MEMORANDUM REPORT ARBRL-MR-03306

DRIFT VELOCITY COMPUTATIONS FOR SHAPED-CHARGE JETS

Steven B. Segletes

September 1983

US ARMY ARMAMENT RESEARCH AND DEVELOPMENT COMMAND
BALLISTIC RESEARCH LABORATORY
ABERDEEN PROVING GROUND, MARYLAND

Destroy this report when it is no longer needed.
Do not return it to the originator.

Additional copies of this report may be obtained from the National Technical Information Service, U. S. Department of Commerce, Springfield, Virginia 22161.

The findings in this report are not to be construed as an official Department of the Army position, unless so designated by other authorized documents.

The use of trade names or manufacturers' names in this report does not constitute indorsement of any commercial product.

UNCLASSIFIED

SECURITY CLASSIFICATION OF THIS PAGE (When Data Entered)

REPORT DOCUMENTATION PAGE	READ INSTRUCTIONS BEFORE COMPLETING FORM
1. REPORT NUMBER: MEMORANDUM REPORT ARBRL-MR-03306	2. GOVT ACCESSION NO.: AD-A133756
3. RECIPIENT'S CATALOG NUMBER	
4. TITLE (and Subtitle): DRIFT VELOCITY COMPUTATIONS FOR SHAPED-CHARGE JETS	5. TYPE OF REPORT & PERIOD COVERED
	6. PERFORMING ORG. REPORT NUMBER
7. AUTHOR(s): S. B. Segletes	8. CONTRACT OR GRANT NUMBER(s)
9. PERFORMING ORGANIZATION NAME AND ADDRESS: US Army Ballistic Research Laboratory, ATTN: DRDAR-BLT, Aberdeen Proving Ground, MD 21005	10. PROGRAM ELEMENT, PROJECT, TASK AREA & WORK UNIT NUMBERS: 1L162618AH80
11. CONTROLLING OFFICE NAME AND ADDRESS: US Army Armament Research & Development Command, US Army Ballistic Research Laboratory (DRDAR-BLA-S), Aberdeen Proving Ground, MD 21005	12. REPORT DATE: September 1983
	13. NUMBER OF PAGES: 81
14. MONITORING AGENCY NAME & ADDRESS (if different from Controlling Office)	15. SECURITY CLASS. (of this report): Unclassified
	15a. DECLASSIFICATION/DOWNGRADING SCHEDULE

16. DISTRIBUTION STATEMENT (of this Report)

Approved for public release; distribution unlimited.

17. DISTRIBUTION STATEMENT (of the abstract entered in Block 20, if different from Report)

18. SUPPLEMENTARY NOTES

19. KEY WORDS (Continue on reverse side if necessary and identify by block number)

shaped-charge jet
penetration
drift velocity
transverse velocity
drift distribution
sidewall impact

20. ABSTRACT (Continue on reverse side if necessary and identify by block number) bet/

This work provides quantitative support for the assumption that jet curvature is the major cause for nonideal jet penetration. Jet radiographs were analyzed to ascertain the component of jet velocity normal to the axis of symmetry of the charge for each jet particle. This nonideal velocity component is the drift velocity. The drift velocity distribution determined in this manner was imposed on the jet in a computer simulation of the penetration process. The computer code, referred to as PENJET, was employed to generate penetration-standoff

DD FORM 1 JAN 73 1473 EDITION OF 1 NOV 65 IS OBSOLETE

UNCLASSIFIED

SECURITY CLASSIFICATION OF THIS PAGE (When Data Entered)

curves using the data from a specific round. This curve depicts the penetration-standoff performance for the single round as if it could be shot repeatedly at a variety of standoffs. The curve could then be compared with the actual datum for the round.

TABLE OF CONTENTS

LIST OF ILLUSTRATIONS

LIST OF ILLUSTRATIONS (CONT'D)

I. INTRODUCTION

Theories to predict penetration of shaped charges have met with varying degrees of success. Except for relatively short standoffs, penetrations diverge greatly and never really approach idealized values. Inspection of jets through the use of flash radiographs reveals why idealized penetration is not a reality: because the idealized jet is not a reality. The presence of drift velocity (seen in a radiograph as jet curvature) is suggested as being the main cause for the variance in jet penetrations. Transverse (or alternately drift) velocity refers to the motion of shaped-charge jet particles in the plane perpendicular to the charge axis of the warhead (drift or transverse plane). The distance travelled by a jet particle in the transverse plane is referred to as the particle deviance.

All shaped charge jets contain drift velocity to some degree or another. The origins of drift are naturally linked to imperfections in the warhead itself. Lack of uniformity of liner thickness, nonhomogeneous explosive, as well as asymmetric liner confinements must all be considered as possible causes of drift velocity in any given round. Fissures in the explosive material and uncentered boosters can also contribute to jet performance that is less than perfect. With respect to the rounds studied in this analysis, it was also noticed that rounds with pressed explosive possessed consistently lower penetration capabilities than their cast explosive counterparts. One theory is that the high pressures (20,000 psi) required to press the explosive were capable of distorting the liner. The problems characterizing these pressed rounds were typical of the early days of pressing. Technology in the area of pressing explosives has since improved to a point where many of the problems then inherent in the rounds studied have been corrected. Some uncased pressed rounds now show penetrations of 5.5 calibers at 24 caliber standoff. Nonetheless, the pressed rounds that were studied possessed adverse qualities that manifested themselves in poor jets. Thus, with a multitude of sources for asymmetric conditions always present, it is not surprising to find the regularity with which drift velocity occurs in jets.

An algebraic analysis can be performed to evaluate numerically the drift velocities of the particles of a given jet. Preliminary and somewhat simplified computations indicate that drift velocity alone is sufficient to account for major variations in jet penetration.

II. MEASURING THE DRIFT VELOCITY OF A PARTICLE

The flash radiograph is the best tool to perform detailed analysis of the shaped charge jet in flight. It would, therefore, be appropriate to explain the nature and setup of the apparatus and how it relates to the data obtained and used in the analysis. A diagram of the apparatus is shown in Figure 1. The jet is radiographed from three different angles at three different times before it finally penetrates the target. The angular separation of each of the x-ray tubes is 45°. A sample radiograph of one of the rounds studied is shown in Figure 2. Note the fiducial markings which

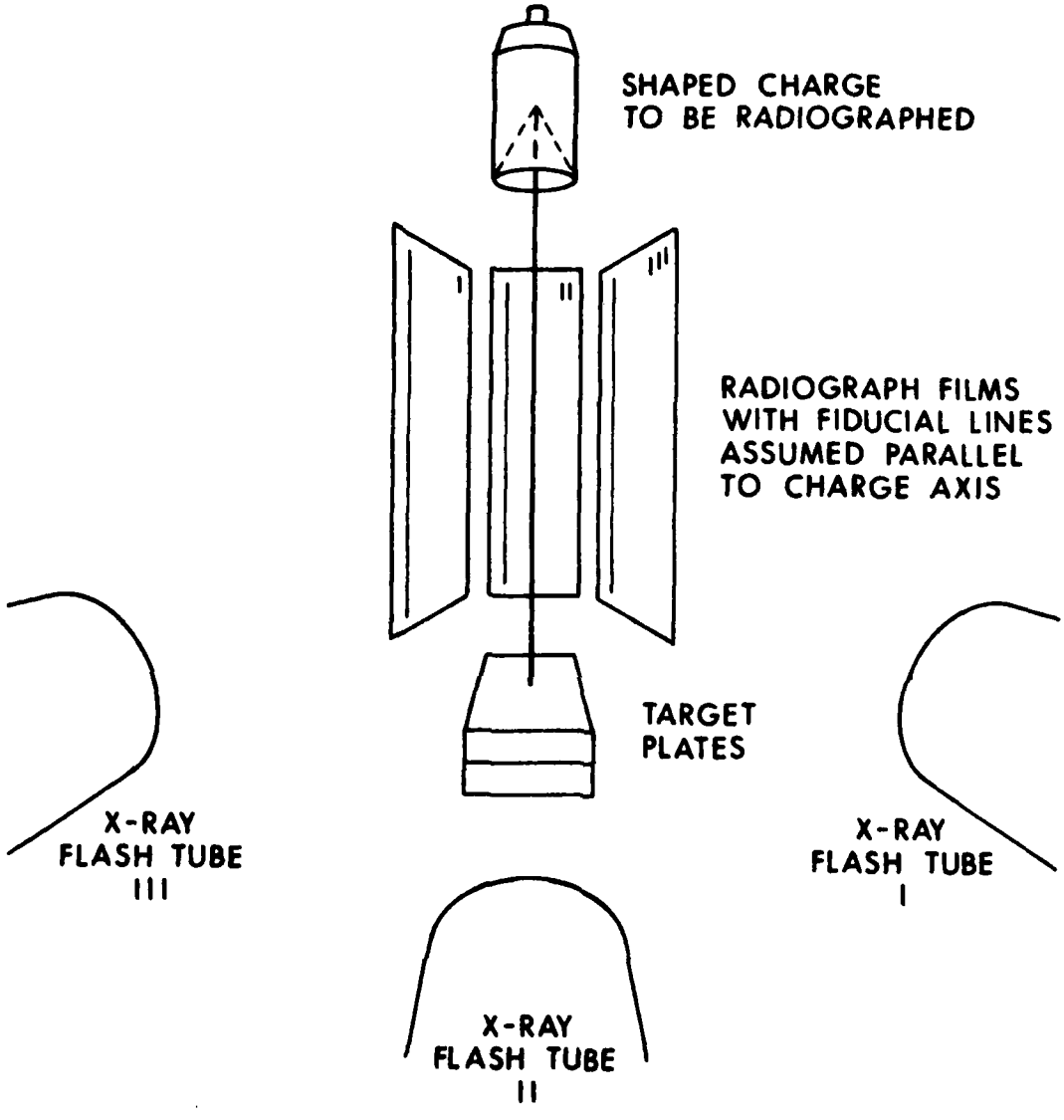

Figure 1. Radiographic Apparatus Used to Record Flight of Shaped-Charge Jet

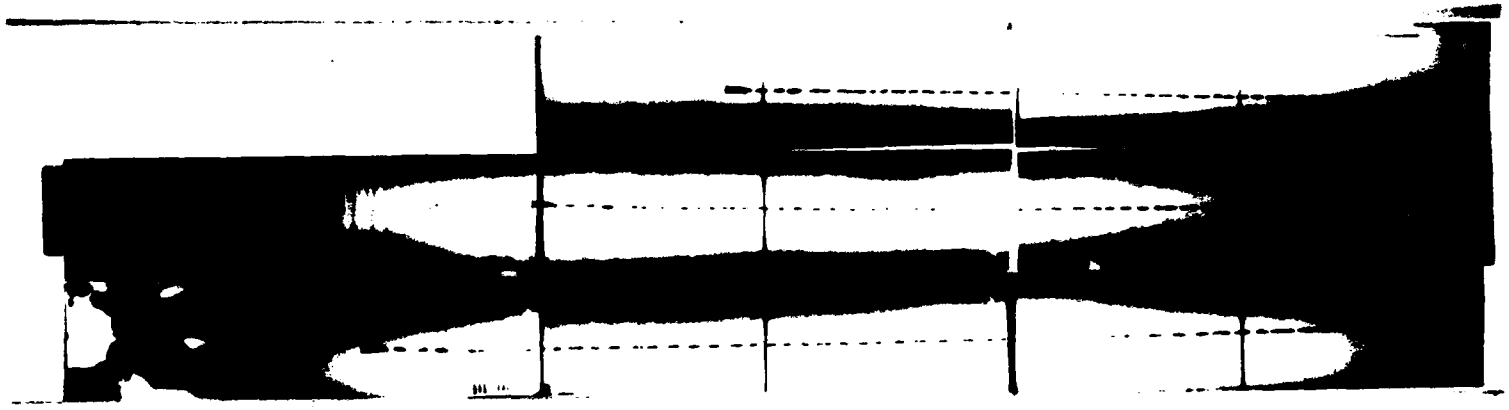

Figure 2. Sample Radiograph of a Shaped-Charge Jet in Flight

lie not on but parallel to the charge axis. Data are extracted from the radiographs by a digitizing process whereby each particle on the film is defined by six points located on the perimeter of the particle. By this means, calculations are made for each particle's length, diameter, velocity, mass, momentum, and kinetic energy using procedures described by Blische and Simmons.[1]

If it is assumed that the fiducials are parallel to the charge axis of a round, the radiograph of an ideal jet would contain an image of the jet parallel to the fiducials on all exposures. This assumption is not strictly true, but shall be discussed in Section IV. With near perfect jets rarely being observed, it becomes important to measure the transverse movement of particles with respect to the charge axis. However, the location of the charge axis is, in itself, unknown. One assumes that the charge axis is parallel to the fiducials on all radiograph exposures, though it is not coincident with any one of them. It becomes necessary, therefore, to choose a workable reference. The rear of the jet has always been considered the most stable portion. For this reason, a particle near the rear of the jet that is readily definable in all three radiographs is chosen as the reference. The reference axis is an axis parallel to the warhead charge axis on which the reference particle lies. If the reference particle is not drifting in the transverse plane, the reference axis will be coincident with the charge axis.

To see how the transverse velocity of a particle might be measured, it would be convenient to imagine looking down the charge axis, as if from liner to target. Ignoring all particles of the jet except the reference particle and the particle in question, the charge axis view of the situation could be described by Figure 3. Note that the film shown in the figure is just the "edge" of the film since the view is down the charge axis. The deviance (perpendicular distance between the reference axis and the particle in question) that is seen in the radiograph is less than or at most equal to the actual deviance due to the cosine effect. Given the apparatus of Figure 1, and having exposed the three radiographs simultaneously, the reference particle and the particle in question could be precisely located with respect to each other in the transverse or drift plane. This situation is illustrated in Figure 4. The time delay that actually exists among the three exposures complicates matters little and three governing equations are readily derived:

$$V_T^* = \frac{D_1/\cos(\theta+45°)}{t_1} \qquad (1)$$

$$V_T^* = \frac{D_2/\cos\theta}{t_2} \qquad (2)$$

---

[1] J. Blische, B. Simmons, "A Method for Reducing Data from Radiographs of Shaped-Charge Jets," BRL Report ARBRL-TR-02330, Jun 81 (AD A102770).

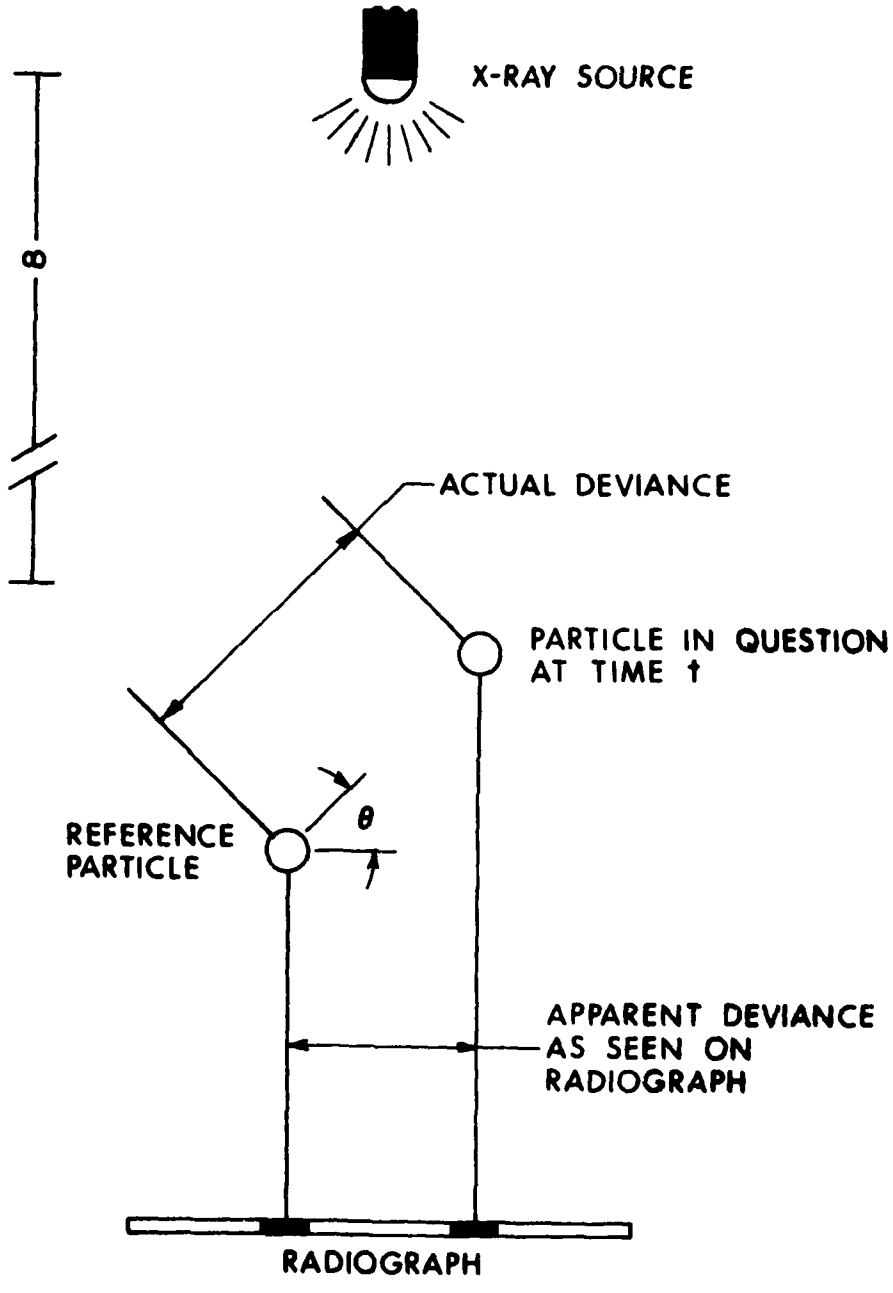

Figure 3. View of Particle Deviation as Projected onto the Transverse Plane

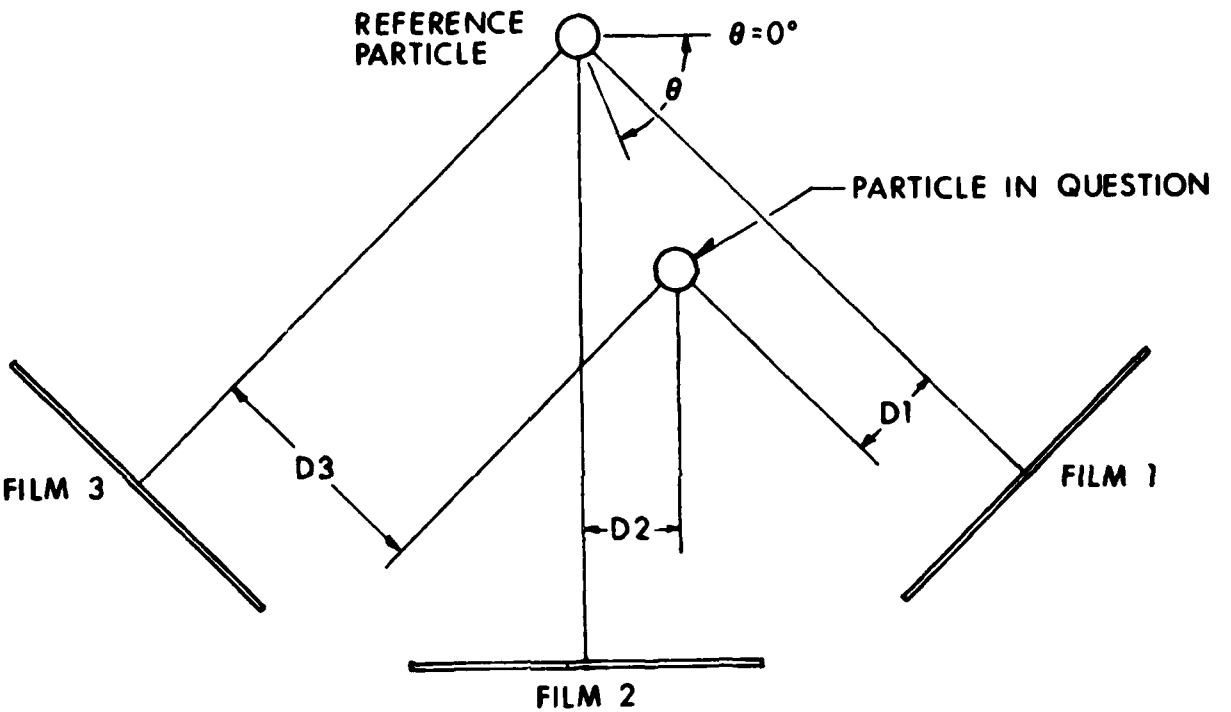

Figure 4. Locating a Particle in the Transverse Plane Through the Use of Three Radiographs

$$V_T^* = \frac{D_3/\cos(\theta-45°)}{t_3} \quad (3)$$

where D_k - apparent deviance read off the K'th radiograph

t_k - the time between particle formation and the K'th exposure

θ - deviation angle between path of deviation and some arbitrary reference (chosen parallel to film 2)

Equations (1), (2), and (3) all contain two unknowns, namely magnitude of drift velocity (V_T^*) and angle of deviation (θ). Any two of these three equations can be solved simultaneously to yield a result for transverse velocity, both in magnitude and direction. In reality, the equations are solved in all three combinations, and a weighted average is taken depending on the particle's orientation with the radiographs. This velocity shall be called by the name of relative drift velocity since the particles are moving with respect to a moving reference (the reference particle).

III. THE DRIFT VELOCITY DISTRIBUTION FOR A GIVEN ROUND

When relative transverse velocities are evaluated for all the particles of a jet, a polar plot can be made whereby a line segment with length proportional to the magnitude of drift velocity is plotted at the appropriate deviation angle in the transverse plane. A sample velocity fan is shown in Figure 5. This relative velocity fan shows a kind of spray of the jet particles away from the reference particle in the deviation plane.

When a plot is made of the axial versus transverse particle velocity for a given round, a graph similar to Figure 6 frequently results. The data seems to be of the form:

$$V_A = KV_T^* + V_{REF} \quad (4)$$

where: V_A - axial velocity of particle

V_T^* - relative transverse velocity of particle

K - constant varying from round to round

V_{REF} - axial velocity of the reference particle

Most rounds studied were in high correlation with Equation (4).

The next quantity to determine is the drift velocity of the reference particle from which all the calculations were made. If we assume that the reference drift velocity is negligible, then the separation distance between impacts of the jet tip and the reference particle would routinely exceed

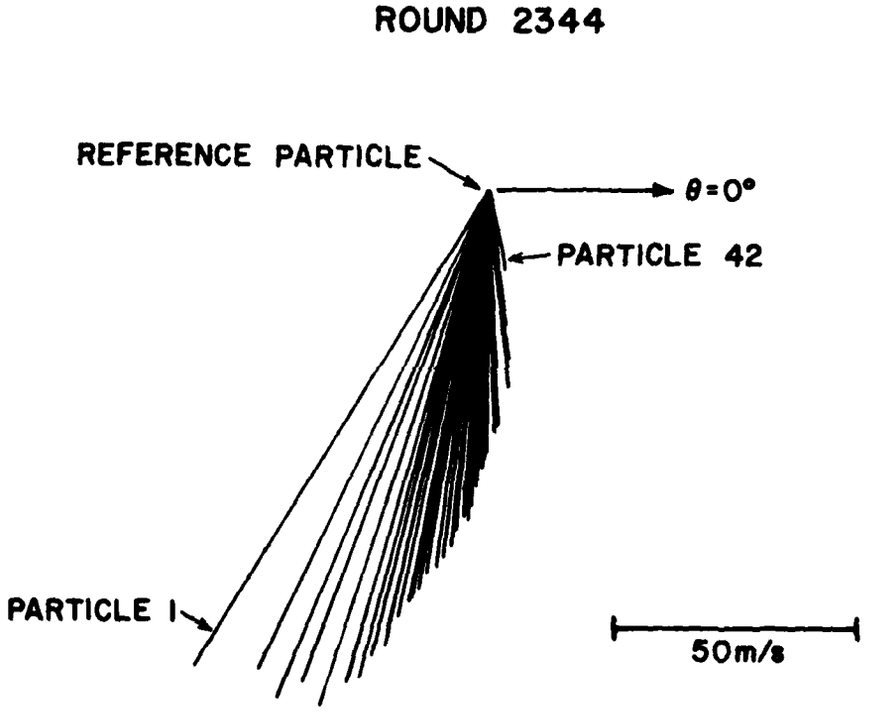

Figure 5. Relative Velocity Fan Showing the Pattern Formed by the Drifting Jet Particles

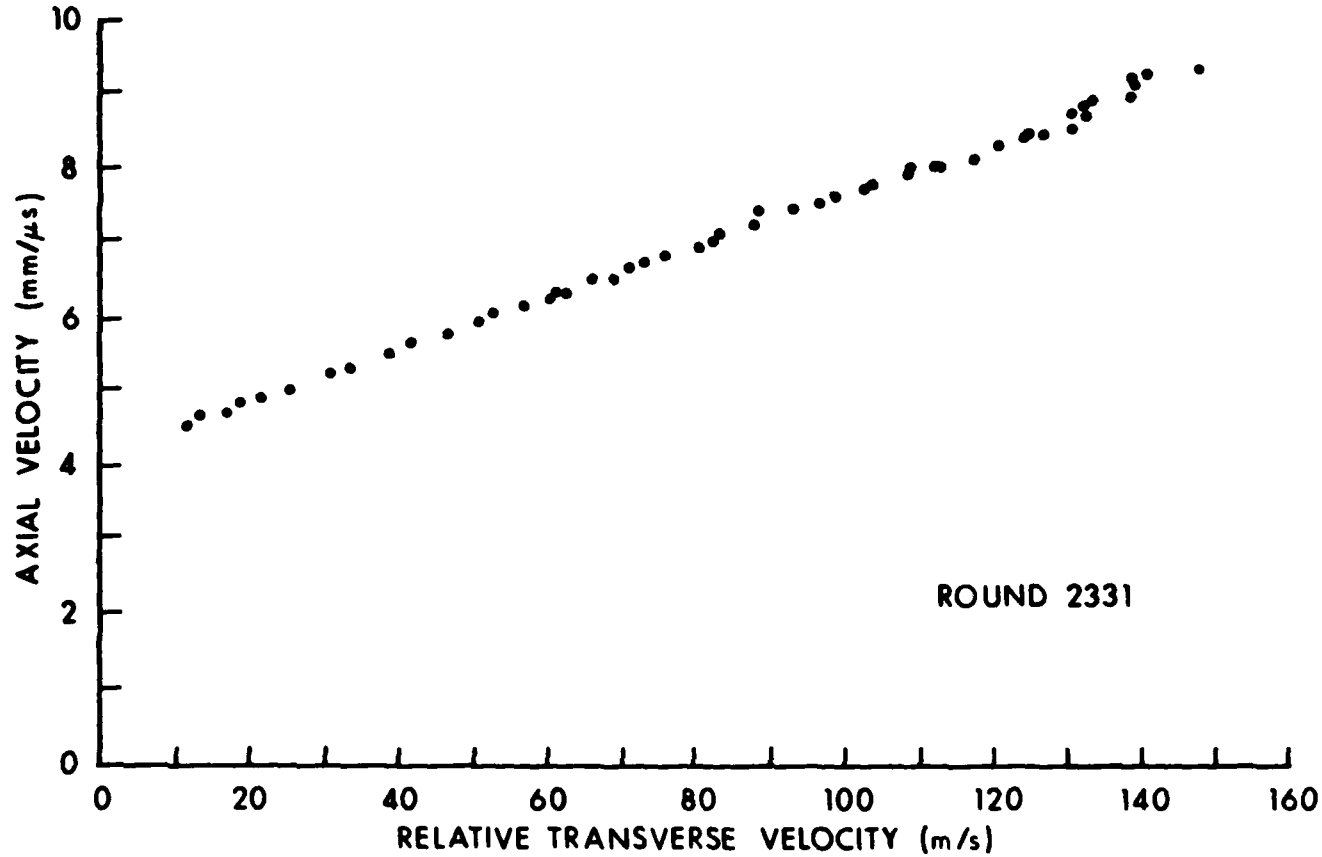

Figure 6. Typical Plot of Axial vs. Transverse Velocity for Particles of a Given Round

1/2 charge diameter (CD) at a 24 CD standoff for typical drift distributions studied. Under such conditions, the reference particle will never enter the crater created by the jet tip because of excessive drift. However, it is not uncommon for a jet to produce a single entrance hole into the target at 24 CD standoff. Thus, the reference must possess a drift velocity which will tend to bring the reference into the crater formed by the jet tip. An equation is needed which expresses that the reference particle should deviate the same distance from the charge axis as the jet tip upon reaching a target block at a given standoff. Mathematically, the assumption is:

$$D_R = D_j \tag{5}$$

where: D_R - the distance the reference has deviated upon reaching the target surface (magnitude only)

D_j - the distance the jet tip has deviated upon reaching the target surface (magnitude only)

Equation (5) does not preclude drift among the jet particles since it pertains to magnitude only. An angular separation of the drifting particles still exists and will tend to separate the jet particles at extended standoff. For a small angular deviation among jet particles however, Equation (5) gives jets the ability to produce single crater target impacts. It is suggested solely because a compensatory reference particle drift was required and is the best which can be proposed at this time. Since drift velocity is assumed to be constant after a particle's formation, Equation (5) can be expressed as:

$$V_{T_R} t_R = V_{T_j} t_j \tag{6}$$

where: V_T - the absolute drift velocity of the associated particle

t - the time required for the associated particle to reach the target surface

R - the reference particle

j - an arbitrary jet particle

But the time required for a particle to reach the target surface is equal to the standoff as measured from the virtual origin (Z_o) divided by the particle's axial velocity (V_A). Therefore, Equation (6) expands to:

$$V_{T_R} \frac{Z_o}{V_{A_R}} = V_{T_j} \frac{Z_o}{V_{A_j}} \tag{7}$$

Simplifying:

$$\frac{V_{A_R}}{V_{T_R}} = \frac{V_{A_j}}{V_{T_j}} \tag{8}$$

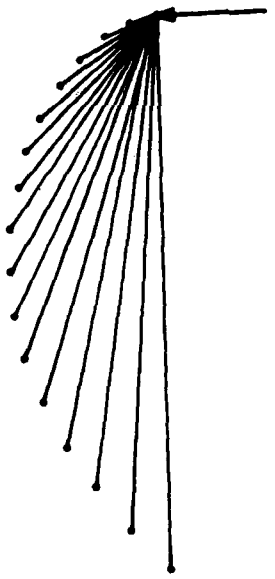

A RELATIVE VELOCITY FAN WITH SCALED REFERENCE VELOCITY ARROW INDICATING MAGNITUDE AND DIRECTION OF REFERENCE DRIFT. THE APEX OF THE FAN REPRESENTS THE REFERENCE PARTICLE FROM WHICH DRIFT MEASUREMENTS WERE ORIGINALLY TAKEN.

AN ABSOLUTE VELOCITY FAN IS CREATED BY CONNECTING THE TAIL OF THE REFERENCE VECTOR TO THE RELATIVE VELOCITY FAN. THE APEX OF THE FAN LOCATES THE CHARGE AXIS IN THE TRANSVERSE PLANE. THE REFERENCE PARTICLE NOW BECOMES JUST ANOTHER DRIFTING PARTICLE.

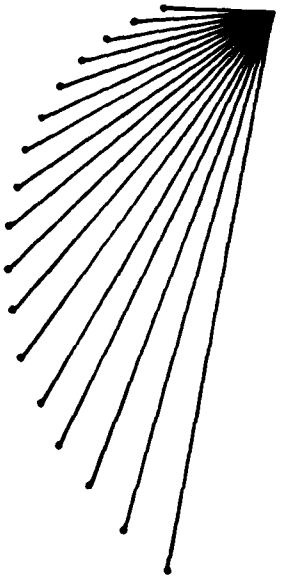

Figure 7. Transformation of Relative Fan Into Absolute Fan for a Hypothetical Drift Distribution

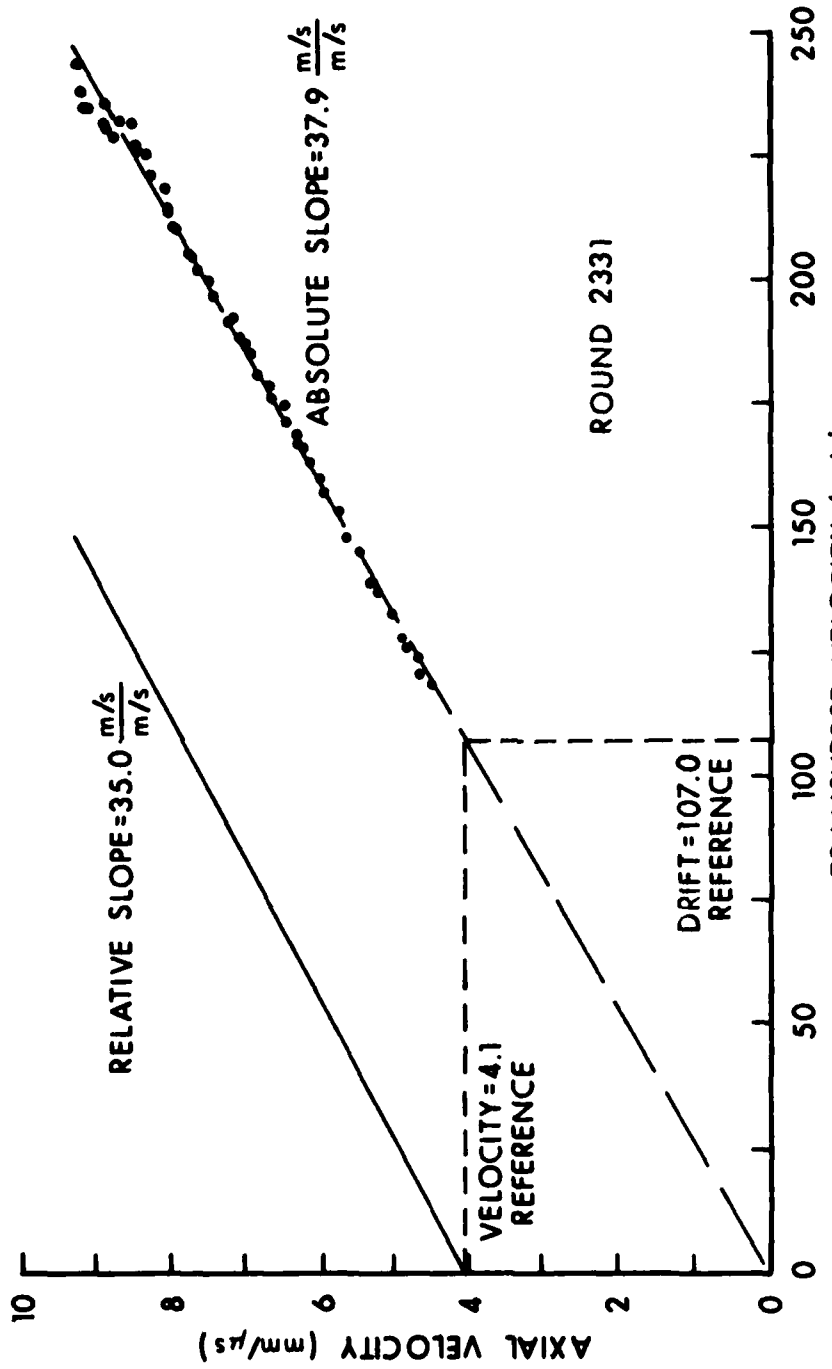

Figure 8. Effect of Transformation from Relative to Absolute Drift Velocity on the Slope of the Curve

For a crater profile in which all particles of the jet enter the target surface at the same point, Equation (5) must hold for all particles, implying:

$$\frac{V_A}{V_T} = \text{constant} \qquad (9)$$

Since the reference is at the apex of the relative transverse velocity fan, the reference velocity would appear as a vector with its tip attached to the apex of the relative velocity fan. Its length corresponds to the drift velocity of the reference particle and its direction indicates the direction in which the reference is deviated. Its direction of deviation is assumed to be about the same as that of the slowest digitized particle. The absolute velocities of the balance of the particles are calculated by vectorially adding the reference velocity to the relative velocities of the respective particles. Thus, an absolute drift velocity fan is created by drawing the segments from the tail of the reference vector to the tips of the relative drift velocity fan. (See Figure 7.) Graphically, Equation 9 implies a linear V_A vs. V_T plot which intercepts the origin. With the proper vectorial addition of the reference drift as just described, relative drift distributions like Figure 6 readily map into absolute drift distributions which satisfy Equation 9. (See Figure 8.)

There is no way to know whether this transformation into absolute velocities is the correct one. However, it is believed that the directional assumption of the reference is a safe one, and that the Equation (5) assumption is as good as any considering the need for the drift correction of particles. In addition, the results obtained from the transformation are supported by the experimental data. Note that Equation (9) does not guarantee that all particles will only form a one-crater hole profile even though all the particles should deviate the same distance from the charge axis. A large angular spread in a jet (characterized by a wide absolute velocity fan) may produce enough relative deviation among the particles so as to cause multiple impacts at long standoff. Thus, the deviating factors in jets are both the angular spread and the magnitudes of the drift velocities.

IV. THE QUESTION OF TILT

A possible and potentially fatal flaw in the previous discussion concerns the presence of tilt. The word tilt is taken to mean a charge axis that is not parallel to the radiograph fiducials. An original assumption was that there was no tilt, or that charge axis and fiducials were aligned. It is obvious that some sort of tilt must exist, however small. The answer as to when tilt becomes critical is a bit disconcerting. Depending on the jet, a one-degree tilt of the charge axis off the fiducials could induce an apparent drift velocity of 160 m/sec in the jet tip as measured with respect to the fiducials. It is likely that uncertainties of this magnitude exist regularly.

The consequence of tilt on a jet is an apparent drift velocity distribution, which is also governed by Equation (9), which is the assumed relation for actual drift velocity. One may rightfully wonder whether all of the drift velocities read off the radiographs are due completely to tilt, and whether graphs like that of Figure 6 are a consequence of tilt alone. In fact, what is read off the radiographs is the superposition of both tilt and real drift velocity distributions. However, it should be noted that an important aspect of tilt is that it cannot produce a velocity fan. All of the particles of a jet under the influence of tilt exclusively would appear to drift in a uniform direction. Yet, Equation (9) has been seen to hold for jets with velocity fans spanning in excess of 90°.

The concern here is whether a nonlinear drift distribution could be "tilted" into appearing linear on the radiographs, and thus explain the data without having the actual drift obey Equation (9). Such could only be the case if the magnitude of actual drift were small in relation to tilted drift. If this were the case, however, the angular spans of the velocity distributions would also be quite small, which is usually not the case. Thus, it appears that the actual drift velocities are at least of the same order of magnitude as the apparent drift velocities due to tilt. Thus, it seems that the actual drift distributions, though probably different from the measured drift distributions, can still be adequately described by Equation (9). This belief is based only on the rounds studied. No explanation is offered as to why there might be a relation between the axial and transverse velocities of jet particles. Also, it is uncertain as to whether this may be a general phenomena or characteristic only of the rounds studied.

Support for Equation (9) was found in work done by Aerojet General Corporation.[2] Aerojet was interested in the crater formation of individually impacting particles. A shaped charge supplied the particles for their experiment. The method employed for dispersion of the particles was asymmetric initiation. Considering that it was desired to induce much drift velocity in the particles, the effects of tilt could be neglected in this experiment. The target plate used in their experiment is shown in Figure 9. The particle impacts generally lie at a constant distance from the slug impact. Assuming the slug flight path to be coincident with the charge axis, Equation 9 is the governing equation.

A penetration code was created to predict penetrations for nonideal shaped-charge jets. Unlike the DSM model,[3] which can express penetration in a single equation, the model developed analyzes the jet piecemeal. It is described in detail in the following section.

---

[2] K. N. Kreyenhagen, J. E. Ferguson, R. R. Randall, J. P. Joyce, "Special Explosive Projectors," Proc. 6th Symposium Hypervelocity Impact, Vol. I (Held Cleveland, Ohio, April 30-May 2, 1963).

[3] R. DiPersio, J. Simon, A. Merendino, "Penetration of Shaped-Charge Jets Into Metallic Targets," Ballistic Research Laboratory Report No. 1296, September, 1965 (AD 476717).

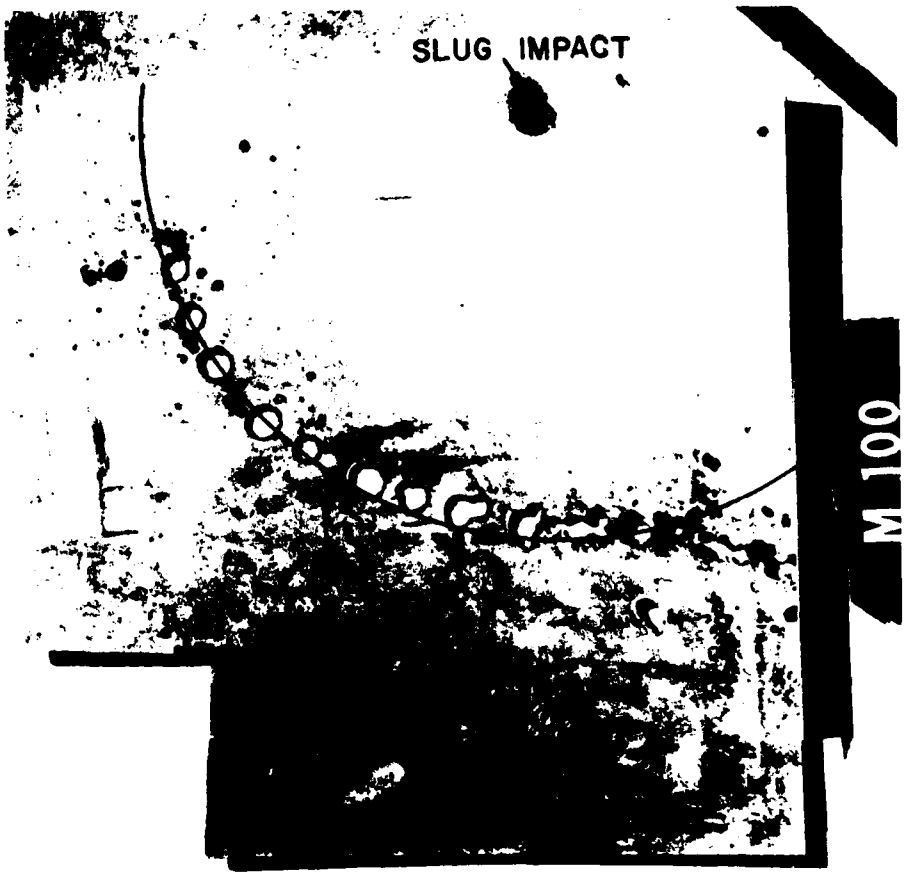

Figure 9. Target Plate for Asymmetrically Initiated Shaped Charge (Reference 2)

V. THE CREATION OF A PENETRATION CODE TO ANALYZE DRIFT

The purpose of analyzing drift velocity distributions of shaped-charge jets is to see how these distributions affect penetration. The dynamics of penetration is not, however, a thoroughly understood subject. Many theories exist in attempts to discribe the mechanical properties of matter. Classical, empirical and even wave mechanical concepts are used in pursuit of the subject. Consequently, rather than adding to the spectrum of theories that already exist, the author chose to draw upon information already available on the subject whenever possible and to combine views in a seemingly compatible manner.

One shaped-charge penetration model that has received much attention in recent years was formulated by DiPersio, Simon, and Merendino (the DSM model).[3] This model does a good job at predicting penetration of shaped charges even at extended standoffs. The model accomplished this however, by implying that there exists a cutoff penetration velocity, a minimum penetration velocity below which a jet cannot penetrate. Unfortunately, the DSM cutoff penetration velocity implies that jet material traveling below certain hypervelocity speeds is incapable of penetrating target material. Substantial quantities of jet material are thus eliminated from the penetration process. The DSM model is empirically based and really attempts only to describe the data at hand and does not enter an intense theoretical discussion to describe the origins of jet cutoff other than citing that it exists experimentally. The work presented in this report suggests that the drift of particles off axis is largely responsible for reduced jet penetration, whereby drifting particles strike the target not at the bottom of the hole but somewhere up the hole profile. This commencement of sidewall impacts frequently seems to constitute a cutoff in jet penetration, since the overall depth of penetration is not altered by a sidewall impact.

A method, therefore, had to be devised which would allow penetration to be a function of drift velocity. Three-dimensional finite difference codes were not considered due to a coupling of availability and cost. Yet, a three-dimensional description of penetration was required since the source of altered penetration is the spread of the particles off of the one-dimensional axis. Consequently, all aspects of particle penetration would have to be considered: size, shape, and orientation of crater formation in a three-dimensional target block.

The code developed in the present work (referred to as PENJET) includes many simplifications and assumptions. The first assumption concerns the shape of crater formed by an impinging jet particle. The chosen shape was that of an ellipsoid, with the ellipsoid being characterized by a position in three-dimensional space, dimensions along the axes, as well as an orientation in space (as shown in Figure 10). The position of particle impact is determined by using the velocity fan of a round to trace the particles' flight through three-dimensional space and time in order to locate the particle position with respect to the instantaneous hole profile (formed by earlier particles of the jet). If a particle is found to strike any point within the target, PENJET then proceeds through a series of calculations to determine the remainder of crater parameters. Once the crater formed by a particle is effectively evaluated, PENJET proceeds through subsequent particles of the jet until impacts for all digitized particles have been evaluated. Thus,

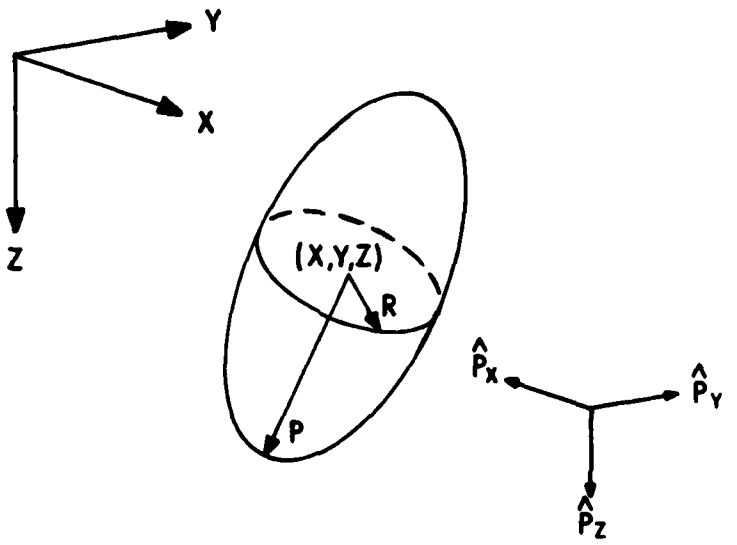

(X,Y,Z)	LOCATION OF IMPACT IN 3-D SPACE
P	MAGNITUDE OF PARTICLE PENETRATION
R	MAGNITUDE OF CRATER RADIUS
$\hat{P}_X, \hat{P}_Y, \hat{P}_Z$	PENETRATION AXIS (A UNIT VECTOR IN 3-D SPACE)

Figure 10. Parameters Generated by PENJET to Describe Crater Formed by Impinging Jet Particle

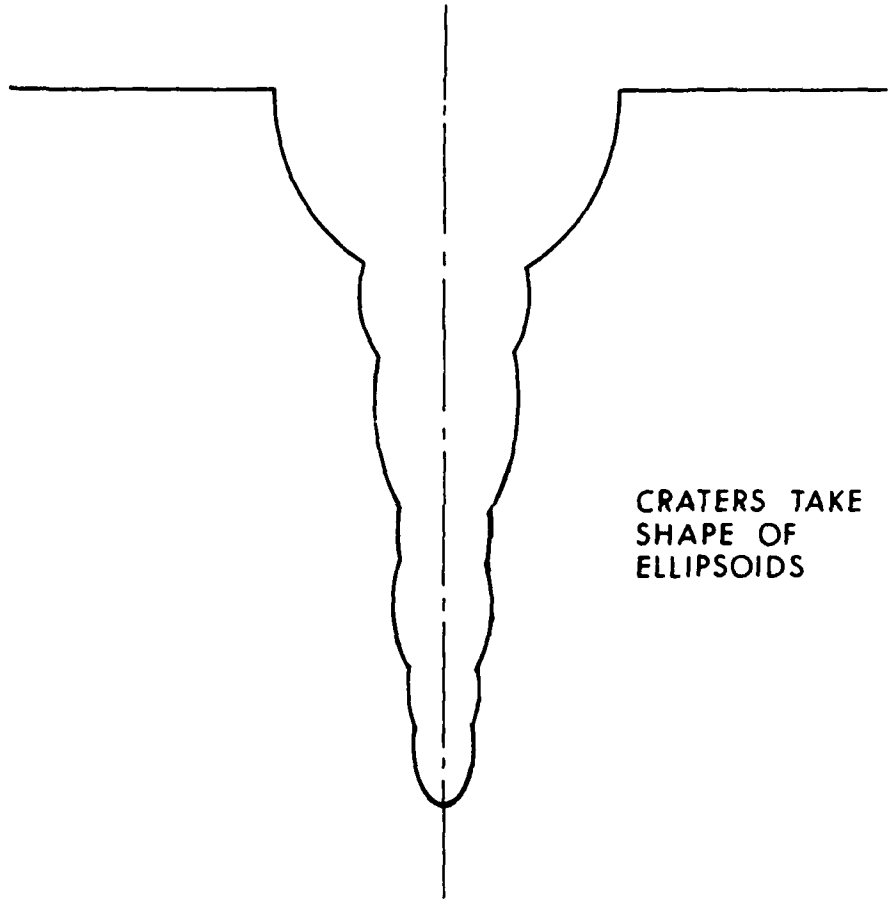

Figure 11. PENJET Hole Profile Results from Ellipsoid Superposition

a hole profile for a complete jet is just the superposition of ellipsoids from each of the particle impacts. A two-dimensional representation of a three-dimensional hole profile is shown in Figure 11 for a fictitious nondrifting jet. When evaluating the crater formed by an impinging jet particle, crater volume is a constraining factor. That is to say, crater volume is calculated independently of other crater parameters and is assumed to be a function of particle kinetic energy alone. Subsequent calculations for actual crater dimensions are, therefore, constrained by the allowable volumetric target displacement a given particle can produce. The function governing the volume energy relationship is a linear one, similar to that adopted by DiPersio, Simon, and Merendino.[3] The distinction arises in the fact that the DSM model expresses its proportionality constant as a relationship between total jet kinetic energy and total hole volume. PENJET, on the other hand, bases its constant on the energy of the individual particle. It is not surprising to find, therefore, that the DSM constant differs from its PENJET counterpart. Consider also, that the energy constant of PENJET does not strictly define an exact amount of displaced target material. As mentioned previously, the hole profile of PENJET is the superposition of ellipsoid craters corresponding to each of the jet particles. The orientation of these ellipsoids will greatly affect the spacial overlap of the ellipsoids, and thus the overall volumetric target displacement of a given jet. Because of this spacial overlap of particle craters, the overall crater volume as calculated by PENJET is not the summation of particle energies divided by the energy constant. Estimation of the constant was gotten empirically through examination of target blocks as well as hole profile data.

The crater shape of an individual impact is prescribed (as an ellipsoid) and the particle's crater volume is proportional to its own kinetic energy. Therefore, knowledge of a particle's penetration capability will allow the particle's hole radius to be computed and vice versa. In PENJET, depth of penetration is computed, with crater radius being subsequently determined. The model of particle penetration used in the code is based on the work of Fitzgerald,[4] who draws on the work of Kineke[5] to imply that crater formation occurs in a direction perpendicular to the stricken surface. Fitzgerald calls this phenomenon the wave refraction theory and shows that it applied to a single particle striking a flat plate at some obliquity (Figure 12). PENJET uses the concept in a more general sense by applying the wave refraction theory to local obliquities as well. Local obliquity is defined as the angle between the particle flight axis and the normal to the impact plane. Unless the impinging particle strikes exactly at the bottom of the hole profile, the refracted penetration wave will not be normal to the original target surface (Figure 13). In the strict sense, the refracted wave theory should only be applicable in the regime of hydrodynamic penetration. A large majority of particle impacts studied did not fit the qualification for hydrodynamic penetration. For these cases, the direction of penetration would be somewhere between the particle flight axis and the refracted wave axis. It was later noted that the penetration of a particle typically varied less than 5% because of the refracted wave assumption.

[4] *E. Fitzgerald, Particle Waves and Deformation in Crystalline Solids, Interscience Publishers, New York, 1966.*

[5] *J. Kineke, Jr. "An Experimental Study of Crater Formation in Metallic Targets," Proc. 4th Symposium Hypervelocity Impact, Vol. I (Held Eglin AFB, Florida, April 26-28, 1960).*

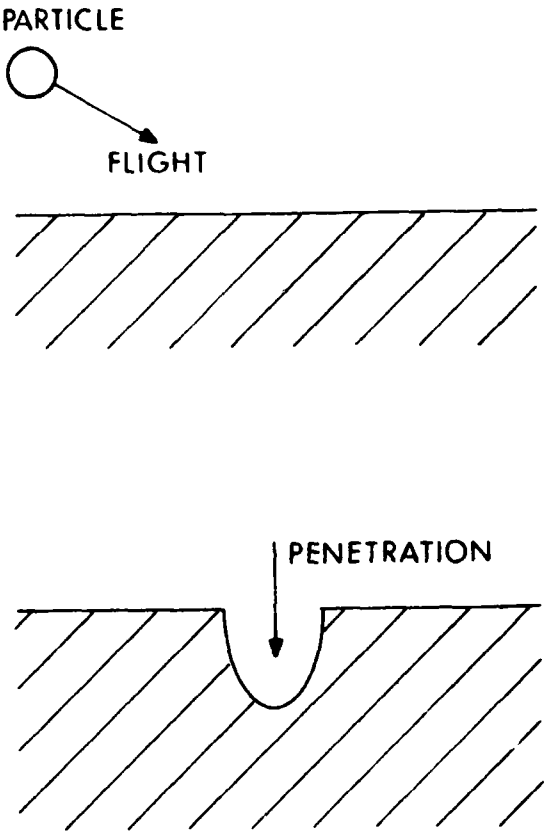

Figure 12. Crater Formation According to Refracted Particle Wave Theory

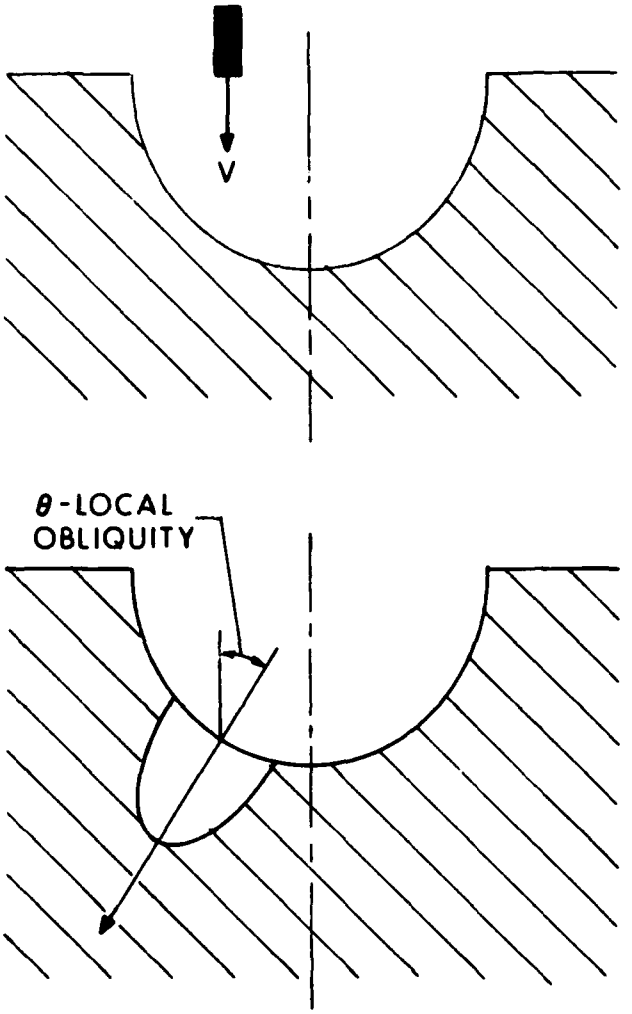

Figure 13. Refracted Particle Wave Theory Applied to Local Obliquity

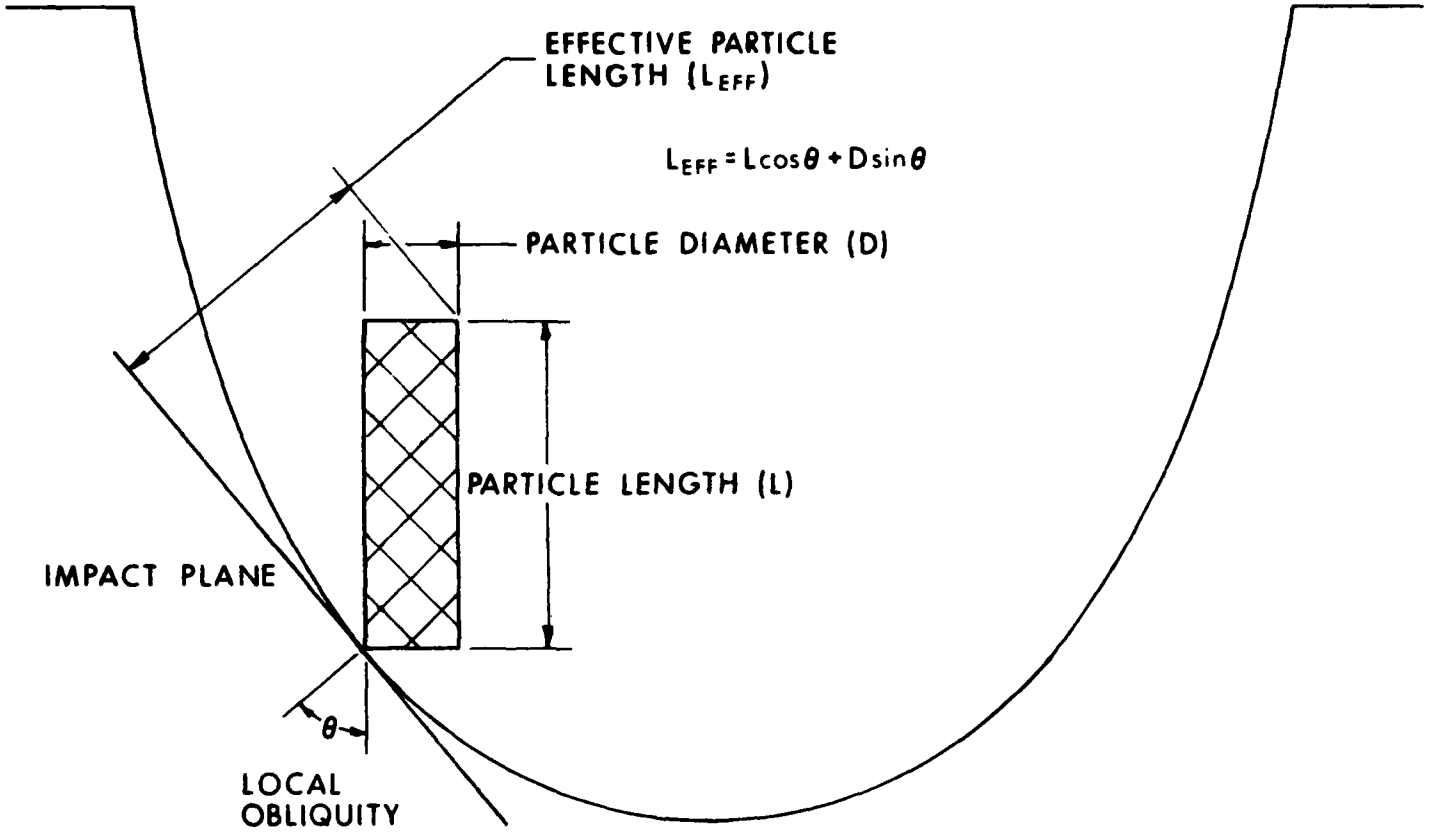

Figure 14. Concept of Effective Length as Seen by Impact Plane

Jet penetration in the continuous mode is quite a different matter from in the particulate mode. Modifications, therefore, had to be included to describe continuous jet penetration. The criterion on which to base mode of penetration is that of breakup time. PENJET uses a linear breakup equation whereby the jet tip particulates at some t_{min} and subsequent particle breakup occurs at regular Δt intervals. Estimates of jet particulation are obtained through examination of the radiographs for the three different exposures. These estimates are then used in a least squares fit to evaluate t_{min} and Δt. Based on the estimated breakup time, it can be established whether a given particle will be penetrating continuously or particulately at a given standoff. If continuous, the length of the particle is re-evaluated such that:

$$\ell_{CONTINUOUS} = \frac{t_{IMPACT}}{t_{BREAK}} \ell_{PARTICULATED} \qquad (10)$$

Also, it is assumed that jet penetrating in the continuous mode does not experience the refracted particle wave of Figure 12. This must, of course, be the case since the continuous particle is essentially beginning its penetration exactly when and where the previous particle leaves off.

PENJET also considers particle orientation with respect to the stricken crater surface. The assumed shape of a shaped-charge particle is cylindrical, being characterized by a length and diameter. As local obliquity is increased, the length of the particle as seen by the impact point is effectively changed. (See Figure 14.) The extreme case is when local obliquity approaches 90°. In this case, the effective length of the particle approaches the diameter of the particle. Hydrodynamically, the penetration of a particle is proportional to the particle length. Thus, the effective particle length replaces the particle length in penetration calculations.

The presence of obliquity raises more questions. The larger the obliquity, the smaller the component of particle velocity perpendicular to the stricken surface. Once in the hypervelocity regime, large changes in particle velocity produce relatively small changes in penetration. If particle velocity is too small, however, the strength of the target and jet play a major role in reducing the penetration of that particle. Besides the effective particle length that the target "sees", it is believed that an effective velocity also plays a role in determining depth of penetration. Whereas penetration is assumed to be directly proportional to effective length, the role that effective velocity plays is not nearly so profound. As long as the effective velocity is in the hypervelocity regime (arbitrarily chosen as any velocity above 2mm/μsec), penetration is assumed greater than the effective particle length for copper jet into an RHA target. As effective velocity increases, penetration is assumed to asymptotically approach the hydrodynamically idealized value. That is:

$$\Delta P \rightarrow L_{eff}/\gamma \text{ where } \gamma = \sqrt{\rho_T/\rho_j} \quad .$$

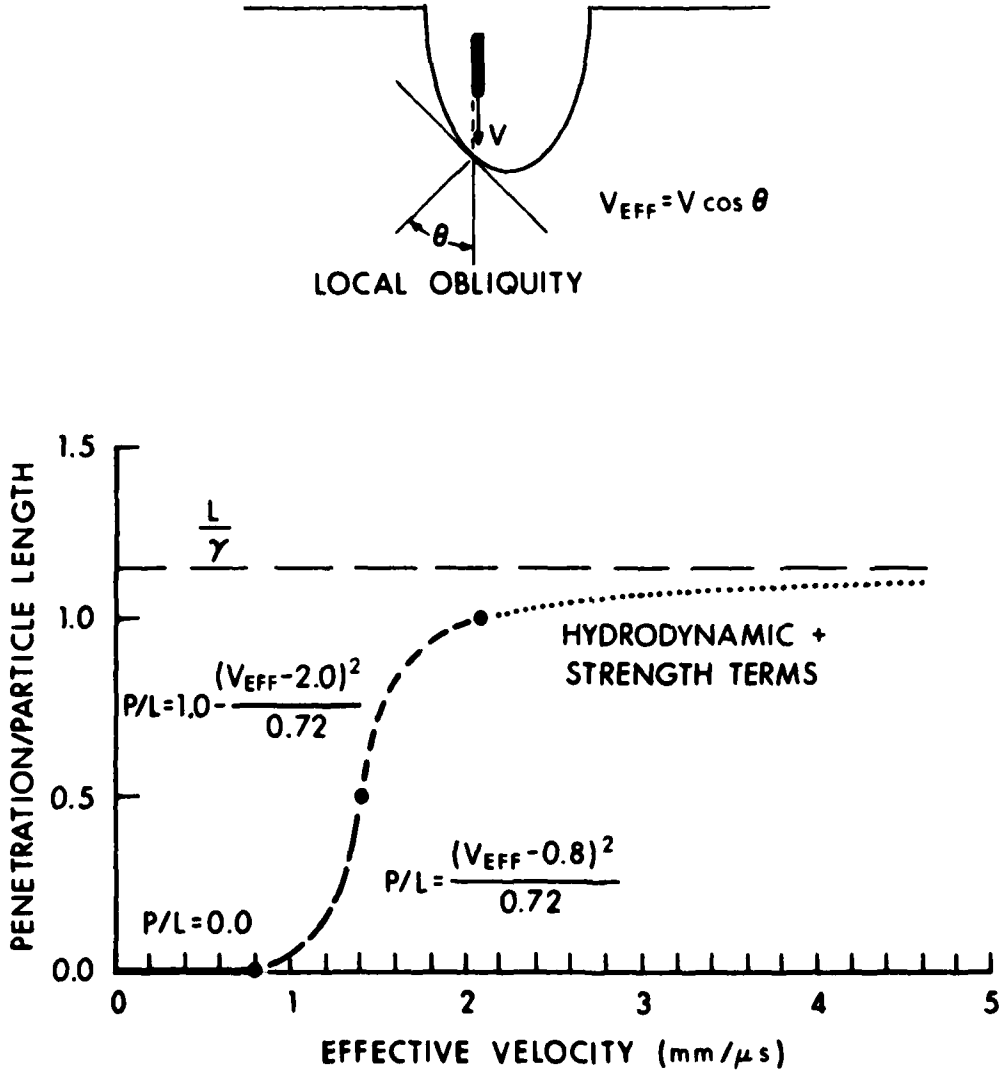

Figure 15. The Role of Effective Velocity in Penetration Calculations Involving Copper Jets Against Steel Targets

The asymptotic approach is generated using the hydrodynamic equations, including strength terms. For effective velocities below 2mm/μsec, penetration rapidly decreases in a manner expressed in Figure 15 so that no penetration is induced when the effective particle velocity is lowered beyond .8 mm/μsec. Data for the effective velocity curve in the low velocity regime was gathered from work by Weirauch.[6] Impacts of this nature may be the source of particle residue shown by Simon and DiPersio[7] to accumulate at the bottom of the hole profile. PENJET, however, does not consider this type of interference.

VI. APPLYING THE CODE TO DATA

Given a set of digitized radiographic data, PENJET will go through all of the mentioned calculations for each digitized particle of the jet to eventually create a three-dimensional hole profile for a given round at a given standoff. If the code is told to use the data of a given round to perform penetration calculations at a variety of standoffs, a theoretical penetration standoff curve can be generated for each round. This curve is, of course, only valid for a particular round. Thus, each generated curve is as individual as the data from which it was generated, and does not, in general, pertain to all rounds of the same type.

The code has both its good and bad aspects. A major consequence is that tilt has no direct effect on the code's ability to calculate penetration. This happens because tilt does not misalign the particles. Rather, it only redefines the charge axis. The particles still drift with respect to each other in the same fashion despite measurements including tilt. Much emphasis was previously placed on tilt for the reason that it would be advantageous to obtain drift distributions unbiased by tilt. In terms of the penetration calculations, though, tilt of and by itself has no effect.

Tilt does, however, indirectly affect the situation in terms of reference drift calculations. As relative drift velocity (as calculated from the radiographs) is the superposition of tilted and actual drift, abnormal relative drift distributions can occasionally result depending on how the two components of measured drift interact with each other. Correspondingly, abnormal relative drift distributions lead to abnormal extrapolations of reference drift, thus making the calculated reference drift suspect. After all, the calculation of reference drift is only an educated approximation: Direction of the drift is based on jet particle orientation, while magnitude of drift velocity is based on Equation (9). Therefore, unlike relative drift computations, which are as good as accuracy of measurement, reference drift is only as good as the governing assumptions. Thus, the poorer the approximation at reference drift, the poorer the quality of penetration calculations.

---

[6] *G. Weirauch, "The Behavior of Copper Pins Upon Impacting Various Materials With Velocities Between 50 m/s and 1650 m/s," (Doctoral Thesis) University of Karlsruhe, 1971.*

[7] *J. Simon, R. DiPersio, "Experimental Verification of Standoff Effects on Shaped-Charge Jet Cutoff in Solid Targets," Ballistic Research Laboratory Memorandum No. 1976, May 1969 (AD 854396).*

Another drawback to the code results from the radiographs themselves. The code can only analyze particles that have been digitized. In most radiographs some portion of the jet that is visible has not yet particulated. Attempting to separate the continuous jet into digitizable portions has met with some success, though likely at the cost of accuracy of particle length, since the continuous particles are still stretching when digitized. Also, most radiographs don't even contain the complete jet, for there is still jet matter that hasn't reached the plane of the film by the time it is exposed. Thus, there is no way to digitize these particles. For the rounds studied, it is estimated that over 40% of the jet was routinely nondigitizable.

To what extent the ability to digitize particles affects the penetration code predictions depends on the quality of the jet. In fact, the poorer the jet is, the less predictions are affected. If the undigitized particles drift far enough off course from the front portion of the jet, they will never make it to the bottom of the hole profile to add to penetration. In this situation, calculations based only on the particles digitized should produce results compatible with calculations involving all particles. Since distance of deviation is directly proportional to time in flight which is directly proportional to standoff, longer standoffs will also decrease the penetration effectiveness of the rear of the jet. Thus, penetration predictions at short standoff are subject to unavoidable error since the undigitized jet portion is still capable of increasing jet penetration. The fact that the penetration effectiveness of the jet rear is predicted to decrease with increasing standoff correlates with the DSM concept of minimum jet velocity increasing with standoff. [3]

Having kept these reservations in mind, the results of the code based on data from four rounds are illustrated in Figures 16-19. The only factor governing the choice of these particular four rounds was penetration; that is, rounds were chosen with varying penetrations ranging from poor to good. The code was run at standoff increments out to 38 CD. The actual rounds were fired at 24 CD standoff to allow radiography, and the actual penetrations achieved are shown on each of the graphs as a single datum. Steplike variations in the code's predictions result because of the discreteness of the impacting particles: Either a particle made it to the bottom of a hole profile or it did not. Major fluctuations in the code predictions can be taken to imply uncertainty in the jet performance. Uncertainty as to whether two or three given particles make it to the bottom of the hole profile can create penetration variations in excess of 1/2 CD. A curve was drawn to fit the code's predictions on each of the rounds, though a band width of uncertainty should be realized as well. This curve is PENJET's prediction of penetration, assuming that one could fire the exact same round over and over again at various standoffs. Since we know that the predictions at short standoff are inaccurate due to nondigitizable jet, the code's predictions on Figures 16-19 are generally unreliable below 10 CD. The curve, however, should be valid at the standoff of 24 CD at which the rounds were actually fired.

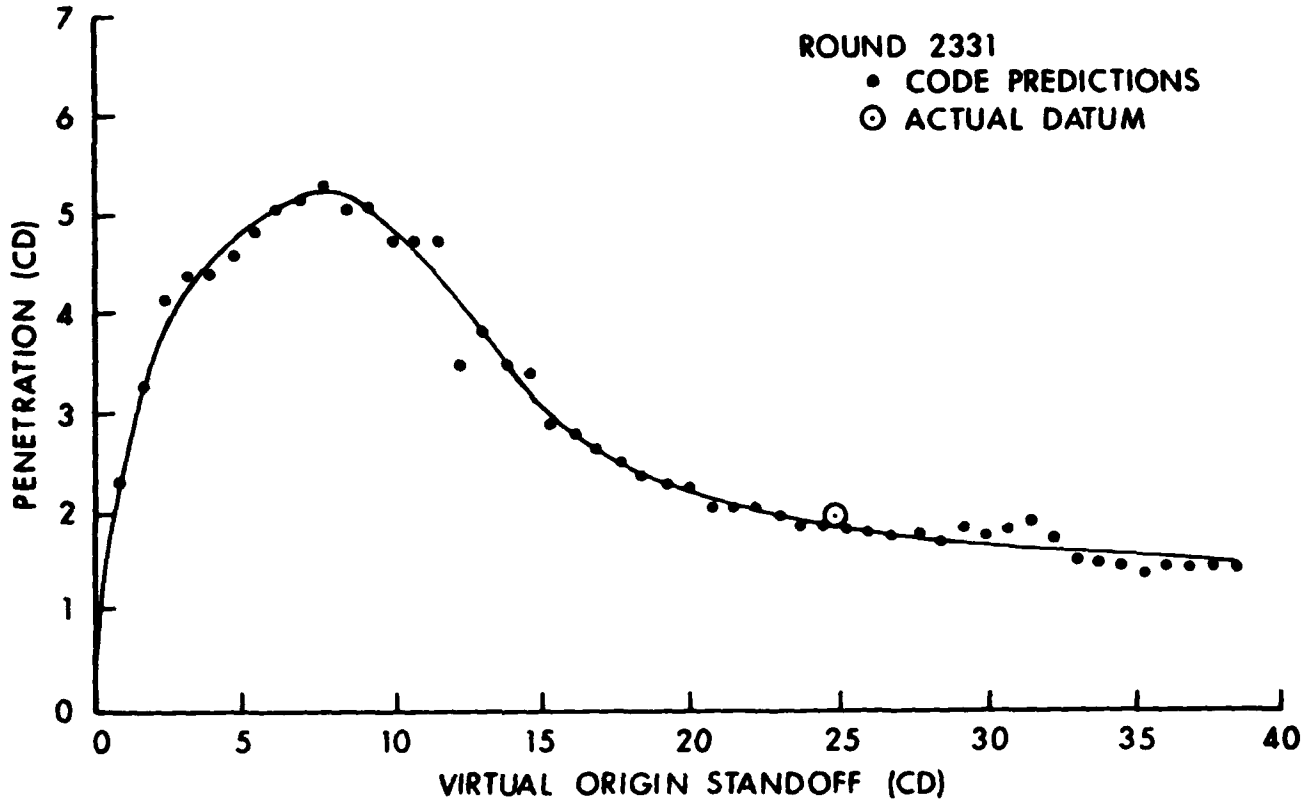

Figure 16. Analysis of Round 2331

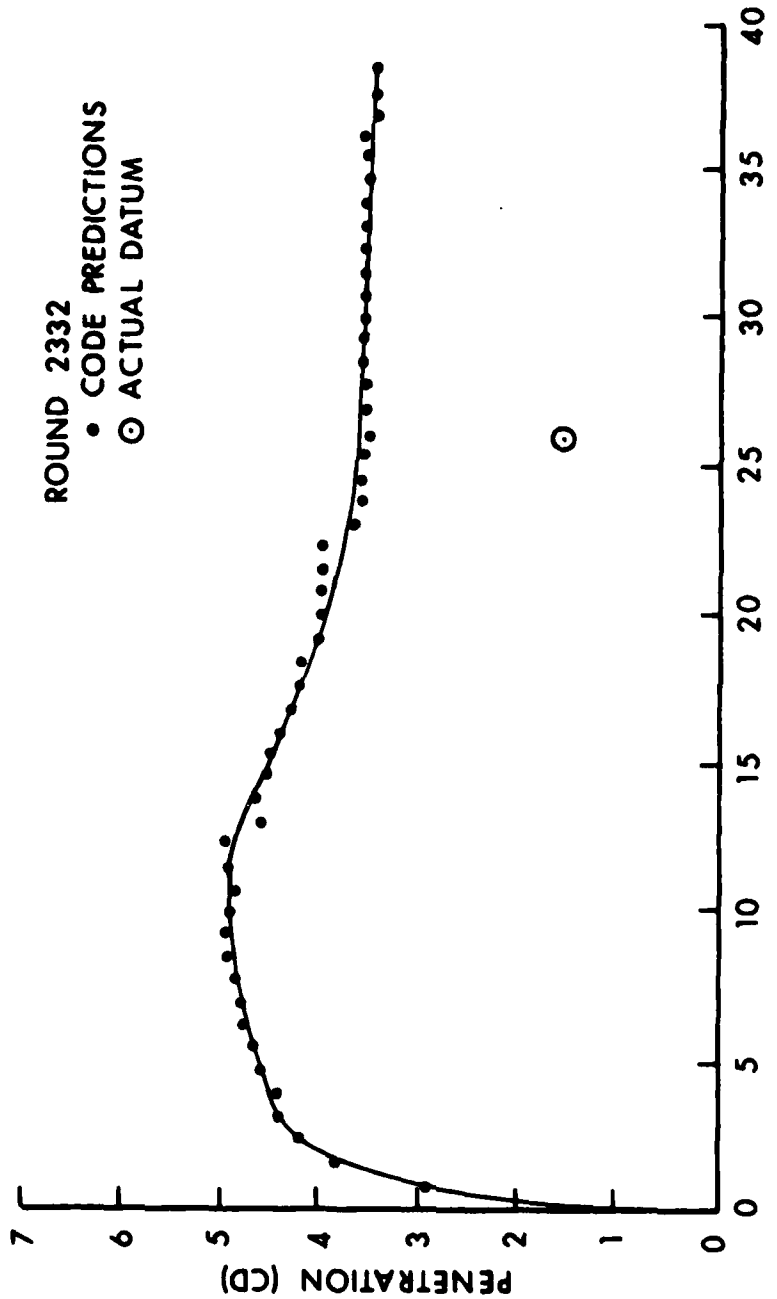

Figure 17. Analysis of Round 2332

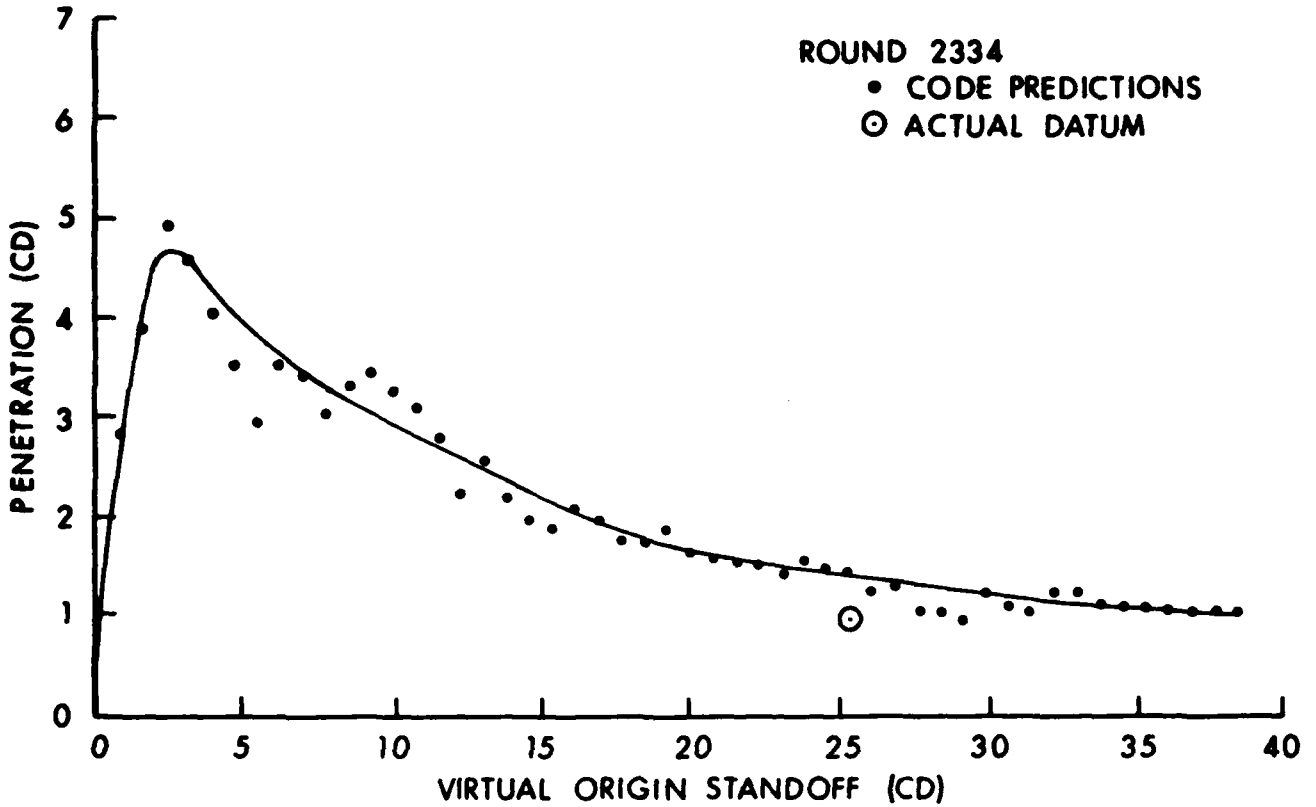

Figure 18. Analysis of Round 2334

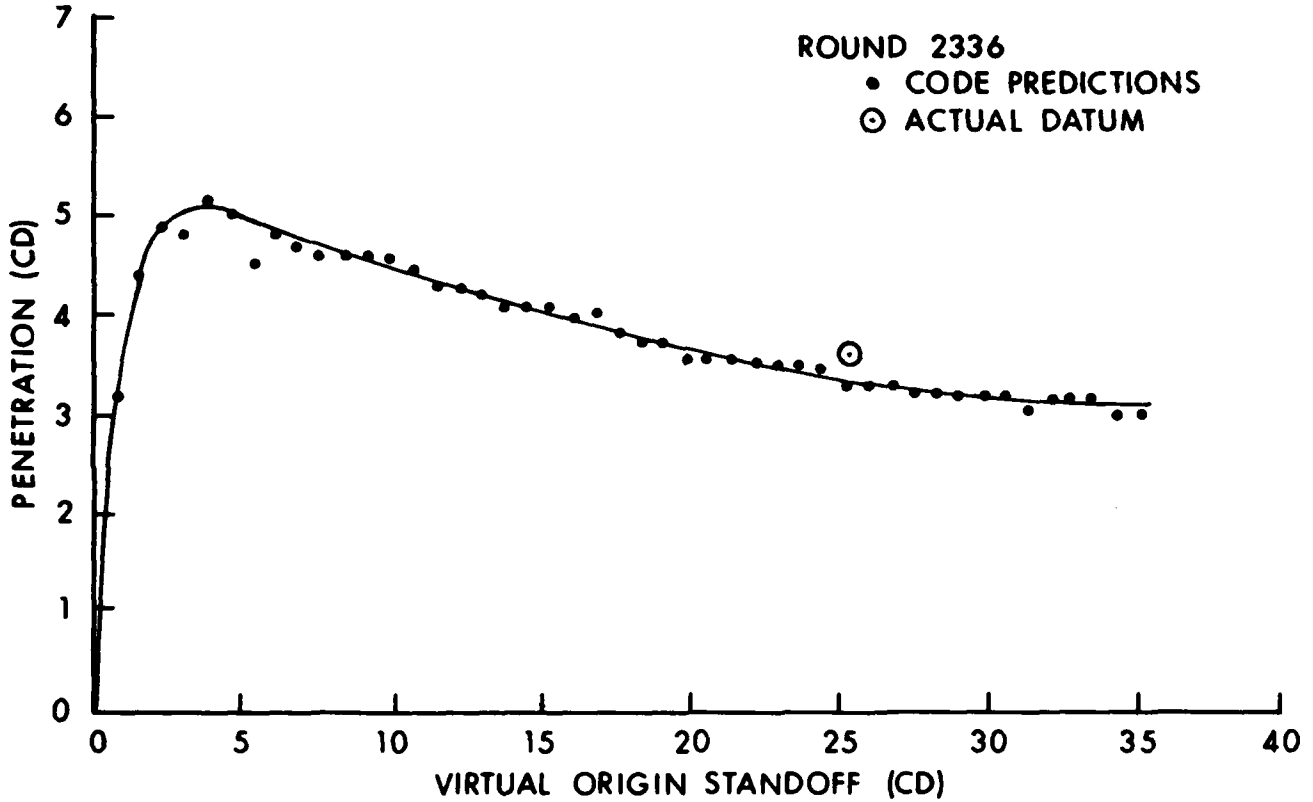

Figure 19. Analysis of Round 2336

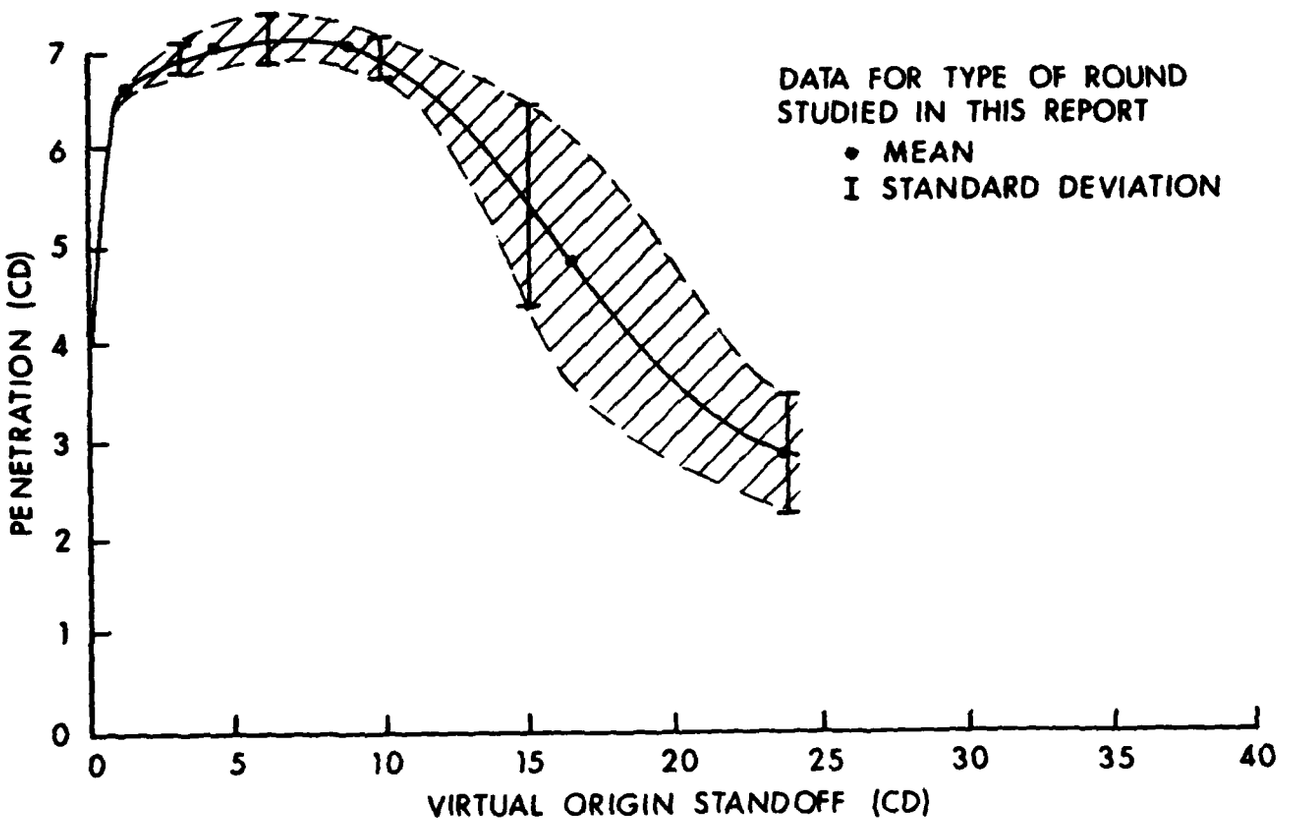

Figure 20. Routine Performance for Type of Round Analyzed

All of the codes's predictions were in reasonable agreement with experiment except for Round 2332. Upon studying this round for possible causes of discrepancy, it was noted that the round uniquely had what shall be called a switchback angular spiral. This falls into the category of abnormal relative drift distributions. Most jets contain drift distributions such that the jet particles spiral in only one direction (either clockwise or counterclockwise) throughout the jet. Figure 5, for example, shows a jet spiralling counterclockwise from jet tip to tail. A switchback angular spiral is one in which one part of the jet spirals in one direction, while the subsequent portion of the jet spirals in the opposite direction. Switchback is thought to be a product of abnormal tilt/drift combinations such that subsequent computation of reference drift might be quite inaccurate. As set forth before, an inaccurate reference extrapolation leads to inaccurate penetration calculations.

Figure 20 shows how the actual weapon routinely performs. In order to test whether PENJET could predict the average penetration at standoffs near the peak performance of the round, a radiograph containing a complete and fully particulated jet would be required for digitization. As mentioned previously, no available radiographs fulfilled these requirements. A radiograph was obtained, however, of a complete jet which was not fully particulated. Though not completely digitizable, the presence of a complete jet greatly facilitated estimation of many jet parameters (e.g. velocity of jet rear, drift with respect to jet rear, and total jet length). By this means, the rear of the jet which was not digitizable could be simulated into particles based on analysis of the radiograph containing the continuous jet rear.

Figure 21 shows the PENJET prediction of the round that includes the jet rear simulation. The actual datum as well as optimum performance for this type of round are included in order to put PENJET calculations in perspective.

The importance of a complete jet at short standoff is shown in Figure 22. The penetration standoff curve for Round 2331 is shown here. Superimposed upon it are curves showing the amount of residual penetration resulting from different fractions of the complete jet. The points at which the curves meet signify that the number of particles producing the superimposed curves are also the same number of particles producing the total residual penetration at that point. For example, PENJET's predictions at 11.5 CD standoff imply that predicting penetration using 40 particles would be just as accurate as using 51 particles. Anything less than 40 particles at that standoff would, however, produce inaccurate results. For the 24 CD standoff at which the round was actually fired, less than 20 digitized particles would be required for an accurate description of penetration. At short standoff, however, even 51 particles do not completely describe the penetration capabilities of Round 2331. Estimates are that below 8 CD standoff, particles beyond particle 51 were also capable of adding to penetration. For better quality rounds, though, as illustrated by Round 2937 in Figure 23, more particles are required even at longer standoffs to accurately describe penetration. For example, more than 50 digitized particles would be required for standoffs out to 25 CD for this particular round.

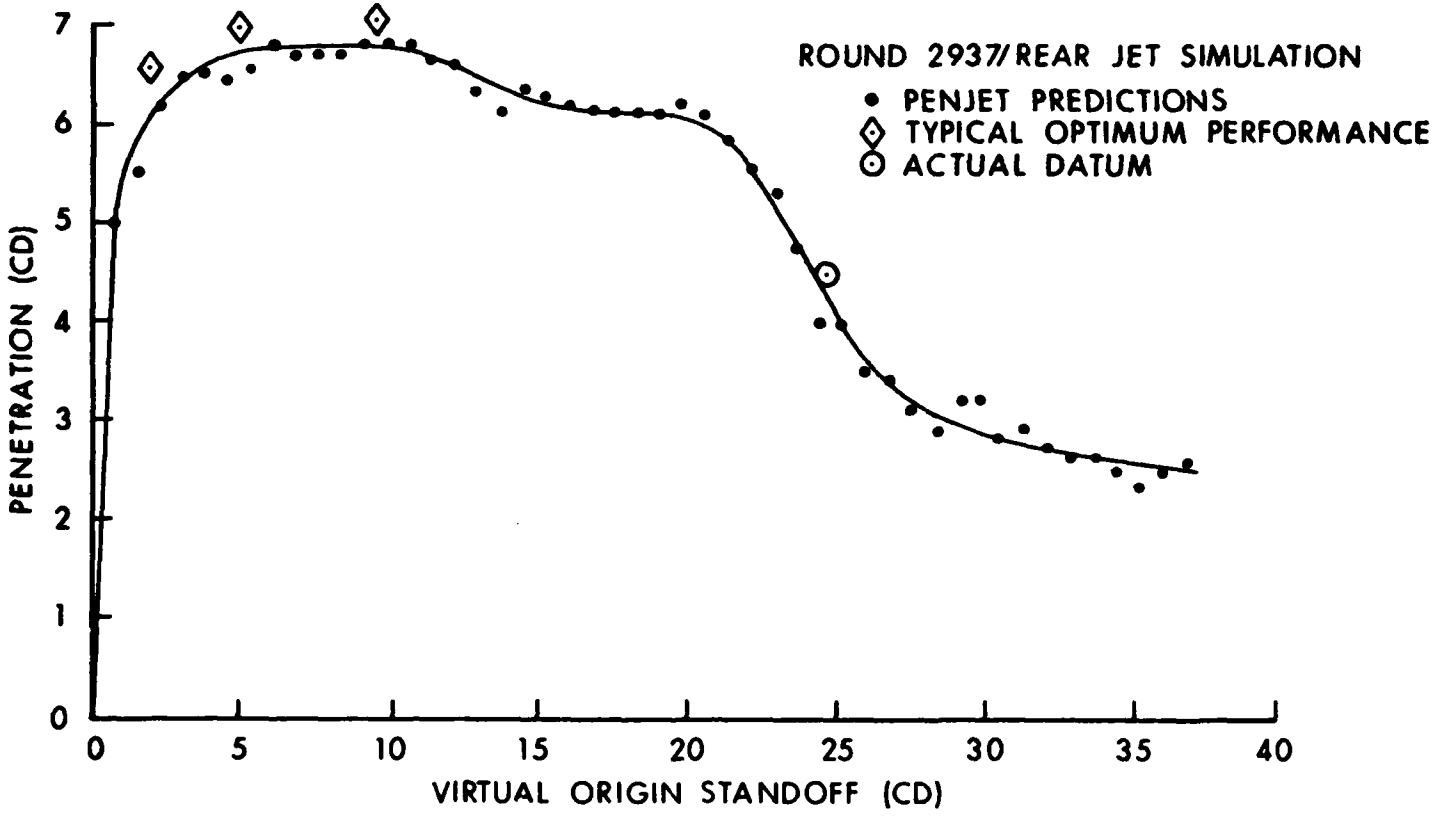

Figure 21. Analysis of Round 2937 with the Included Jet Rear Simulation
Note: Optimum Performance Data Transferred from Figure 20.

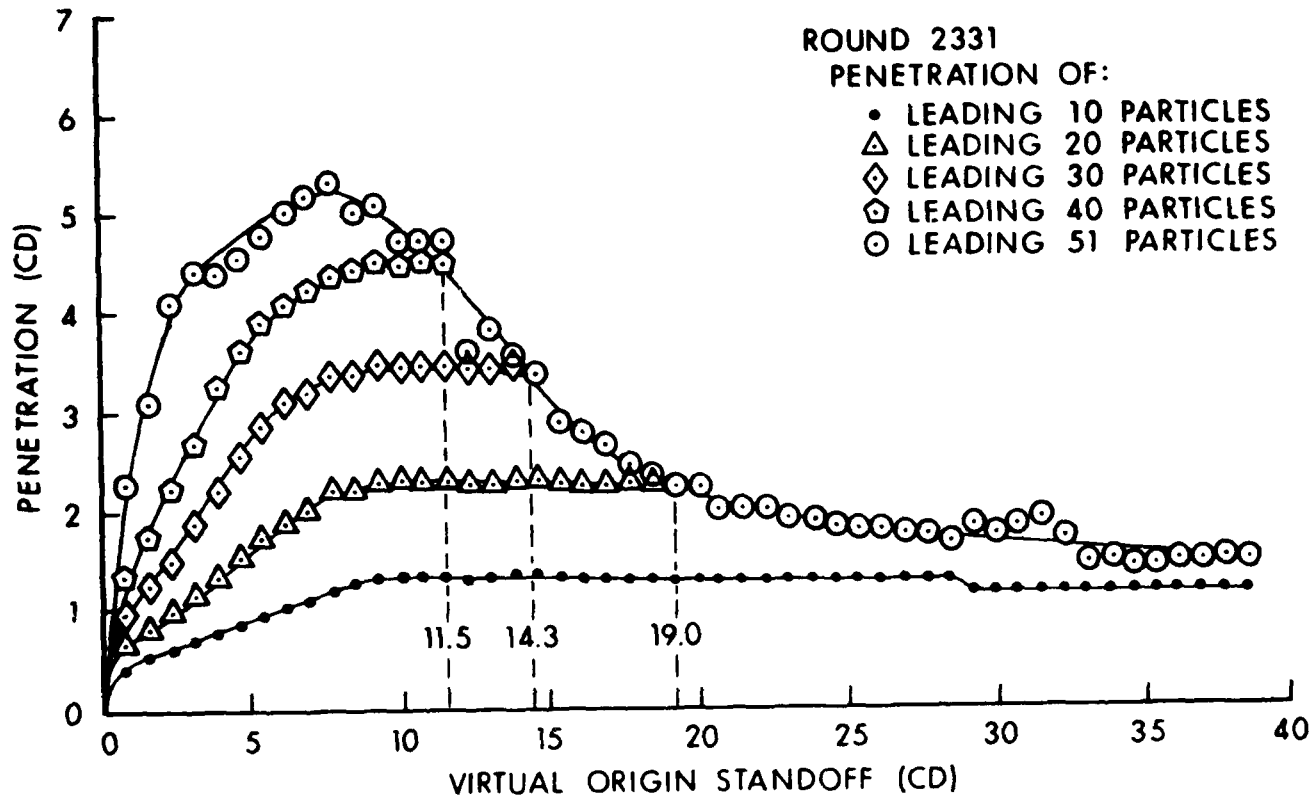

Figure 22. Penetration Capability of Distinct Jet Portions of Round 2331

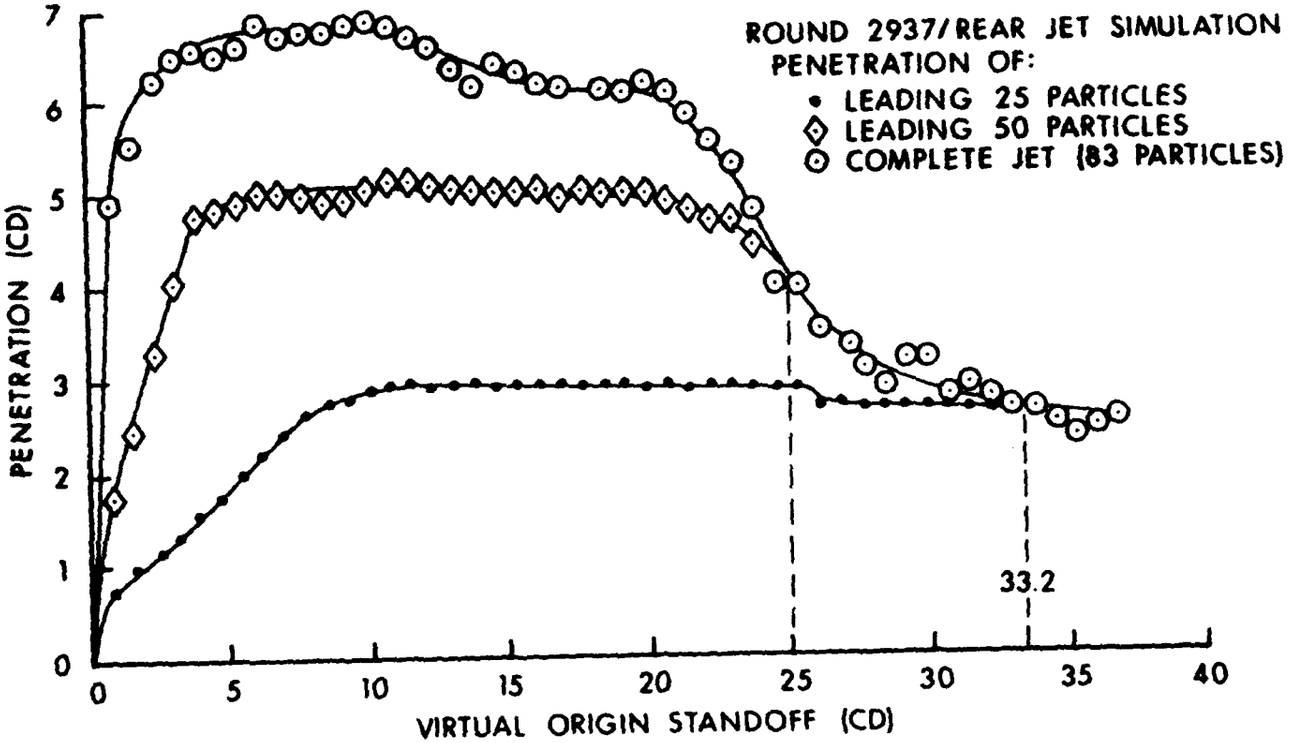

Figure 23. Penetration Capability of Distinct Jet Portions of Round 2937

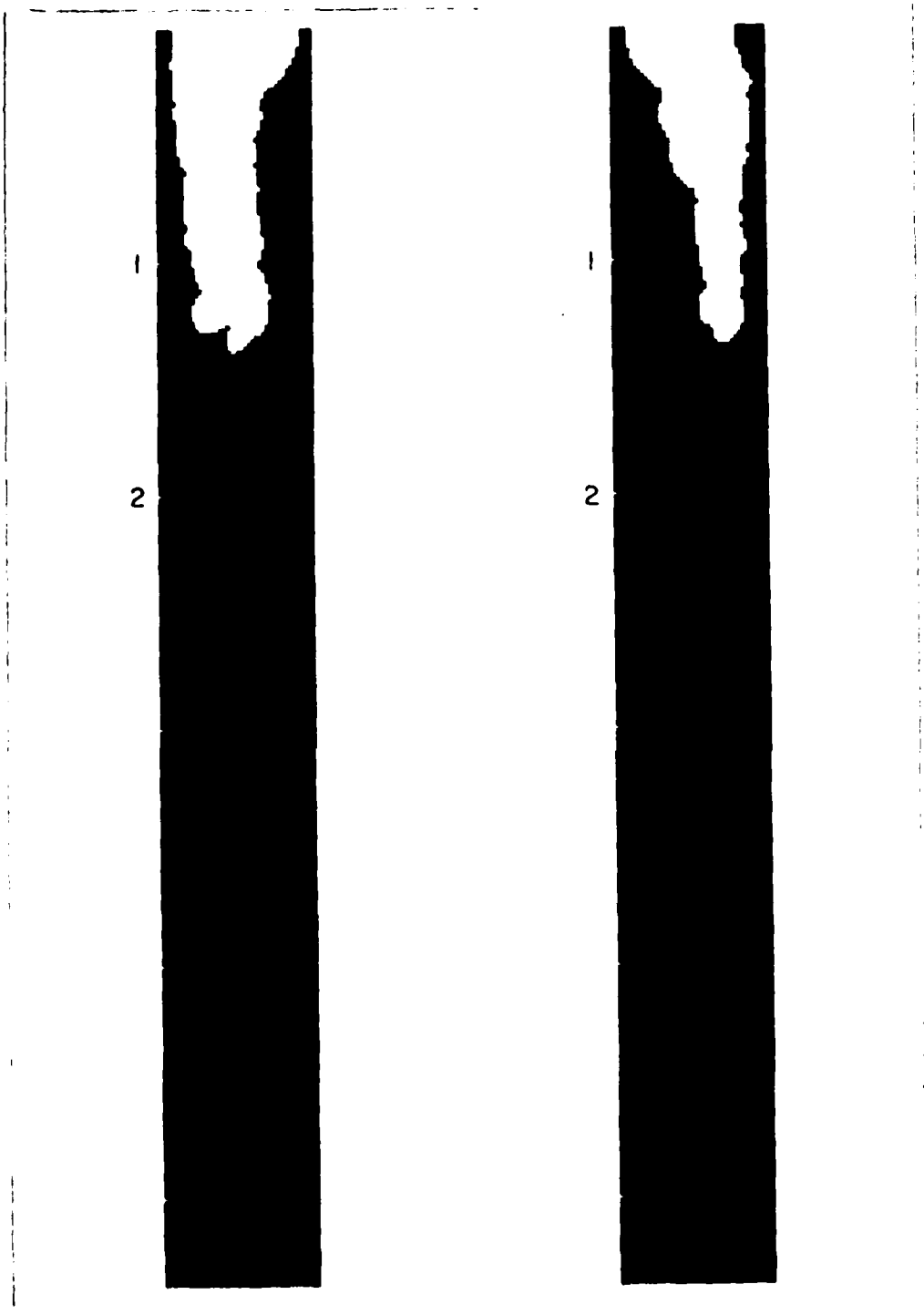

Figure 24. PENJET Predictions of Hole Profile for Round 2334 at 23 CD Standoff. Penetration in Cone Diameters.

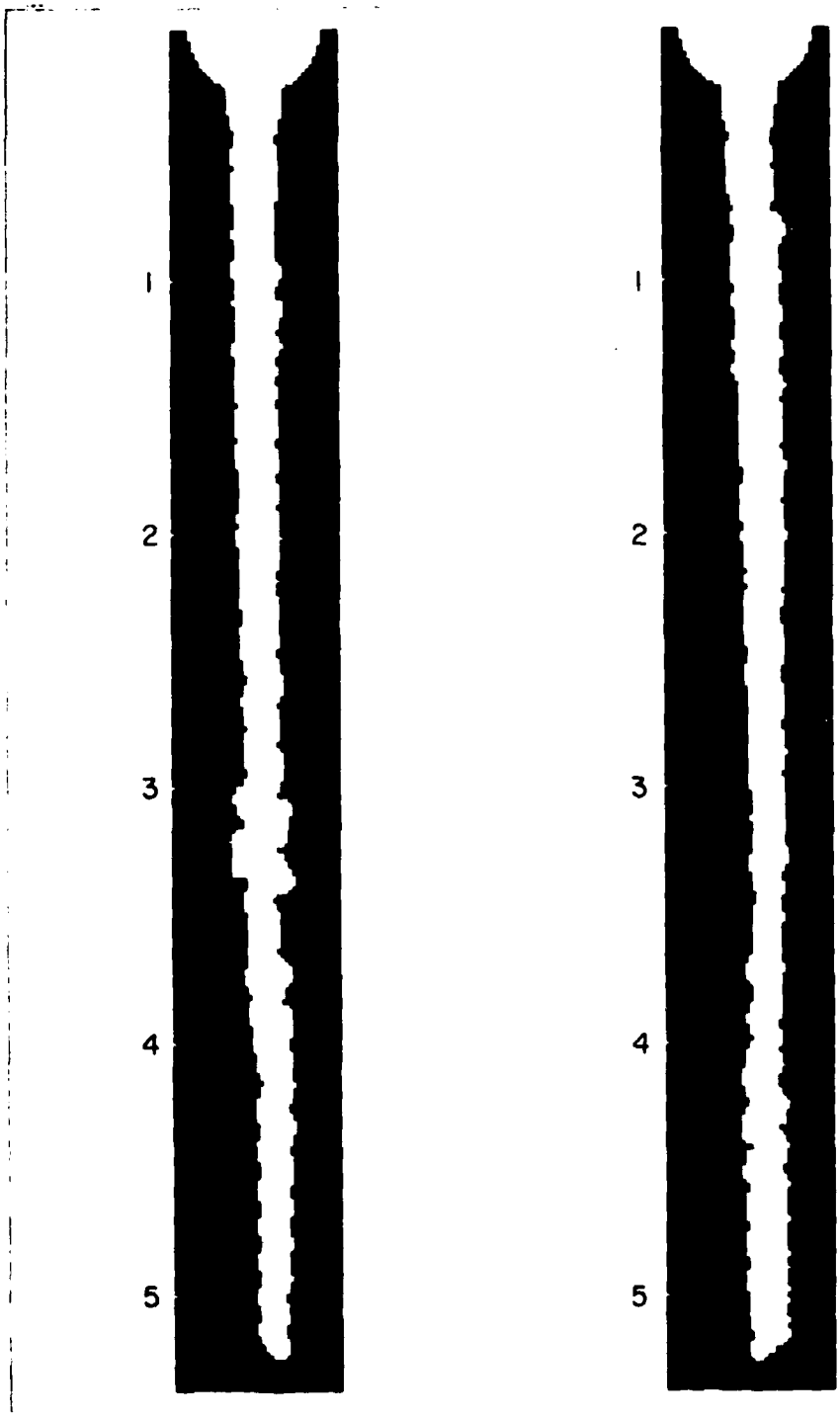

Figure 25. PENJET Predictions of Hole Profile for Round 2937 at 23 CD Standoff. Penetration in Cone Diameters.

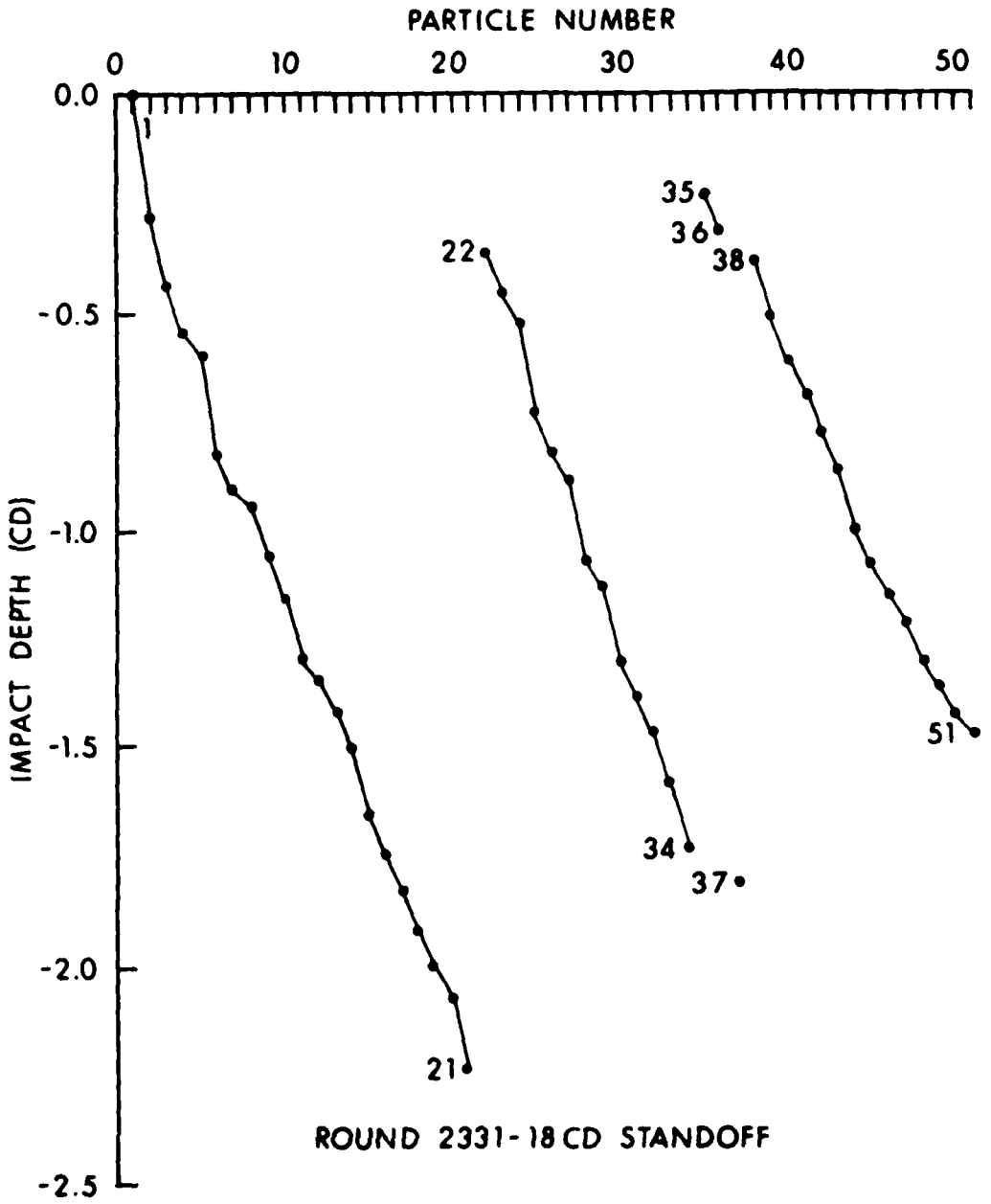

Figure 26. Code Predictions of Rear-Jet Ineffectiveness Due to Side Wall Impacts of Drifting Particles

Figure 27. Orthogonal Views of Projected Hole Profile of Round 2331 at 18 CD Standoff as Predicted by PENJET. Penetration in Cone Diameters.

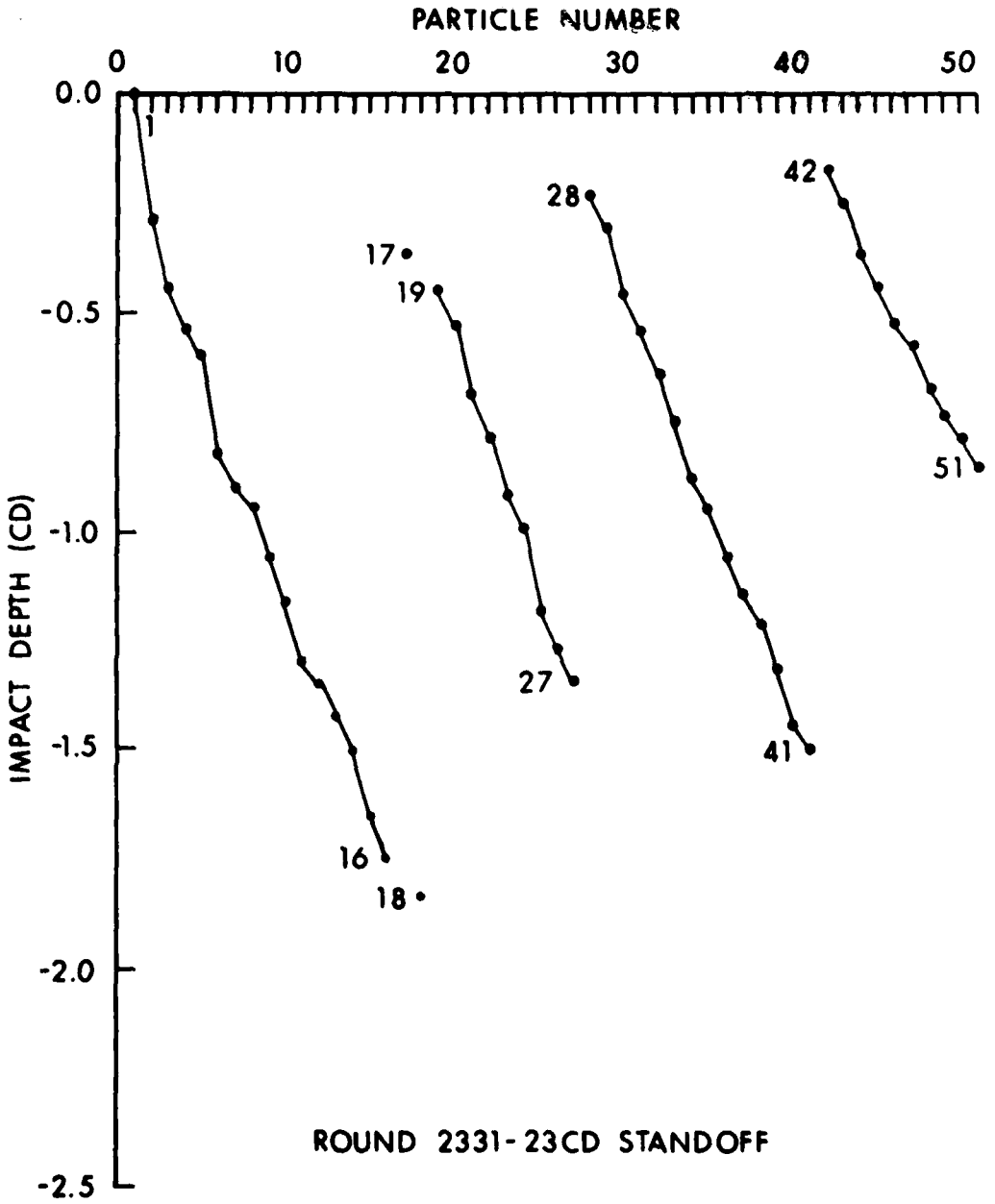

Figure 28. Increase of Side-Wall Impacts Predicted at Longer Standoffs

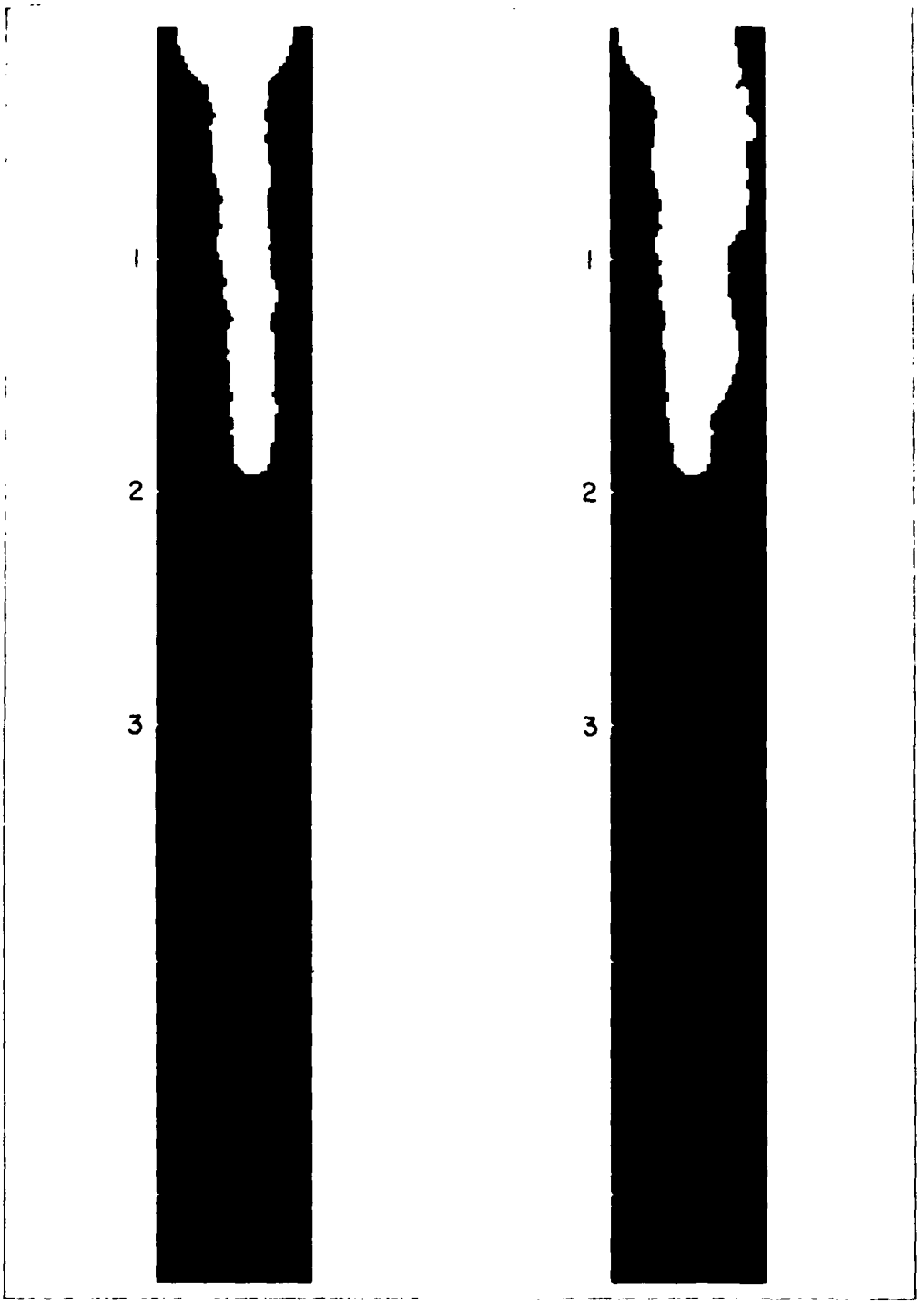

Figure 29. Orthogonal Views of Projected Hole Profile of Round 2331 at 23 CD Standoff as Predicted by PENJET. Penetration in Cone Diameters.

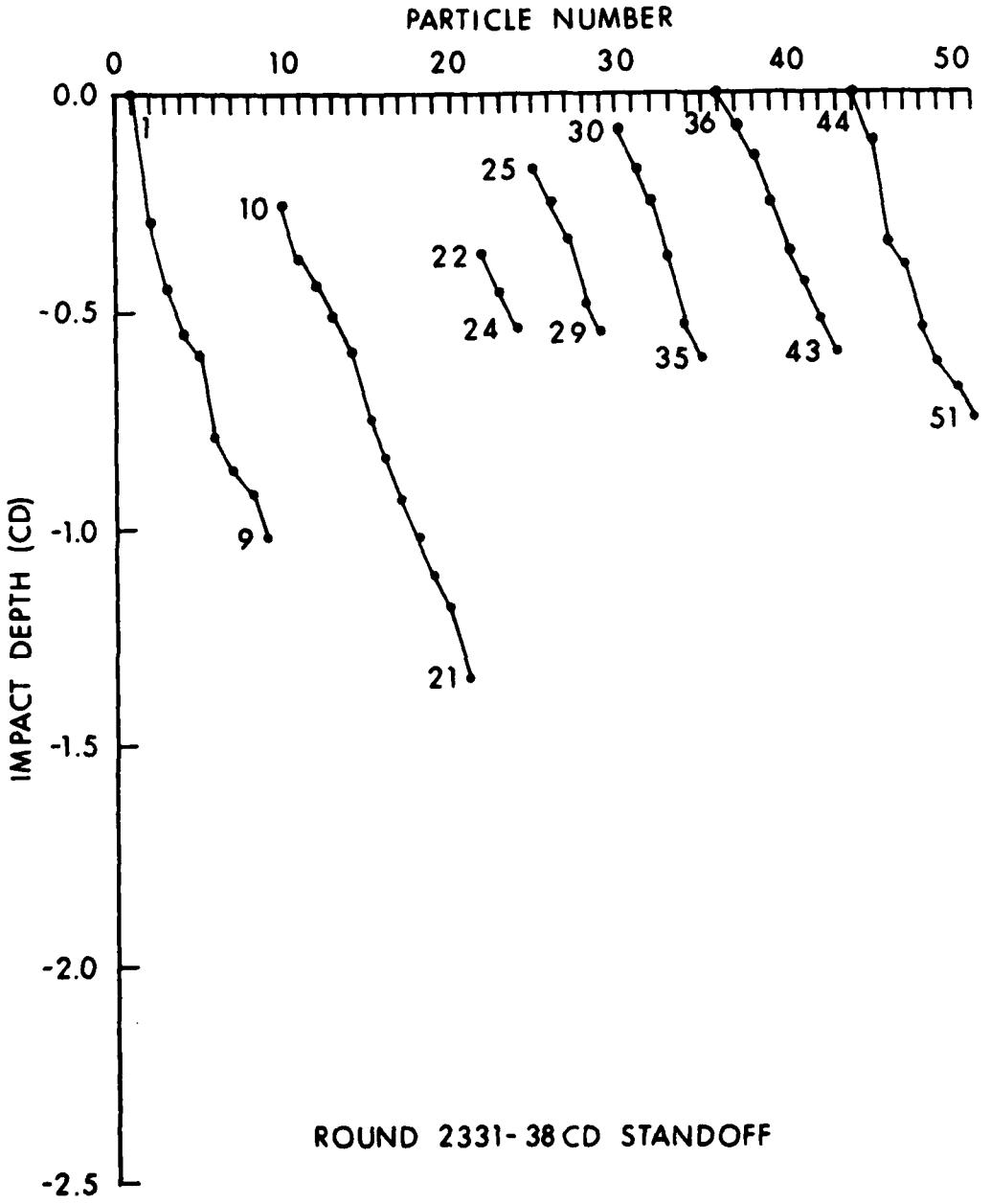

Figure 30. *The Effect of Side Wall Impacts is Not Only to Decrease Penetration, But to Widen Crater.*

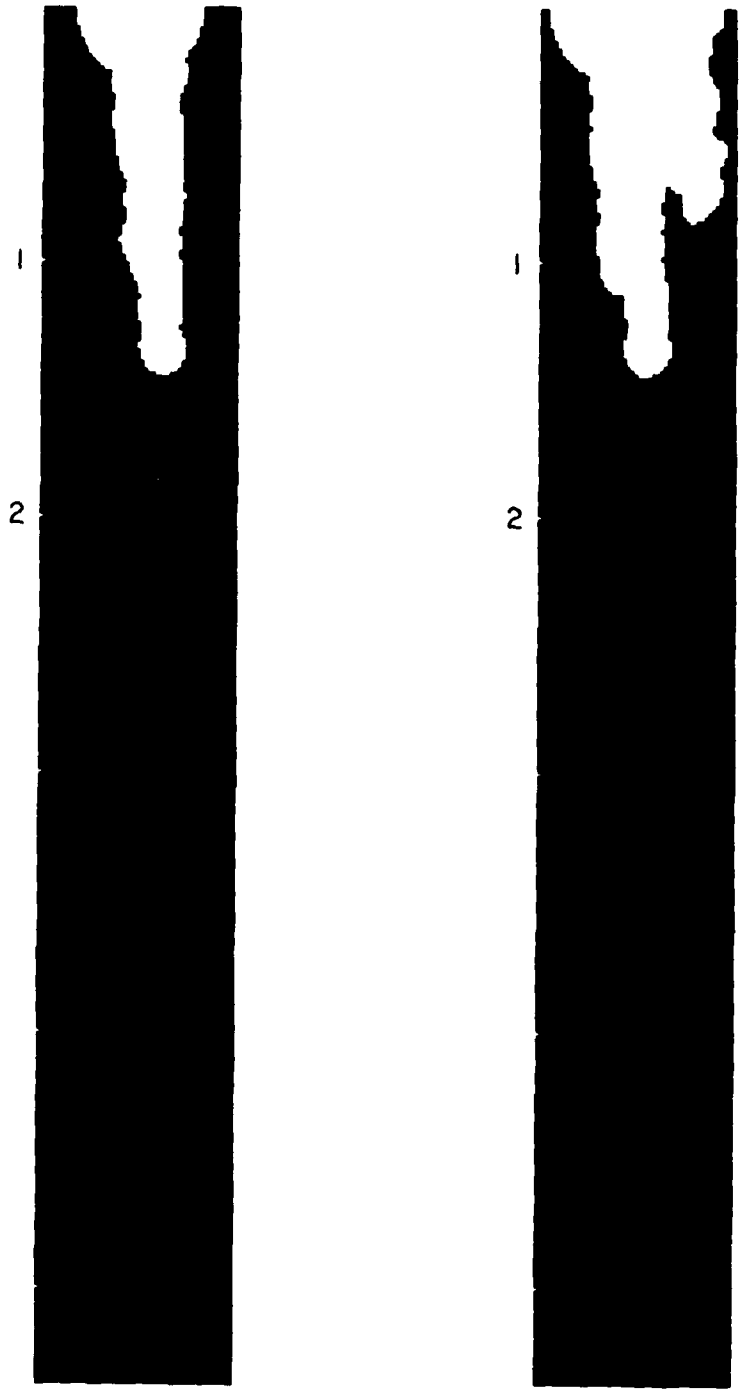

Figure 31. Orthogonal Views of Projected Hole Profile of Round 2331 at 38 CD Standoff as Predicted by PENJET. Penetration in Cone Diameters.

Besides showing a semblance of agreement between code and experiment, Figures 16-19 show that drift alone can easily account for rapid decreases in penetration as is often experienced by rounds at extended standoffs. The process by which penetration is decreased is one of sidewall impacts. This process was briefly mentioned before as a phenomenon which sometimes renders a particle ineffectual. The majority of sidewall impacts, though, are not so oblique as to disrupt penetration; most sidewall impacts go into creating wider hole profiles.

As an example of the devastating effects of drift velocity on jet penetration, a comparison of PENJET's hole profile predictions is shown for two separate rounds in Figures 24 and 25. The plots represent orthogonal views of the target block as described by PENJET. Both sets of calculations were performed at the same standoff (23 CD). The stark contrast of jet performance is noted not only in terms of depth of penetration, but also in terms of crater width. Sidewall impacts do not occur until much later in the penetration process for Round 2937, thus allowing more of the jet to contribute to the overall penetration.

Figure 26 is PENJET's prediction as to where in the hole profile each particle of Round 2331 strikes the target block at 18 CD standoff. Note that particle number is in order of formation. (Jet tip is particle 1.) It is seen that once a particle is blocked from reaching the bottom of the hole, it will usually begin the widening process somewhere up the profile. Subsequent particles try to work their way back down again. This process continues until no jet is left with which to penetrate the target. A plot of the hole profile as generated by PENJET is shown in Figure 27 as two orthogonal views of the target block. Graphs and plots for the same round are shown again at longer standoffs in Figures 28-31. It is seen that penetration is progressively lower because sidewall impacts occur earlier in the penetration process. Consequently, crater diameter progressively increases at longer standoffs. Thus, for Round 2331 at a standoff of 23 CD the total penetration capability of the jet as predicted by PENJET is contained within the first 18 particles.

The profile at 38 CD sharply illustrates the effects of drift velocity on jet penetration. The spread of the particles was so great as to cause the beginnings of a dual crater within 1 CD of the target surface. Thus, the ineffectiveness of the jet rear is seen. Any nondigitized portion of Round 2331 would probably produce its penetration in the vicinity of the particle 51 crater, far from the point of maximum penetration.

Thus, the decreases in penetration as predicted by PENJET are due mainly to the presence of drift velocities among the particles. Drift causes scattering of the particles and eventually, at some critical standoff, elimination of the particles from the crater deepening process via the mechanism of sidewall impacts.

VII. CONCLUSIONS

The ability to compute drift velocities for the particles of a shaped-charge jet is thought to be significant. In its own right, quantification of drift velocity aids in understanding the nature of the nonideal jet. A degree of imperfection may also be placed upon the jet in hopes of classifying a jet with regard to its quality.

The concept of how a jet penetrates is better understood when drift velocity is considered in the penetration picture. The process of sidewall impacts as a hinderance to penetration can be verified by inspection of actual target blocks. This process is reminiscent of the jet cutoff velocity which varies with standoff as proposed by Dipersio, Simon, and Merendino,[3] in that the velocity of the particle striking deepest in the hole profile can be considered a cutoff velocity with respect to jet penetration. Implications here are that a jet could approach ideal penetration had drift velocity not been present. Larger craters would also make jets more insensitive to drift. Weaker targets allow for a wider crater for a given jet particle. Thus, the reduced probability of sidewall impact would allow greater penetration.

Compared to armor, a target of mild steel hydrodynamically should not affect the penetration of a given jet. It will affect penetration, however, when drift velocity is present in the jet. DiPersio and Simon[8] verified this experimentally by firing jets into steel targets of varying hardness. Increasing crater size could alternately be accomplished by means of increasing the jet's energy. If dynamic impact did not induce additional drift in the jet, projecting the round into the target, as is the case under field conditions, should produce greater penetration than the static detonation of the same round. This cannot be verified experimentally, however, due mainly to the complexity of dynamic impact. Besides possessing possible yaw and pitch, the dynamic round is moving with respect to the target during the jet formation process. This relative motion can manifest itself in the form of drift. Dynamically detonated rounds do, however, create wider craters than their static counterparts as expected.

It is suggested that future investigations attempt to analyze drift from the viewpoint of warhead causes. The first step in understanding penetration in terms of drift has hopefully been set forth in this report. The ability to analyze drift as a function of the warhead would be the link between the imperfect warhead and nonideal penetration. Eventually, the possibility exists where warhead tolerances may be used to place limits upon the drift velocity distributions for a round so that penetration might be expressible as a function of charge tolerances.

---

[8] *R. DiPersio, J. Simon, "The Effect of Target Hardness on the Penetration Capability of Shaped-Charge Jets," BRL Report No. 1408, July 1968 (AD 838991).*

ACKNOWLEDGEMENTS

The author wishes to acknowledge the following members and emeriti of the Warhead Mechanics Branch of the U.S. Army Ballistic Research Laboratory for their encouraging support of this analysis: R. Jameson, M. Lampson, and J. Simon for technical consultations; V. Kucher for assistance rendered regarding computer related procedures; M. Scarborough and B. Simmons for having radiographs digitized and ready for use as computer data.

REFERENCE LIST

1. J. Blische, B. Simmons, "A Method for Reducing Data from Radiographs of Shaped-Charge Jets," BRL Report ARBRL-TR-02330, Jun 81 (AD A102770).

2. K. N. Kreyenhagen, J. E. Ferguson, R. R. Randall, J. P. Joyce, "Special Explosive Projectors," Proc. 6th Symposium Hypervelocity Impact, Vol. I (Held Cleveland, Ohio, April 30-May 2, 1963).

3. R. DiPersio, J. Simon, A. Merendino, "Penetration of Shaped-Charge Jets Into Metallic Targets," Ballistic Research Laboratory Report No. 1296, September 1965 (AD 476717).

4. E. Fitzgerald, Particle Waves and Deformation in Crystalline Solids, Interscience Publishers, New York, 1966.

5. J. Kineke, Jr. "An Experimental Study of Crater Formation in Metallic Targets," Proc. 4th Symposium Hypervelocity Impact, Vol. I (Held Eglin AFB, Florida, April 26-28, 1960).

6. G. Weihrauch, "The Behavior of Copper Pins Upon Impacting Various Materials with Velocities Between 50 m/s and 1650 m/s," (Doctoral Thesis) University of Karlsruhe, 1971.

7. J. Simon, R. DiPersio, "Experimental Verification of Standoff Effects on Shaped-Charge Jet Cutoff in Solid Targets," Ballistic Research Laboratory Memorandum No. 1976, May 1969 (AD 854396).

8. R. DiPersio, J. Simon, "The Effect of Target Hardness on the Penetration Capability of Shaped-Charge Jets," BRL Report No. 1408, July 1968 (AD 838991).

APPENDIX A

PROGRAM LISTING

AND

VARIABLE NAME DESCRIPTIONS

The drift velocity and PENJET programs were written as direct additions to Blische's and Simmons' radiograph-data-reduction program (Reference 1) introduced in BRL Report 2330. Therefore, a listing of PENJET must be accompanied by the program which generates data for use within PENJET. The right-hand edge of the listing reveals where the statements in question originated. "GETREADY" are nonexecutable statements required for BRL Report 2330, PENJET, or both. "BRL 2330" is the bulk of Blische's and Simmons' program with minor revisions for PENJET applicability. "JETBREAK" is a revision for jet breakup calculations. "DRIFT" is used to calculate the drift distribution for a round while "PENJET" is the jet penetration program. The program is written in FORTRAN IV. An explanation of the program variables is inserted after the program listing.

It should be noted that even though Blische's and Simmons' program is versatile enough to run using data from only two X-ray flash exposures, PENJET is geared to the standard 3 flash setup and will require modifications to run otherwise.

Explanation for the program variable names found in the program segment identified as "BRL 2330" can be found in BRL Report 2330 (Reference 1). Should one wish to identify variables within the program segment "GETREADY," the other segments should be consulted, as all "GETREADY" variables are contained within other segments. All other significant variables are listed under their appropriate program segment.

```
      PROGRAM MAIN(INPUT,OUTPUT,TAPE5=INPUT,TAPE6=OUTPUT)                GETREADY    2
      DIMENSION S1(100),S2(100),S3(100),VOL(100),XL(100),DIA(100),       GETREADY    3
     1V1(100),V2(100),V3(100),VEL(100),XMASS(100),XKE(100),SUMKE(100),   GETREADY    4
     2ELOD(100),XXL(100),SUML(100),IX(6),IY(6),ZX(6),ZY(6),              GETREADY    5
     3BREAK(100),SUMMAS(100),B(10000),DA(3),DB(3),XMAG(3)               GETREADY    6
      DIMENSION AA(2,3),CC(2),RR(500),AF(500),STG(2),TT(2)               GETREADY    7
      DIMENSION DS(3),THETA(100),VETRAV(100),T1(100),T2(100),T3(100),    GETREADY    8
     1          REF(3)                                                   GETREADY    9
      DIMENSION AVST(100),BETA(100)                                      GETREADY   10
      DIMENSION PHI(100),PHIR(100),VTABS(100)                            GETREADY   11
      DIMENSION EPS(6,100),WT(6)                                         GETREADY   12
      DIMENSION VX(100),VY(100)                                          GETREADY   13
      DIMENSION R(2)                                                     GETREADY   14
      DIMENSION VTB(100)                                                 GETREADY   15
      DIMENSION T(100),X(100),Y(100),Z(100),U(100),RADIUS(100),PEN(100), GETREADY   16
     1          HVOL(100)                                                GETREADY   17
      DIMENSION NCC(100)                                                 GETREADY   18
      DIMENSION ZSUB(100),PENT(100),PENMAX(100)                          GETREADY   19
      DIMENSION V(100,3),VM(100),VA(100,3),VAM(100),VP(100,3),VPM(100),  GETREADY   20
     1          RGRAD(100,3),RGM(100),GRAD(100,3),AR(100,3),PR(100,3)    GETREADY   21
      DIMENSION RL(100),RVEL(100)                                        GETREADY   22
      DIMENSION OL(100),XVAL(100),TAU(100)                               GETREADY   23
      DIMENSION TP(100),RD(100)                                          GETREADY   24
      REAL KD12,KD23,KD13                                                GETREADY   25
      REAL INCR                                                          GETREADY   26
      DIMENSION SA(10),SB(10),SC(10),SD(10),SE(10),SF(10),SL1(10),       GETREADY   27
     1SL2(10),SL3(10),ST(10),L1(100),L2(100),L3(100)                     GETREADY   28
      DIMENSION P(100),TOTP(100),SUMDIA(100),SUMLEN(100),XDIA(100),DELV( GETREADY   29
     1100),SDELV(100),SUMDEL(100)                                        GETREADY   30
      DIMENSION XVOL(3,100)                                              GETREADY   31
      DIMENSION AZ(100,100)                                              GETREADY   32
      DATA SA(1),SA(2),SA(3)/10HVELOCITY (,10HMM/MICROSE,3HC)>/          GETREADY   33
      DATA SB(1),SB(2),SB(3)/10HCUMULATIVE,10H MASS (GRA,4HMS)>/         GETREADY   34
      DATA SC(1),SC(2),SC(3),SC(4)/10HPOSITION A,10HLONG JET L,1CHENGTH  GETREADY   35
     1(MM),1H>/                                                          GETREADY   36
      DATA SD(1),SD(2),SD(3)/10HCUMULATIVE,10H K.E. (JOU,5HLES)>/        GETREADY   37
      DATA SE(1),SE(2),SE(3),SE(4)/10HDISTANCE F,10HROM CHARGE,1CH BASE  GETREADY   38
     1(MM),1H>/                                                          GETREADY   39
      DATA SF(1),SF(2),SF(3)/10HBREAK-UP T,10HIME (MICRO,5HSEC)>/        GETREADY   40
      DATA SL1(1)/8HFLASH 1>/                                            GETREADY   41
      DATA SL2(1)/8HFLASH 2>/                                            GETREADY   42
      DATA SL3(1)/8HFLASH 3>/                                            GETREADY   43
      DATA MPA,MPAR,MPART,MCO,MCON,MCONT/4HPART,4HICUL,4HATED,4H CON,4HT GETREADY   44
     1INU,4HOUS /                                                        GETREADY   45
    1 FORMAT(3I5,F5.2,6F10.5)                                           BRL2330    2
    2 FORMAT(7F10.5)                                                    BRL2330    3
    6 FORMAT(8F10.5)                                                    BRL2330    4
   21 FORMAT(2I5)                                                       BRL2330    5
   30 FORMAT(12I5,2X,I1,2X,3I5)                                         BRL2330    6
      READ(5,21) ICASES,LCL                                             BRL2330    7
      IF(EOF(5)) 23,23                                                  BRL2330    8
   23 DO 500 I3=1,ICASES                                                BRL2330    9
   22 READ(5,1)NROUND,NPART,NFLASH,RHC,(XMAG(I),I=1,3),FLASH1,FLASH2,   BRL2330   10
     1FLASH3                                                            BRL2330   11
      IF(EOF(5)) 24,24                                                  BRL2330   12
   24 ENCODE(21,20,ST(1)) NROUND                                        BRL2330   13
   20 FORMAT(10HROUND NUMB,4HER  ,I5,2H >)                              BRL2330   14
      READ(5,2) FOCUS1,FOCUS2,FOCUS3,F1A,F2A,F3A,F4A                    BRL2330   15
      IF(EOF(5)) 25,26                                                  BRL2330   16
   25 READ(5,6) F1B,F2B,F3B,F4B,F1C,F2C,F3C,F4C                         BRL2330   17
      IF(EOF(5)) 26,26                                                  BRL2330   18
   26 RO=RHO                                                            BRL2330   19
      IF(LCL.NE.1) GO TO 29                                             BRL2330   20
```

```
      RHO=0.                                                                BRL2330    21
C                                                                           BRL2330    22
C     ROUND INFORMATION CARD NEXT                                           BRL2330    23
   29 PRINT 5                                                               BRL2330    24
      PRINT 3, NROUND,RHO,(XMAG(N),N=1,3),FOCUS1,FOCUS2,FOCUS3,FLASH1,FL    BRL2330    25
     1ASH2,FLASH3                                                           BRL2330    26
    3 FORMAT(/////,20X,'ROUND NUMBER  ',I5,//,20X,'LINER DENSITY(GM/CC)-   BRL2330    27
     1 ',F4.1,/,20X,'MAGNIFICATION FACTOR-',3F9.5,/,20X,'DISTANCE FROM L    BRL2330    28
     2INER BASE TO FOCAL POINT(MM)',/,25X,'FLASH 1- ',F6.1,/,25X,'FLASH     BRL2330    29
     32- ',F6.1,/,25X,'FLASH 3- ',F6.1,/,20X,'DELAY TIMES (MICROSEC)',/,    BRL2330    30
     425X,'FLASH 1- ',F6.1,/,25X,'FLASH 2- ',F6.1,/,25X,'FLASH 3- ',F6.1    BRL2330    31
     5)                                                                     BRL2330    32
      RHO=RO                                                                BRL2330    33
      PRINT 5                                                               BRL2330    34
    5 FORMAT(1H1)                                                           BRL2330    35
      PRINT 4                                                               BRL2330    36
    4 FORMAT(21X,'PARTICLE   AVG. VELOCITY   TOTAL JET     BREAK-UP',/,2    BRL2330    37
     12X,'NUMBER',4X,'(MM/MICROSEC)',3X,'LENGTH(MM)',3X,'(MICROSEC)',/)     BRL2330    38
      PI=3.14159                                                            BRL2330    39
      DO 150 I=1,NFLASH                                                     BRL2330    40
      DO 149 J=1,NPART                                                      BRL2330    41
      READ(5,30)(IX(K),IY(K),K=1,6),L,IFILM,IROUND,IPART                    BRL2330    42
      IF(EOF(5)) 32,32                                                      BRL2330    43
   32 DO 35 M=1,6                                                           BRL2330    44
      ZX(M)=FLOAT(IX(M))/15.5906                                            BRL2330    45
   35 ZY(M)=FLOAT(IY(M))/15.5906                                            BRL2330    46
      AZ(I,J)=((ZY(2)+ZY(5))/2.)*XMAG(I)                                    BRL2330    47
      IF(ZX(1).EQ.ZX(2)) GO TO 40                                           BRL2330    48
      R1=.5*SQRT((ZX(1)-ZX(6))**2+(ZY(1)-ZY(6))**2)*XMAG(I)                 BRL2330    49
      R2=.5*SQRT((ZX(2)-ZX(5))**2+(ZY(2)-ZY(5))**2)*XMAG(I)                 BRL2330    50
      R3=.5*SQRT((ZX(3)-ZX(4))**2+(ZY(3)-ZY(4))**2)*XMAG(I)                 BRL2330    51
      P1X=(ZX(1)+ZX(6))/2.                                                  BRL2330    52
      P1Y=(ZY(1)+ZY(6))/2.                                                  BRL2330    53
      P2X=(ZX(3)+ZX(4))/2.                                                  BRL2330    54
      P2Y=(ZY(3)+ZY(4))/2.                                                  BRL2330    55
      P3X=(ZX(2)+ZX(5))/2.                                                  BRL2330    56
      P3Y=(ZY(2)+ZY(5))/2.                                                  BRL2330    57
      XH1=SQRT((P1X-P3X)**2+(P1Y-P3Y)**2)*XMAG(I)                           BRL2330    58
      XH2=SQRT((P3X-P2X)**2+(P3Y-P2Y)**2)*XMAG(I)                           BRL2330    59
      P1Z=P1X                                                               BRL2330    60
      P1X=P2X                                                               BRL2330    61
      GOTO 45                                                               BRL2330    62
   40 P1X=ZX(1)                                                             BRL2330    63
   45 IF(L.EQ.2) GOTO 55                                                    BRL2330    64
      IF(L.EQ.3) GOTO 65                                                    BRL2330    65
      IF(IFILM.EQ.2) GO TO 47                                               BRL2330    66
      IF(IFILM.EQ.3) GO TO 48                                               BRL2330    67
      IF(IFILM.EQ.4) GO TO 49                                               BRL2330    68
      S1(J)=FOCUS1-(F1A-P1X)*XMAG(I)                                        BRL2330    69
      GO TO 15                                                              BRL2330    70
   47 S1(J)=FOCUS1-(F2A-P1X)*XMAG(I)                                        BRL2330    71
      GO TO 15                                                              BRL2330    72
   48 S1(J)=FOCUS1+(F3A+P1X)*XMAG(I)                                        BRL2330    73
      GO TO 15                                                              BRL2330    74
   49 S1(J)=FOCUS1+(F4A+P1X)*XMAG(I)                                        BRL2330    75
   15 IF(ZX(1).EQ.ZX(2)) GO TO 50                                           BRL2330    76
      L1(J)=0                                                               BRL2330    77
      GOTO 75                                                               BRL2330    78
   50 L1(J)=1                                                               BRL2330    79
      GOTO 80                                                               BRL2330    80
   55 IF(IFILM.EQ.2) GO TO 57                                               BRL2330    81
      IF(IFILM.EQ.3) GO TO 58                                               BRL2330    82
      IF(IFILM.EQ.4) GO TO 59                                               BRL2330    83
      S2(J)=FOCUS2-(F1B-P1X)*XMAG(I)                                        BRL2330    84
```

```
      GO TO 16                                                          BRL2330    85
   87 S2(J)=FOCUS2-(F2B-P1X)*XMAG(I)                                    BRL2330    86
      GO TO 16                                                          BRL2330    87
   88 S2(J)=FOCUS2+(F3B+P1X)*XMAG(I)                                    BRL2330    88
      GO TO 16                                                          BRL2330    89
   89 S2(J)=FOCUS2+(F4B+P1X)*XMAG(I)                                    BRL2330    90
   16 V1(J)=(S2(J)-S1(J))/(FLASH2-FLASH1)                               BRL2330    91
      IF(ZX(1).EQ.ZX(2)) GO TO 60                                       BRL2330    92
      L2(J)=0                                                           BRL2330    93
      GOTO 75                                                           BRL2330    94
   60 L2(J)=1                                                           BRL2330    95
      GOTO 80                                                           BRL2330    96
   65 IF(NFLASH.EQ.2) GOTO 80                                           BRL2330    97
      IF(IFILM.EQ.2) GO TO 67                                           BRL2330    98
      IF(IFILM.EQ.3) GO TO 68                                           BRL2330    99
      IF(IFILM.EQ.4) GO TO 69                                           BRL2330   100
      S3(J)=FOCUS3-(F1C-P1X)*XMAG(I)                                    BRL2330   101
      GO TO 17                                                          BRL2330   102
   67 S3(J)=FOCUS3-(F2C-P1X)*XMAG(I)                                    BRL2330   103
      GO TO 17                                                          BRL2330   104
   68 S3(J)=FOCUS3+(F3C+P1X)*XMAG(I)                                    BRL2330   105
      GO TO 17                                                          BRL2330   106
   69 S3(J)=FOCUS3+(F4C+P1X)*XMAG(I)                                    BRL2330   107
   17 V2(J)=(S3(J)-S2(J))/(FLASH3-FLASH2)                               BRL2330   108
      V3(J)=(S3(J)-S1(J))/(FLASH3-FLASH1)                               BRL2330   109
      IF(ZX(1).EQ.ZX(2)) GO TO 70                                       BRL2330   110
      L3(J)=0                                                           BRL2330   111
      GOTO 75                                                           BRL2330   112
   70 L3(J)=1                                                           BRL2330   113
      GOTO 80                                                           BRL2330   114
   75 VOL(J)= VOL(J)+(PI*XH1/3.*(R1**2+R1*R2+R2**2)+PI*XH2/3.*(R2**2+R2* BRL2330   115
     1R3+R3**2))                                                        BRL2330   116
      P1X=P1Z                                                           BRL2330   117
      XVOL(I,J)= PI*XH1/3.*(R1**2+R1*R2+R2**2)+PI*XH2/3.*(R2**2+R2*R3+  BRL2330   118
     1R3**2)                                                            BRL2330   119
      XVOL(I,J)= XVOL(I,J)*.001*RHO                                     BRL2330   120
      XL(J)=XL(J)+SQRT((P1X-P2X)**2+(P1Y-P2Y)**2)*XMAG(I)               BRL2330   121
      DIA(J)=DIA(J)+2.*R2                                               BRL2330   122
   80 CONTINUE                                                          BRL2330   123
      IF(I.LT.NFLASH) GOTO 149                                          BRL2330   124
      IF(NFLASH.EQ.2) GOTO 85                                           BRL2330   125
      IF(L1(J).EQ.1.AND.L2(J).EQ.1.AND.L3(J).EQ.1) GO TO 149            BRL2330   126
      IF(L1(J).EQ.0.AND.L2(J).EQ.0.AND.L3(J).EQ.0) GO TO 90             BRL2330   127
      IF(L2(J).EQ.1.AND.L3(J).EQ.1) GO TO 95                            BRL2330   128
      IF(L1(J).EQ.1.AND.L3(J).EQ.1) GO TO 95                            BRL2330   129
      IF(L1(J).EQ.1.AND.L2(J).EQ.1) GO TO 95                            BRL2330   130
      IF(L2(J).EQ.0.AND.L3(J).EQ.0) GO TO 100                           BRL2330   131
      IF(L1(J).EQ.0.AND.L3(J).EQ.0) GO TO 100                           BRL2330   132
      IF(L1(J).EQ.0.AND.L2(J).EQ.0) GO TO 100                           BRL2330   133
   85 IF(L1(J).EQ.1.AND.L2(J).EQ.1) GO TO 149                           BRL2330   134
      IF(L1(J).EQ.0.AND.L2(J).EQ.0) GO TO 100                           BRL2330   135
      IF(L1(J).EQ.0.OR.L2(J).EQ.0) GO TO 95                             BRL2330   136
   90 XMASS(J)=VOL(J)*.001/3.*RHO                                       BRL2330   137
      XL(J)=XL(J)/3.                                                    BRL2330   138
      DIA(J)=DIA(J)/3.                                                  BRL2330   139
      GOTO 149                                                          BRL2330   140
   95 XMASS(J)=VOL(J)*.001*RHO                                          BRL2330   141
      GOTO 149                                                          BRL2330   142
  100 XMASS(J)=VOL(J)*.001/2.*RHO                                       BRL2330   143
      XL(J)=XL(J)/2.                                                    BRL2330   144
      DIA(J)=DIA(J)/2.                                                  BRL2330   145
  149 CONTINUE                                                          BRL2330   146
  150 CONTINUE                                                          BRL2330   147
C                                                                       JETBREAK    1
```

```
C     BROK IS THE NUMBER OF JET PARTICLES THAT HAVE PARTICULATED AS OF   JETBREAK    2
C     EXPOSURE TIMES 1, 2, AND 3 RESPECTIVELY.  TDLAY IS THE DELAY TIME  JETBREAK    3
C     BETWEEN DETONATION AND JET FORMATION (MICROSEC).                   JETBREAK    4
C                                                                        JETBREAK    5
      READ(5,*) BROK1,BROK2,BROK3,TDLAY                                  JETBREAK    6
      PZ=BROK1+BROK2+BROK3                                               JETBREAK    7
      TZ=FLASH1+FLASH2+FLASH3                                            JETBREAK    8
      PBYTZ=BROK1*FLASH1+BROK2*FLASH2+BROK3*FLASH3                       JETBREAK    9
      PBYPZ=BROK1**2+BROK2**2+BROK3**2                                   JETBREAK   10
      Z1=(PBYTZ-(PZ*TZ/3.))/(PBYPZ-(PZ**2/3.))                          JETBREAK   11
      PBAR=PZ/3.                                                         JETBREAK   12
      TAVG=TZ/3.                                                         JETBREAK   13
      DO 170 N=1,NPART                                                   BRL2330   148
      IF(NFLASH.EQ.2)GOTO 155                                            BRL2330   149
      VEL(N)=(V1(N)+V2(N)+V3(N))/3.*.1                                   BRL2330   150
      GOTO 160                                                           BRL2330   151
  155 VEL(N)=V1(N)*.1                                                    BRL2330   152
  160 SUML(N)=XL(N)+SUML(N-1)                                            BRL2330   153
      SUMMAS(N)=XMASS(N)+SUMMAS(N-1)                                     BRL2330   154
      ELOD(N)=XL(N)/DIA(N)                                               BRL2330   155
      VEL(N)=VEL(N)*10.                                                  BRL2330   156
      XKE(N)=.5*XMASS(N)*.001*(VEL(N)*1000.)**2                          BRL2330   157
      SUMKE(N)=XKE(N)+SUMKE(N-1)                                         BRL2330   158
      P(N)=VEL(N)*XMASS(N)                                               BRL2330   159
      TOTP(N)=P(N)+TOTP(N-1)                                             BRL2330   160
      SUMDIA(N)=SUMDIA(N-1)+DIA(N)                                       BRL2330   161
      BREAK(N)=TAVG+Z1*(N-PBAR)-TDLAY                                    JETBREAK   14
      GOTO 170                                                           BRL2330   162
  165 BREAK(1)=0.0                                                       BRL2330   163
  170 PRINT 171, N,VEL(N),SUML(N),BREAK(N)                               BRL2330   164
  171 FORMAT(23X,I2,10X,F6.3,9X,F6.2,7X,F6.1)                            BRL2330   165
      PRINT 52                                                           BRL2330   166
   52 FORMAT(1H1,20X,'PARTICLE',4X,'VELOCITY1',6X,'VELOCITY2',6X,        BRL2330   167
     1'VELOCITY3',/,22X,'NUMBER',3X,'(MM/MICROSEC)',2X,'(MM/MICROSEC)',  BRL2330   168
     22X,'(MM/MICROSEC)',/)                                              BRL2330   169
      DO 172 J=1,NPART                                                   BRL2330   170
  172 PRINT 173, J,V1(J),V2(J),V3(J)                                     BRL2330   171
  173 FORMAT(23X,I2,9X,F6.3,7X,F6.3,9X,F6.3)                             BRL2330   172
      PRINT 175                                                          BRL2330   173
  175 FORMAT(1H1,20X,'PARTICLE   LENGTH   DIA.   L/D    MASS     TOTAL J BRL2330   174
     1ET',/,22X,'NUMBER',5X,'(MM)',4X,'(MM)',9X,'(GRAMS)',2X,'MASS(GRAMS BRL2330   175
     2)',/)                                                              BRL2330   176
      DO 176 I=1,NPART                                                   BRL2330   177
  176 PRINT 177, I,XL(I),DIA(I),ELOD(I),XMASS(I),SUMMAS(I)               BRL2330   178
  177 FORMAT(23X,I2,8X,F4.1,4X,F4.1,2X,F4.1,4X,F9.2,5X,F6.2)             BRL2330   179
      PRINT 603                                                          BRL2330   180
  603 FORMAT(1H1,20X,'PARTICLE',4X,'MASS1',9X,'MASS2',9X,'MASS3',/,22X,  BRL2330   181
     1'NUMBER',4X,'(GRAMS)',7X,'(GRAMS)',7X,'(GRAMS)',/)                 BRL2330   182
      DO 600 J=1,NPART                                                   BRL2330   183
      I=1                                                                BRL2330   184
  600 WRITE(6,602) (J,XVOL(I,J),XVOL(I+1,J),XVOL(I+2,J))                 BRL2330   185
  602 FORMAT(23X,I2,6X,F8.4,6X,F8.4,6X,F8.4)                             BRL2330   186
      PRINT 180                                                          BRL2330   187
  180 FORMAT(1HI,20X,'PARTICLE     K.E.     TOTAL JET   DISTANCE FROM CH BRL2330   188
     1ARGE BASE',/,22X,'NUMBER',4X,'(JOULES)',3X,'KE(JOULES)',2X,'FLASH  BRL2330   189
     21',2X,'FLASH 2',2X,'FLASH 3',/)                                    BRL2330   190
      DO 181 I=1,NPART                                                   BRL2330   191
  181 PRINT 182, I,XKE(I),SUMKE(I),S1(I),S2(I),S3(I)                     BRL2330   192
  182 FORMAT(23X,I2,7X,F8.0,4X,F8.0,4X,F9.0,4X,F9.0,4X,F9.0)             BRL2330   193
      PRINT 183                                                          BRL2330   194
  183 FORMAT(1H1,20X,'PARTICLE',4X,'MOMENTUM',4X,'TOTAL JET',/,22X,'NUMB BRL2330   195
     1ER',4X,'(KG-M/SEC)',3X,'MOMENTUM',/)                               BRL2330   196
      DO 185 I=1,NPART                                                   BRL2330   197
  185 PRINT 184,I,P(I),TOTP(I)                                           BRL2330   198
```

```
  184 FORMAT(23X,I2,9X,F6.2,7X,F6.2)                                    BRL2330   199
      DO 192 N=2,NPART                                                  BRL2330   200
      SUMLEN(N)=SUMLEN(N-1)+XL(N)                                       BRL2330   201
      XDIA(N)=XDIA(N-1)+DIA(N)                                          BRL2330   202
      IF(N.EQ.2) GO TO 191                                              BRL2330   203
      DELV(N)=VEL(N-1)-VEL(N)                                           BRL2330   204
      GO TO 192                                                         BRL2330   205
  191 DELV(N)=VEL(1)-VEL(N)                                             BRL2330   206
  192 SDELV(N)=SDELV(N-1)+DELV(N)                                       BRL2330   207
      DO 195 J=3,NPART                                                  BRL2330   208
  195 SUMDEL(J)=DELV(8)+SUMDEL(J-1)                                     BRL2330   209
      AVL1=SUML(NPART)/FLOAT(NPART)                                     BRL2330   210
      AVL2=SUMLEN(NPART)/FLOAT(NPART-1)                                 BRL2330   211
      AVD1=SUMDIA(NPART)/FLOAT(NPART)                                   BRL2330   212
      AVD2=XDIA(NPART)/FLOAT(NPART-1)                                   BRL2330   213
      ADELV1=SDELV(NPART)/FLOAT(NPART-1)                                BRL2330   214
      ADELV2=SUMDEL(NPART)/FLOAT(NPART-2)                               BRL2330   215
      PRINT 200, AVL1,AVL2,AVD1,AVD2,ADELV1,ADELV2                      BRL2330   216
  200 FORMAT(1H1,///7X,47X,'WITH JET TIP    W/O TIP',//,20X,'AVERAGE PART BRL2330   217
     1ICLE LENGTH',7X,F6.2,7X,F6.2,//,20X,'AVERAGE PARTICLE DIAMETER',6X,  BRL2330   218
     2F5.2,8X,F5.2,//,20X,'AVERAGE CHANGE IN VELOCITY',6X,F4.2,9X,F4.2)    BRL2330   219
      PRINT 909                                                         BRL2330   220
      NRA=2                                                             BRL2330   221
      NN=1                                                              BRL2330   222
      IC=0                                                              BRL2330   223
      CALL POLYLS(VEL,S1,NPART,AA,NRA,NN,CC,RR,AF,ERMS,SIG,TT,DET,IC)   BRL2330   224
      WRITE(6,41) CC(1)                                                 BRL2330   225
      DS(1)=CC(1)                                                       BRL2330   226
   41 FORMAT(20X,' VIRTUAL ORIGIN FOR FLASH 1=',F12.6)                  BRL2330   227
      CALL POLYLS(VEL,S2,NPART,AA,NRA,NN,CC,RR,AF,ERMS,SIG,TT,DET,IC)   BRL2330   228
      WRITE(6,42) CC(1)                                                 BRL2330   229
      DS(2)=CC(1)                                                       BRL2330   230
   42 FORMAT(20X,' VIRTUAL ORIGIN FOR FLASH 2=',F12.6)                  BRL2330   231
      IF(L.LT.3) GO TO 515                                              BRL2330   232
      CALL POLYLS(VEL,S3,NPART,AA,NRA,NN,CC,RR,AF,ERMS,SIG,TT,DET,IC)   BRL2330   233
      WRITE(6,43) CC(1)                                                 BRL2330   234
      DS(3)=CC(1)                                                       BRL2330   235
   43 FORMAT(20X,' VIRTUAL ORIGIN FOR FLASH 3=',F12.6)                  BRL2330   236
C                                                                       DRIFT       1
C     DRIFT CALCULATIONS                                                DRIFT       2
C                                                                       DRIFT       3
C                                                                       DRIFT       4
C     EACH REF REFERS TO THE DISTANCE BETWEEN THE REFERENCE PARTICLE    DRIFT       5
C     AND THE FEDUCIAL FROM WHERE ALL OTHER MEASUREMENTS ARE TAKEN.     DRIFT       6
C     REF IS TAKEN IN MM AND SHOULD BE THE ACTUAL DISTANCE READ OFF OF  DRIFT       7
C     THE FILM.  IT WILL THEN BE MULTIPLIED BY THE MAG FACTOR(WHICH     DRIFT       8
C     SHOULD HAVE BEEN ENTERED AS DATA IN BRL2330) NOTE, IF XMAG IS     DRIFT       9
C     LESS THAN 1. , THEN THE FILM PORTRAYS AN IMAGE LARGER THAN REALITY DRIFT      10
C                                                                       DRIFT      11
      READ(5,*) REF(1),REF(2),REF(3)                                    DRIFT      12
      REF(1)=REF(1)*XMAG(1)                                             DRIFT      13
      REF(2)=REF(2)*XMAG(2)                                             DRIFT      14
      REF(3)=REF(3)*XMAG(3)                                             DRIFT      15
      DO 401 J=1,3                                                      DRIFT      16
      DO 400 I=1,NPART                                                  DRIFT      17
  400 AZ(J,I)=AZ(J,I)-REF(J)                                            DRIFT      18
  401 CONTINUE                                                          DRIFT      19
      PRINT 33                                                          DRIFT      20
   33 FORMAT(1H1,21X,'PARTICLE',8X,'DEVIANCE FROM PATH (MM)',//,23X,    DRIFT      21
     1'NUMBER',6X,'FLASH 1    FLASH 2    FLASH 3',/)                   DRIFT      22
      DO 800 JJJ=1,NPART                                                DRIFT      23
      WRITE (6,36) JJJ,AZ(1,JJJ),AZ(2,JJJ),AZ(3,JJJ)                    DRIFT      24
   36 FORMAT(24X,I2,8X,F8.3,3X,F8.3,3X,F8.3)                            DRIFT      25
  800 CONTINUE                                                          DRIFT      26
```

```
      DO 491 I=1,NPART                                                  DRIFT    27
      T1(I)=(S1(I)-DS(1))/VEL(I)                                        DRIFT    28
      T2(I)=(S2(I)-DS(2))/VEL(I)                                        DRIFT    29
      T3(I)=(S3(I)-DS(3))/VEL(I)                                        DRIFT    30
      KD12=AZ(1,I)*T2(I)/(AZ(2,I)*T1(I))                                DRIFT    31
      KD23=AZ(2,I)*T3(I)/(AZ(3,I)*T2(I))                                DRIFT    32
      KD13=AZ(1,I)*T3(I)/(AZ(3,I)*T1(I))                                DRIFT    33
      DO 405 J=1,3                                                      DRIFT    34
      IF(AZ(J,I)-REF(J)) 405,402,405                                    DRIFT    35
  402 THETA(I)=0.0                                                      DRIFT    36
      VETRAV(I)=0.0                                                     DRIFT    37
      GO TO 491                                                         DRIFT    38
  405 CONTINUE                                                          DRIFT    39
C                                                                       DRIFT    40
C     SOLVING FOR THETA USING FIRST TWO GOVERNING EQUATIONS             DRIFT    41
C                                                                       DRIFT    42
      TH12=ATAN(2.0*KD12/SQRT(2.0)-1.0)                                 DRIFT    43
      IF(TH12.LT.0.0)TH12=TH12+PI                                       DRIFT    44
C                                                                       DRIFT    45
C     SOLVING FOR THETA USING LAST TWO GOVERNING EQUATIONS              DRIFT    46
C                                                                       DRIFT    47
      TH23=ATAN(1.0-2.0/(SQRT(2.0)*KD23))                               DRIFT    48
      IF(TH23.LT.0.0)TH23=TH23+PI                                       DRIFT    49
  450 IF(ABS(TH12-TH23).LT.PI/2.0)GO TO 449                             DRIFT    50
      IF(TH23.LT.TH12)GO TO 448                                         DRIFT    51
      TH12=TH12+PI                                                      DRIFT    52
      GO TO 449                                                         DRIFT    53
  448 TH12=TH12-PI                                                      DRIFT    54
C                                                                       DRIFT    55
C     SOLVING FOR THETA USING FIRST AND LAST GOVERNING EQUATIONS        DRIFT    56
C                                                                       DRIFT    57
  449 TH13=ATAN((KD13-1.0)/(KD13+1.0))                                  DRIFT    58
      IF(TH13.LT.0.0)TH13=TH13+PI                                       DRIFT    59
  470 IF(ABS(TH23-TH13).LT.PI/2.0)GO TO 469                             DRIFT    60
      IF(TH23.LT.TH13)GO TO 468                                         DRIFT    61
      TH13=TH13+PI                                                      DRIFT    62
      GO TO 469                                                         DRIFT    63
  468 TH13=TH13-PI                                                      DRIFT    64
C                                                                       DRIFT    65
C     FINDING AN AVERAGE VALUE FOR THETA AND PLACING IT IN THE PROPER   DRIFT    66
C     QUADRANT                                                          DRIFT    67
C                                                                       DRIFT    68
  469 THV=(TH12+TH23+TH13)/3.0                                          DRIFT    69
      IF((TH23-PI/2.0)*AZ(2,I)) 471,473,472                             DRIFT    70
  471 THETA(I)=THV                                                      DRIFT    71
      GO TO 480                                                         DRIFT    72
  472 THETA(I)=THV+PI                                                   DRIFT    73
      TH12=TH12+PI                                                      DRIFT    74
      TH23=TH23+PI                                                      DRIFT    75
      TH13=TH13+PI                                                      DRIFT    76
      IF(THETA(I)-THV.GT.1.7)THV=THV+PI                                 DRIFT    77
      GO TO 480                                                         DRIFT    78
  473 IF(TH13) 474,475,475                                              DRIFT    79
  474 THETA(I)=THV+PI                                                   DRIFT    80
      TH12=TH12+PI                                                      DRIFT    81
      TH23=TH23+PI                                                      DRIFT    82
       TH13=TH13+PI                                                     DRIFT    83
       IF(THETA(I)-THV.GT.1.7)THV=THV+PI                                DRIFT    84
      GO TO 480                                                         DRIFT    85
  475 THETA(I)=THV                                                      DRIFT    86
C                                                                       DRIFT    87
C     CALCULATING RELATIVE TRANSVERSE VELOCITIES WHILE ASSIGNING        DRIFT    88
C     WEIGHTED VALUES...(DEPENDING ON THE PARTICLES' ORIENTATION        DRIFT    89
C     WITH THE FLASH X-RAY)                                             DRIFT    90
```

```
C                                                                       DRIFT      91
  480 VETR12=AZ(1,I)/(COS(TH12-PI/4.0)*T1(I))*1000.0                    DRIFT      92
      VETR23=AZ(2,I)/(COS(TH23)*T2(I))*1000.0                           DRIFT      93
      VETR13=AZ(3,I)/(COS(TH13+PI/4.0)*T3(I))*1000.0                    DRIFT      94
      EPS(1,I)=AZ(1,I)*SIN(TH12-PI/4.0)*(TH12-THV)/T1(I)*1000.0         DRIFT      95
     1          /(COS(TH12-PI/4.0))**2                                 DRIFT      96
      EPS(2,I)=AZ(2,I)*SIN(TH23)*(TH23-THV)*1000.0/T2(I)                DRIFT      97
     1          /(COS(TH23))**2                                        DRIFT      98
      EPS(3,I)=AZ(3,I)*SIN(TH13+PI/4.0)*(TH13-THV)/T3(I)*1000.0         DRIFT      99
     1          /(COS(TH13+PI/4.0))**2                                 DRIFT     100
      EPS(4,I)=AZ(1,I)*SIN(TH13-PI/4.0)*(TH13-THV)/T1(I)*1000.0         DRIFT     101
     1          /(COS(TH13-PI/4.0))**2                                 DRIFT     102
      EPS(5,I)=AZ(2,I)*SIN(TH12)*(TH12-THV)*1000.0/T2(I)                DRIFT     103
     1          /(COS(TH12))**2                                        DRIFT     104
      EPS(6,I)=AZ(3,I)*SIN(TH23+PI/4.0)*(TH23-THV)/T3(I)*1000.0         DRIFT     105
     1          /(COS(TH23+PI/4.0))**2                                 DRIFT     106
      DO 481 J=1,6                                                      DRIFT     107
  481 EPS(J,I)=ABS(EPS(J,I))                                            DRIFT     108
      EPSUM=0.0                                                         DRIFT     109
      DO 482 J=1,6                                                      DRIFT     110
  482 EPSUM=1.0/EPS(J,I)+EPSUM                                          DRIFT     111
      DO 483 J=1,6                                                      DRIFT     112
  483 WT(J)=1.0/(EPS(J,I)*EPSUM)                                        DRIFT     113
      VETRAV(I)=WT(1)*VETR12+WT(2)*VETR23+WT(3)*VETR13+WT(4)*VETR12     DRIFT     114
     1          +WT(5)*VETR23+WT(6)*VETR13                              DRIFT     115
                                                                        DRIFT     116
C                                                                       DRIFT     117
C     CONVERT THETA TO DEGREES                                          DRIFT     118
C                                                                       DRIFT     119
  490 THETA(I)=180.0*THETA(I)/PI                                        DRIFT     120
  491 CONTINUE                                                          DRIFT     121
      PRINT 492                                                         DRIFT     122
  492 FORMAT(1H1,21X,'PARTICLE',5X,'RELATIVE TRANSVERSE',5X,'RELATIVE ',DRIFT     123
     1       'DEVIANCE',/,23X,'NUMBER',8X,'VELOCITY (M/S)',9X,'ANGLE',  DRIFT     124
     2       ' (DEGREES)',/)                                            DRIFT     125
      DO 495 K=1,NPART                                                  DRIFT     126
      WRITE(6,496) K,VETRAV(K),THETA(K)                                 DRIFT     127
  496 FORMAT(24X,I2,18X,F6.2,17X,F5.1)                                  DRIFT     128
  495 CONTINUE                                                          DRIFT     129
C                                                                       DRIFT     130
C     TRANSLATE APPARENT VALUES INTO ABSOLUTE VALUES                    DRIFT     131
C                                                                       DRIFT     132
      R(2)=0.0                                                          DRIFT     133
C                                                                       DRIFT     134
C     GUESSING AT AN INITIAL DEVIANCE ANGLE FOR THE REFERENCE           DRIFT     135
C                                                                       DRIFT     136
      TMIN=THETA(1)                                                     DRIFT     137
      TMAX=THETA(1)                                                     DRIFT     138
      MINDEX=1                                                          DRIFT     139
      MAXDEX=1                                                          DRIFT     140
      DO 391 I=2,NPART                                                  DRIFT     141
      IF(THETA(I).LT.TMIN.OR.TMIN-THETA(I).LT.-300.)GO TO 392           DRIFT     142
      GO TO 393                                                         DRIFT     143
  392 TMIN=THETA(I)                                                     DRIFT     144
      MINDEX=I                                                          DRIFT     145
      GO TO 391                                                         DRIFT     146
  393 IF(THETA(I).GT.TMAX.OR.TMAX-THETA(I).GT.300.) GO TO 394           DRIFT     147
      GO TO 391                                                         DRIFT     148
  394 TMAX=THETA(I)                                                     DRIFT     149
      MAXDEX=I                                                          DRIFT     150
  391 CONTINUE                                                          DRIFT     151
      IF(MINDEX.GT.MAXDEX) GO TO 395                                    DRIFT     152
      INCR=.0034907                                                     DRIFT     153
      THETA0=THETA(MAXDEX)-180.                                         DRIFT     154
      GO TO 396
```

```
  395 INCR=-.0034907                                                    DRIFT     155
      THETAD=THETA(MINDEX)-180.                                         DRIFT     156
  396 ORCS=0.0                                                          DRIFT     157
      DO 899 I=1,NPART                                                  DRIFT     158
      THETA(I)=THETA(I)*PI/180.0                                        DRIFT     159
      VX(I)=VETRAV(I)*COS(THETA(I))                                     DRIFT     160
  899 VY(I)=VETRAV(I)*SIN(THETA(I))                                     DRIFT     161
      THOR=THETAD*PI/180.0                                              DRIFT     162
  902 R(1)=R(2)                                                         DRIFT     163
      ITOTL=IFIX(.122173/ABS(INCR))                                     DRIFT     164
      DO 1100 NOT=1,ITOTL                                               DRIFT     165
      THOR=THOR+INCR                                                    DRIFT     166
  903 VTO=0.0                                                           DRIFT     167
C                                                                       DRIFT     168
C     FINDING THE MAGNITUDE OF REFERENCE TRANSVERSE VELOCITYTHAT WILL   DRIFT     169
C     MAKE IT PROPORTIONAL TO THE AXIAL VELOCITY                        DRIFT     170
C                                                                       DRIFT     171
      DO 756 I=1,NPART                                                  DRIFT     172
  756 VTABS(I)=VETRAV(I)                                                DRIFT     173
  904 VTO=VTO+10.0                                                      DRIFT     174
      INC=100                                                           DRIFT     175
      GO TO 909                                                         DRIFT     176
  905 VTO=VTO+1.0                                                       DRIFT     177
      INC=10                                                            DRIFT     178
      GO TO 909                                                         DRIFT     179
  906 VTO=VTO+.1                                                        DRIFT     180
      INC=1                                                             DRIFT     181
  909 VXO=VTO*COS(THOR)                                                 DRIFT     182
      VYO=VTO*SIN(THOR)                                                 DRIFT     183
      DO 907 I=1,NPART                                                  DRIFT     184
  907 VTABS(I)=SQRT((VX(I)-VXO)**2+(VY(I)-VYO)**2)                      DRIFT     185
C                                                                       DRIFT     186
C     STATISTICAL CALCULATIONS FOR A LINEAR REGRESSION                  DRIFT     187
C                                                                       DRIFT     188
  802 TS=0.0                                                            DRIFT     189
      AS=0.0                                                            DRIFT     190
      TBYAS=0.0                                                         DRIFT     191
      TBYTS=0.0                                                         DRIFT     192
      ABYAS=0.0                                                         DRIFT     193
      KLESS=0                                                           DRIFT     194
      DO 900 I=1,NPART                                                  DRIFT     195
      IF(ABS(VTABS(I)-VTO) .LE. 1.0) GO TO 700                          DRIFT     196
      TS=VTABS(I)+TS                                                    DRIFT     197
      AS=VEL(I)+AS                                                      DRIFT     198
      TBYAS=VTABS(I)*VEL(I)+TBYAS                                       DRIFT     199
      TBYTS=VTABS(I)**2+TBYTS                                           DRIFT     200
      ABYAS=VEL(I)**2+ABYAS                                             DRIFT     201
      GO TO 900                                                         DRIFT     202
  700 KLESS=KLESS+1                                                     DRIFT     203
  900 CONTINUE                                                          DRIFT     204
      CO1=(TBYAS-(TS*AS/(NPART-KLESS)))/(TBYTS-(TS**2/(NPART-KLESS)))   DRIFT     205
      CO2=(TBYAS-(TS*AS/(NPART-KLESS)))/(ABYAS-(AS**2/(NPART-KLESS)))   DRIFT     206
      CO=(CO1+1.0/CO2)/2.0                                              DRIFT     207
      TBAR=TS/(NPART-KLESS)                                             DRIFT     208
      ABAR=AS/(NPART-KLESS)                                             DRIFT     209
      XINT=TBAR-ABAR/CO                                                 DRIFT     210
      IF(XINT.LT.0.0 .AND. INC.EQ.100) GO TO 904                        DRIFT     211
      IF(XINT.LT.0.0 .AND. INC.EQ.10) GO TO 905                         DRIFT     212
      IF(XINT.LT.0.0 .AND. INC.EQ.1)  GO TO 906                         DRIFT     213
      IF(INC-10) 902,911,910                                            DRIFT     214
  910 VTO=VTO-11.0                                                      DRIFT     215
      GO TO 905                                                         DRIFT     216
  911 VTO=VTO-1.1                                                       DRIFT     217
      GO TO 906                                                         DRIFT     218
```

```
  912 R(2)=SQRT(CO1*CO2)                                                DRIFT     219
      IF(R(2).GT.R(1)) GO TO 1101                                       DRIFT     220
      GO TO 1100                                                        DRIFT     221
 1101 R(1)=R(2)                                                         DRIFT     222
      VTO8=VTO                                                          DRIFT     223
      THOR8=THOR                                                        DRIFT     224
      DO 1102 IB=1,NPART                                                DRIFT     225
 1102 VTB(IB)=VTABS(IB)                                                 DRIFT     226
 1100 CONTINUE                                                          DRIFT     227
      VTO=VTO8                                                          DRIFT     228
      THOR=THOR8                                                        DRIFT     229
      DO 1103 IBI=1,NPART                                               DRIFT     230
 1103 VTABS(IBI)=VTB(IBI)                                               DRIFT     231
  790 DO 815 N=1,NPART                                                  DRIFT     232
      IF((VTABS(N)-VTO).LE. 1.0) GO TO 811                              DRIFT     233
      PHI(N)=THETA(N)-THOR                                              DRIFT     234
      BETA(N)=ASIN(VETRAV(N)*SIN(PHI(N))/VTABS(N))*180.0/PI             DRIFT     235
      AVST(N)=VEL(N)/VTABS(N)*1000.0                                    DRIFT     236
      GO TO 815                                                         DRIFT     237
  811 VTABS(N)=0.0                                                      DRIFT     238
      BETA(N)=0.0                                                       DRIFT     239
      AVST(N)=0.0                                                       DRIFT     240
  815 CONTINUE                                                          DRIFT     241
      PRINT 702                                                         DRIFT     242
  702 FORMAT(1H1,21X,'PARTICLE',5X,'ABSOLUTE TRANSVERSE',9X,'ABSOLUTE ',DRIFT     243
     1       'ANGULAR',5X,'AXIAL VELOCITY OVER',/,23X,'NUMBER',9X,'VEL',DRIFT     244
     2      'OCITY (M/S)',4X,'DEVIANCE WRT REFERENCE  TRANSVERSE VELOC',DRIFT     245
     3       'ITY',/)                                                   DRIFT     246
      DO 710 J=1,NPART                                                  DRIFT     247
      WRITE(6,707) J,VTABS(J),BETA(J),AVST(J)                           DRIFT     248
  707 FORMAT(24X,I2,16X,F6.2,19X,F6.1,17X,F6.2)                         DRIFT     249
  710 CONTINUE                                                          DRIFT     250
      PRINT 712,VTO                                                     DRIFT     251
  712 FORMAT(/,22X,'THE TRANSVERSE VELOCITY OF THE REFERENCE IS ',      DRIFT     252
     1       F6.2,' M/S')                                               DRIFT     253
      PRINT 713, R(2)                                                   DRIFT     254
  713 FORMAT(/,22X,'THE CORRELATION COEFFICIENT FOR THIS REGRESSION',   DRIFT     255
     1       ' IS ',F9.4)                                               DRIFT     256
C                                                                       PENJET      1
C     * * * * * P E N J E T * * * * *                                   PENJET      2
C                                                                       PENJET      3
C                                                                       PENJET      4
C     ECONST IS THE ENERGY REQUIRED TO CREATE ONE CUBIC-MM OF HOLE      PENJET      5
C     VOLUME.  RHOJ IS JET DENSITY IN G/CU-MM. SIGJ IS JET STRENGTH IN  PENJET      6
C     MEGAPASCALS..  RHOT AND SIGT ARE THE CORRESPONDING TARGET         PENJET      7
C     VARIABLES                                                         PENJET      8
C                                                                       PENJET      9
      READ(5,300)ECONST,RHOJ,SIGJ,RHOT,SIGT                             PENJET     10
  300 FORMAT(5F10.4)                                                    PENJET     11
C                                                                       PENJET     12
C     ZMIN IS THE MINIMUM STANDOFF AT WHICH PENJET WILL EVALUATE THE    PENJET     13
C     GIVEN DRIFT DISTRIBUTION.  ZMAX IS THE MAXIMUM STANDOFF TO BE     PENJET     14
C     ANALYZED.  ZINC IS THE INCREMENT BETWEEN STANDOFF ANALYZATION.    PENJET     15
C     ALL MEASUREMENTS ARE IN MM.                                       PENJET     16
C                                                                       PENJET     17
      READ(5,397)ZMIN,ZMAX,ZINC                                         PENJET     18
  397 FORMAT(3F10.1)                                                    PENJET     19
      DO 301 I=1,NPART                                                  PENJET     20
      BETA(I)=BETA(I)*3.14159/180.                                      PENJET     21
      RADIUS(I)=0.0                                                     PENJET     22
      PEN(I)=0.0                                                        PENJET     23
      RL(I)=XL(I)                                                       PENJET     24
      RVEL(I)=VEL(I)                                                    PENJET     25
  301 CONTINUE                                                          PENJET     26
```

```
      NM1=NPART-1                                                       PENJET     27
      GAMMA=SQRT(RHOT/RHOJ)                                             PENJET     28
      ZSUBO=ZMIN-ZINC                                                   PENJET     29
      KZSUM=0                                                           PENJET     30
  280 ZSUBO=ZSUBO+ZINC                                                  PENJET     31
      KZSUM=KZSUM+1                                                     PENJET     32
      PENMAX(KZSUM)=0.                                                  PENJET     33
      ZSUB(KZSUM)=ZSUBO                                                 PENJET     34
C                                                                       PENJET     35
C     THIS LOOP EVALUATES EACH DIGITIZED PARTICLE                       PENJET     36
C                                                                       PENJET     37
  291 DO 209 I=1,NPART                                                  PENJET     38
      NCC(I)=0                                                          PENJET     39
      NQ=0                                                              PENJET     40
  269 T(I)=(ZSUBO-XL(I)-(DS(1)+DS(2)+DS(3))/3.-2.999)/VEL(I)            PENJET     41
      DELT=3./VEL(I)                                                    PENJET     42
      JMIN=1                                                            PENJET     43
C                                                                       PENJET     44
C     LOCATING A PARTICLE IN 3-D SPACE...THEN FINDING WHETHER IT STRIKES PENJET     45
C     THE HOLE PROFILE.  IF IT DOESN'T, THEN TIME IS INCREMENTED UNTIL  PENJET     46
C     IMPACT OCCURS.                                                    PENJET     47
C                                                                       PENJET     48
  201 T(I)=T(I)+DELT                                                    PENJET     49
  205 X(I)=VEL(I)/AVST(I)*T(I)*COS(BETA(I))                             PENJET     50
      Y(I)=X(I)*TAN(BETA(I))                                            PENJET     51
      Z(I)=VEL(I)*T(I)-ZSUBO+XL(I)+(DS(1)+DS(2)+DS(3))/3.               PENJET     52
      IF(NQ.EQ.2)  GO TO 210                                            PENJET     53
      IF(Z(I).LT.0.0) GO TO 201                                         PENJET     54
      IF(I.EQ.1 .AND. T(I).LT.BREAK(I))GOTO 202                         PENJET     55
      IF(I.EQ.1)GO TO 210                                               PENJET     56
      KLESS=I-1                                                         PENJET     57
      DO 206 J=JMIN,KLESS                                               PENJET     58
      IF(PEN(J).LT..01)GO TO 206                                        PENJET     59
      V(I,1)=X(I)-X(J)                                                  PENJET     60
      V(I,2)=Y(I)-Y(J)                                                  PENJET     61
      V(I,3)=Z(I)-Z(J)                                                  PENJET     62
      VM(I)=SQRT(V(I,1)**2+V(I,2)**2+V(I,3)**2)                         PENJET     63
      VAM(I)=V(I,1)*GRAD(J,1)+V(I,2)*GRAD(J,2)+V(I,3)*GRAD(J,3)         PENJET     64
      VAM(I)=ABS(VAM(I))                                                PENJET     65
      VPM(I)=SQRT(ABS(VM(I)**2-VAM(I)**2))                              PENJET     66
      IF((VPM(I)+DIA(I)/2.)**2/RADIUS(J)**2+VAM(I)**2/PEN(J)**2.GT.1.0) PENJET     67
     1     GO TO 206                                                    PENJET     68
      IF(NQ.EQ.1)GO TO 210                                              PENJET     69
      JMIN=J                                                            PENJET     70
      GO TO 201                                                         PENJET     71
  206 CONTINUE                                                          PENJET     72
  207 NQ=1                                                              PENJET     73
      IF(JMIN.EQ.KLESS .AND. Z(I).LE..1) GO TO 208                      PENJET     74
      T(I)=T(I)-DELT/6.0                                                PENJET     75
      GO TO 205                                                         PENJET     76
  208 T(I)=(ZSUBO-XL(I)-(DS(1)+DS(2)+DS(3))/3.)/VEL(I)                  PENJET     77
      NQ=2                                                              PENJET     78
      GO TO 205                                                         PENJET     79
C                                                                       PENJET     80
C     FINDING THE EFFECTS OF THE PARTICLE PENETRATION                   PENJET     81
C                                                                       PENJET     82
  210 IF(I.NE.1 .AND. NQ.NE.2)GO TO 202                                 PENJET     83
      GRAD(1,1)=0.0                                                     PENJET     84
      GRAD(1,2)=0.0                                                     PENJET     85
      GRAD(I,3)=1.0                                                     PENJET     86
      GO TO 291                                                         PENJET     87
C                                                                       PENJET     88
C     IF A PARTICLE IS NOT IN THE CONTINUOUS MODE, THE AXIS OF          PENJET     89
C     PENETRATION IS EVALUATED                                          PENJET     90
```

```
C                                                                       PENJET     91
  202 IF(T(I).LT.BREAK(I))NCC(I)=1                                      PENJET     92
      IF(I.EQ.1 .AND. NCC(I).EQ.1)GOTO1999                              PENJET     93
      IF(T(I).LT.BREAK(I))XL(I)=XL(I)*T(I)/BREAK(I)                     PENJET     94
      IM1=I-1                                                           PENJET     95
      IF(T(I).LT.BREAK(I) .AND. Z(I).GT.Z(IM1))GOTO 1999                PENJET     96
      DO 204 LJ=1,3                                                     PENJET     97
      VA(I,LJ)=GRAD(JMIN,LJ)*VAM(I)                                     PENJET     98
      VP(I,LJ)=V(I,LJ)-VA(I,LJ)                                         PENJET     99
      AR(I,LJ)=VA(I,LJ)/VAM(I)                                          PENJET    100
  204 PR(I,LJ)=VP(I,LJ)/VPM(I)                                          PENJET    101
      RGRAD(I,1)=VPM(I)*2./RADIUS(JMIN)**2                              PENJET    102
      RGRAD(I,2)=0.0                                                    PENJET    103
      RGRAD(I,3)=VAM(I)*2./PEN(JMIN)**2                                 PENJET    104
      RGM(I)=SQRT(RGRAD(I,1)**2+RGRAD(I,3)**2)                          PENJET    105
      RGRAD(I,1)=RGRAD(I,1)/RGM(I)                                      PENJET    106
      RGRAD(I,3)=RGRAD(I,3)/RGM(I)                                      PENJET    107
      DO 214 LJ=1,3                                                     PENJET    108
  214 GRAD(I,LJ)=RGRAD(I,1)*PR(I,LJ)+RGRAD(I,3)*AR(I,LJ)                PENJET    109
      GM=SQRT(GRAD(I,1)**2+GRAD(I,2)**2+GRAD(I,3)**2)                   PENJET    110
      DO 219 LJ=1,3                                                     PENJET    111
  219 GRAD(I,LJ)=GRAD(I,LJ)/GM                                          PENJET    112
      GOTO 251                                                          PENJET    113
C                                                                       PENJET    114
C     CONTINUOUS PENETRATION AXIS IS ALONG PARTICLE FLIGHT AXIS.        PENJET    115
C                                                                       PENJET    116
 1999 VECT=SQRT(X(I)**2+Y(I)**2+(Z(I)+ZSUBO-(DS(1)+DS(2)+DS(3))/3.)**2) PENJET    117
      GRAD(I,1)=X(I)/VECT                                               PENJET    118
      GRAD(I,2)=Y(I)/VECT                                               PENJET    119
      GRAD(I,3)=(Z(I)+ZSUBO-(DS(1)+DS(2)+DS(3))/3.)/VECT                PENJET    120
  251 PENMAX(KZSUM)=XL(I)/GAMMA+PENMAX(KZSUM)                           PENJET    121
      IF(I.EQ.1 .OR. NQ.EQ.2 .OR. NCC(I).EQ.1)GOTO 262                  PENJET    122
C                                                                       PENJET    123
C     EFFECTIVE LENGTH AND EFFECTIVE VELOCITY CALCULATIONS.             PENJET    124
C                                                                       PENJET    125
      XL(I)=GRAD(I,3)*XL(I)+SQRT(GRAD(I,1)**2+GRAD(I,2)**2)             PENJET    126
     1      *DTA(I)                                                     PENJET    127
      VEL(I)=GRAD(I,3)*VEL(I)                                           PENJET    128
C                                                                       PENJET    129
C     PENETRATION CALCULATIONS AS A FUNCTION OF EFFECTIVE VELOCITY.     PENJET    130
C                                                                       PENJET    131
      IF(VEL(I).GT. .8) GO TO 260                                       PENJET    132
      PEN(I)=0.0                                                        PENJET    133
      RADIUS(I)=0.0                                                     PENJET    134
      U(I)=0.0                                                          PENJET    135
      HVOL(I)=0.0                                                       PENJET    136
      GO TO 209                                                         PENJET    137
  260 IF(VEL(I).GT.1.4) GO TO 261                                       PENJET    138
      U(I)=0.0                                                          PENJET    139
      HVOL(I)=XKE(I)/ECONST                                             PENJET    140
      PEN(I)=(VEL(I)-.8)**2/.72*XL(I)                                   PENJET    141
      RADIUS(I)=SQRT(3.*HVOL(I) /(2.*3.14159*PEN(I)))                   PENJET    142
      GO TO 209                                                         PENJET    143
  261 IF(VEL(I).GT.2.1)GO TO 262                                        PENJET    144
      U(I)=0.0                                                          PENJET    145
      HVOL(I)=XKE(I)/ECONST                                             PENJET    146
      PEN(I)=(-(VEL(I)-2.)**2/.72+1.)*XL(I)                             PENJET    147
      RADIUS(I)=SQRT(3.*HVOL(I) /(2.*3.14159*PEN(I)))                   PENJET    148
      GO TO 209                                                         PENJET    149
  262 RAD=SQRT(VEL(I)**2*RHOJ*RHOT-2.*(RHOJ-RHOT)*(SIGJ-SIGT)/1.E6)     PENJET    150
      U(I)=(RHOJ*VEL(I)-RAD)/(RHOJ-RHOT)                                PENJET    151
      PEN(I)=(RHOJ*VEL(I)*XL(I)-XL(I)*RAD)/(RAD-RHOT*VEL(I))            PENJET    152
      HVOL(I)=XKE(I)/ECONST                                             PENJET    153
      RADIUS(I)=SQRT(3.*HVOL(I) /(2.*3.14159*PEN(I)))                   PENJET    154
```

```
209 CONTINUE                                                          PENJET   155
279 WRITE(6,211)                                                      PENJET   156
211 FORMAT(1H1,10X,'PARTICLE',5X,'HOLE',6X,'IMPACT',3X,'PENETRATION ', PENJET   157
   1'PENETRATION',6X,'STATUS'/#12X,'NUMBER',5X,'VOLUME',6X,'TIME',17X, PENJET   158
   2     'VELOCITY',/,23X,'(CU.MM)  (MICROSEC)',4X,'(MM)',5X,'(MM/',    PENJET   159
   3       'MICROSEC)',/)                                             PENJET   160
    DO 213 I=1,NPART                                                  PENJET   161
    IF(NCC(I).EQ.1)GOTO 281                                           PENJET   162
    WRITE(6,212)I,HVOL(I),T(I),PEN(I),U(I),NPA,MPAR,MPART             PENJET   163
    GO TO 213                                                         PENJET   164
281 WRITE(6,212)I,HVOL(I),T(I),PEN(I),U(I),MCO,MCON,MCONT             PENJET   165
212 FORMAT(14X,I2,7X,F6.0,4X,F9.1,7X,F4.1,8X,F9.3,7X,3A4)             PENJET   166
213 CONTINUE                                                          PENJET   167
    PMAX=0.0                                                          PENJET   168
    DO 215 I=1,NPART                                                  PENJET   169
    IF(Z(I).LE.PMAX) GO TO 215                                        PENJET   170
    PMAX=Z(I)                                                         PENJET   171
    DPMAX=PEN(I)*GRAD(I,3)                                            PENJET   172
215 CONTINUE                                                          PENJET   173
    PENSUM=PMAX+DPMAX                                                 PENJET   174
    PENT(KZSUM)=PENSUM                                                PENJET   175
    WRITE(6,216)PENSUM                                                PENJET   176
216 FORMAT(1HO,10X,'THE TOTAL PENETRATION PREDICTED BY THIS ',         PENJET   177
   1     'PROGRAM IS ',F6.1,' MM')                                    PENJET   178
    PRINT 257, ZSUBO                                                  PENJET   179
257 FORMAT(1HO,10X,'THESE VALUES WERE CALCULATED AT A  STANDOFF ',     PENJET   180
   1        'OF ',F6.0,' MM.')                                        PENJET   181
    WRITE(6,220)                                                      PENJET   182
220 FORMAT(1H1,14X,'X,Y, AND Z COORDINATES      PENETRATION  MAX CRA', PENJET   183
   1     'TER RADIUS  AXIAL DIRECTION OF PENETRATION')                PENJET   184
    DO 218 I=1,NPART                                                  PENJET   185
    WRITE(6,217)I,X(I),Y(I),Z(I),PEN(I),RADIUS(I),GRAD(I,1),          PENJET   186
   1     GRAD(I,2),GRAD(I,3)                                          PENJET   187
217 FORMAT(11X,I2,5F10.2,3F10.4)                                      PENJET   188
218 CONTINUE                                                          PENJET   189
    DO 263 I=1,NPART                                                  PENJET   190
    VEL(I)=RVEL(I)                                                    PENJET   191
    KWAL(I)=0                                                         PENJET   192
263 XL(I)=RL(I)                                                       PENJET   193
    IF(ZSUBO.LT.ZMAX) GO TO 250                                       PENJET   194
    WRITE(6,290)                                                      PENJET   195
290 FORMAT(1H1,' VIRTUAL ORIGIN ZO(MM)     PENETRATION(MM)     MAX ', PENJET   196
   +     'PENETRATION(MM)',/)                                         PENJET   197
    DO 289 I=1,KZSUM                                                  PENJET   198
289 WRITE(6,292)ZSUB(I),PENT(I),PENMAX(I)                             PENJET   199
292 FORMAT(10X,F5.0,T32,F7.2,T55,F7.2)                                PENJET   200
515 CONTINUE                                                          PENJET   201
505 FORMAT(1H1)                                                       BRL2330  237
    DO 510 JN= 1,NPART                                                BRL2330  238
    VOL(JN)=0.                                                        BRL2330  239
    XL(JN)=0.                                                         BRL2330  240
510 DIA(JN)=0.                                                        BRL2330  241
500 CONTINUE                                                          BRL2330  242
    STOP                                                              BRL2330  243
    END                                                               BRL2330  244
```

BREAK(N) - breakup time of particle N in μsec

BROK (1, 2, 3) - observed number of jet particles already particulated as of exposure (1, 2, 3)

FLASH (1, 2, 3) - time after detonation of round for exposure of film (1, 2, 3)

PBAR -

PBYPZ -

PBYTZ - } statistical variables used in calculation of breakup time

TAVG -

TDLAY - time delay between detonation of round and formation of jet

Z1 - time between breakup of adjacent jet particles

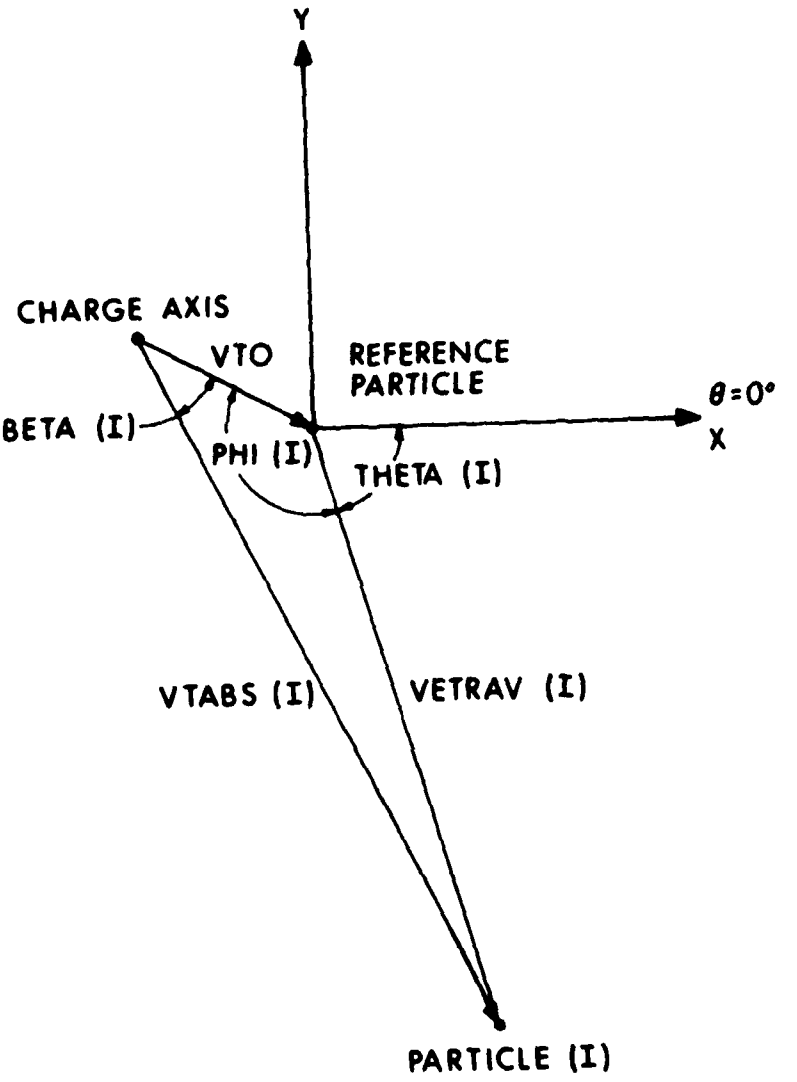

Figure A1. A Diagrammatic Sketch Identifying Some DRIFT Variables

AVST (I) - the axial velocity divided by the transverse velocity for particle I

AZ (1, I)
AZ (2, I) - deviance of particle I with respect to the reference on exposure 1, 2, 3
AZ (3, I)

BETA (I) - absolute angle formed between drifting reference and particle I

DS (1)
DS (2) - virtual origin calculations based on exposure 1, 2, 3
DS (3)

EPS (1, I)
EPS (2, I)
EPS (3, I)
EPS (4, I) - estimate for sensitivity of transverse velocity V with respect to small changes in drift angle Θ (of the form $\frac{dV}{d\Theta}\Delta\Theta$) using all combinations of drift velocities and drift angles calculated from the 3 radiographs
EPS (5, I)

EPSUM - $\sum_{K=1}^{6} \frac{1}{EPS(K, I)}$ a constant used to scale the EPS values to their proper magnitude

KD 12
KD 23 - a constant relating time delay between exposures 1 and 2, 2 and 3, 1 and 3 used in drift velocity calculations
KD 13

MAXDEX - the particle # that satisfies TMAX

MINDEX - the particle # that satisfies TMIN

PHI (I) - the supplementary of the relative drift angle between particle I and the reference

R (2) - correlation coefficient for V_A vs. V_T plot for reference drift angle presently being analyzed.
R (1) previously

S1 (I)
S2 (I) - axial distance from charge base to particle I on exposure 1, 2, 3
S3 (I)

T1 (I)
T2 (I) - estimated existence time from creation of particle I to exposure of film $\begin{matrix}1\\2.\\3\end{matrix}$
T3 (I)

THETAO - initial guess at direction of reference drift

TMAX - the angle of the particle which is most clockwise/counterclockwise
TMIN in the relative angular span.

TH12
TH23 - relative drift angle calculated from governing equations $\begin{matrix}1 & 2\\2 & 3\\1 & 3\end{matrix}$
TH13

THV - the numerical average of TH12, TH23, and TH13

THETA (I) - the relative drift angle of particle I with respect to arbitrary origin (chosen parallel to film 2) (degrees).

THOR - the current reference drift angle being tested

VETR12
VETR23 - relative transverse velocity calculated from equations $\begin{matrix}1 & 2\\2 & 3\\1 & 3\end{matrix}$
VETR13

VETRAV (I) - relative transverse velocity of particle I based on weighted values of VETR12, VETR23, and VETR13 (m/s)

VTABS (I) - absolute transverse velocity of particle I (m/s)

VTO - transverse velocity of particle reference (m/s)

VXO - x component of drift velocity for the reference
VYO - y

VX (I) - x component of relative drift velocity for particle I
VY (I) - y

WT (I) - the percentage weight that an individual drift velocity calculation contributes to the overall average.

ABAR
ABYAS
AS
CO
CO1
CO2
TBAR
TBYAS
TBYTS
TS
XINT

statistical variables used in V_A vs V_T regression

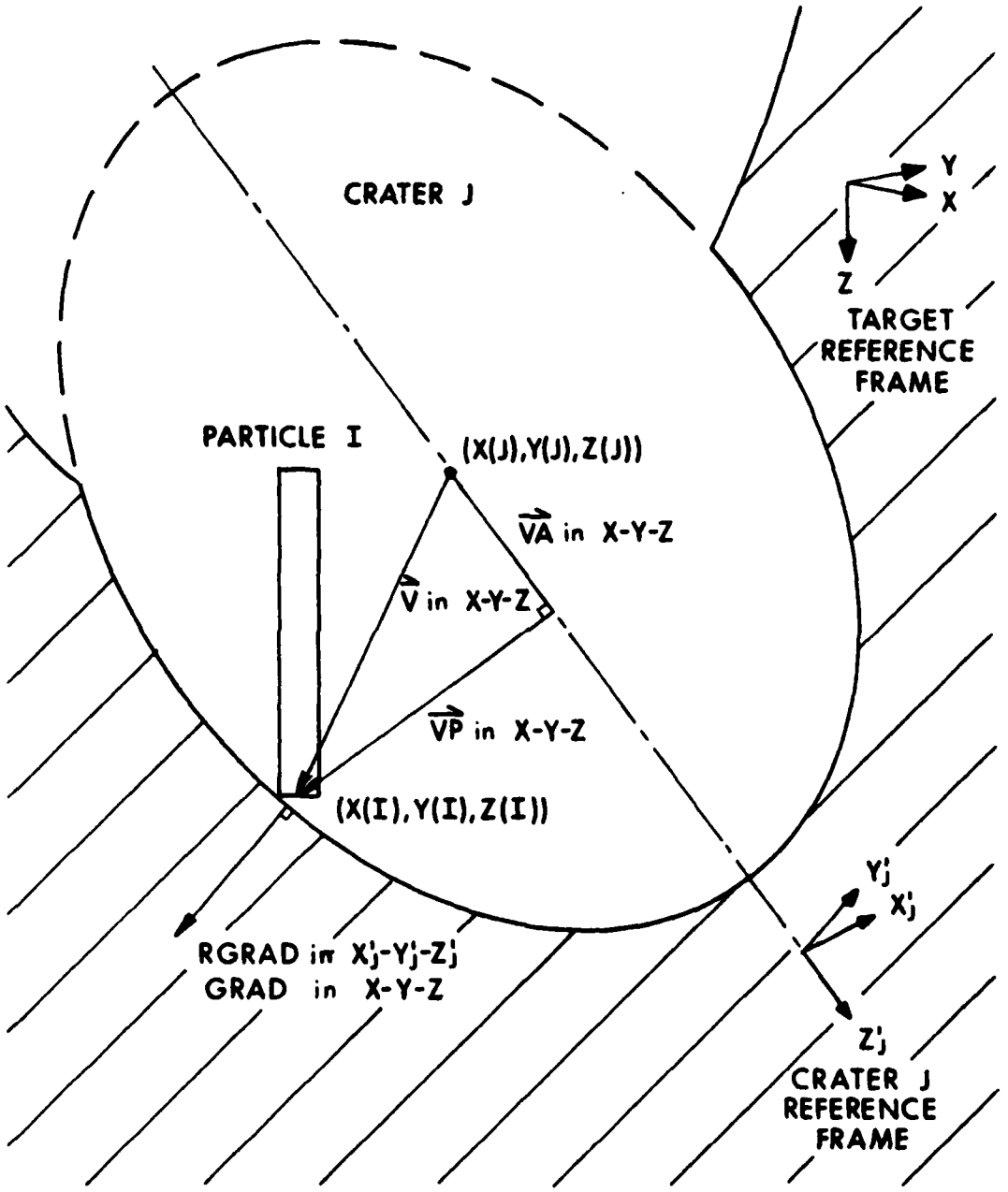

Figure A2: A Diagrammatic Sketch Identifying Some PENJET Variables.

T (I) - impact time of particle I, taken from virtual origin

X (I), Y (I), Z (I) - spacial coordinates for top of particle I at any given time (and eventually upon impact) X = 0, Y = 0 denote where charge axis intersects target plate; Z = 0 is target surface.

DELT - time increment (varied so that particle travels 3 mm/timestep)

U (I) - penetration velocity of particle I (calculated only in the hypervelocity regime e.g. above 2 mm/μsec)

RADIUS (I) - crater radius of particle I

PEN (I) - penetration of particle I

HVOL (I) - hole volume created by particle I

V (I, 1), V (I, 2), V (I, 3) - the x, y, z components of a vector drawn from the center of crater J (through which particle I is instantaneously passing) to the tip of particle I

VM (I) - magnitude of vector $\vec{V}$

VA (I, 1), VA (I, 2), VA (I, 3) - the x, y, z components of vector $\vec{VA}$ which is in itself the component of vector $\vec{V}$ pointing axially down crater J (the crater through which particle I is passing)

VAM (I) - magnitude of vector $\vec{VA}$

VP (I, 1), VP (I, 2), VP (I, 3) - the x, y, z components of vector $\vec{VP}$ which is in itself the component of vector $\vec{V}$ pointing perpendicular to the penetration axis of crater J (through which particle I is passing). Note that $\vec{VA} + \vec{VP} = \vec{V}$

VPM (I) - magnitude of vector $\vec{VP}$

RGRAD (I, 1), RGRAD (I, 2), RGRAD (I, 3) - the x, y, z components of a vector that is perpendicular to crater J at the point of impact of particle I, but in the coordinate system of crater J (e.g., the Z' axis points down the axis of crater J)

RGM (I) - magnitude of vector $\overrightarrow{RGRAD}$

GRAD (I, 1)
GRAD (I, 2)
GRAD (I, 3)
: the x, y, z components of a vector that is perpendicular to crater J at the point of impact of particle I, and in laboratory coordinate system (e.g., the z axis points perpendicular to the target surface); $\overrightarrow{GRAD}$ becomes the axis of penetration for crater I according to refracted particle wave theory

GM (I) - magnitude of vector $\overrightarrow{GRAD}$

AR (I, 1)
AR (I, 2)
AR (I, 3)
: a unit vector version of $\overrightarrow{VA}$

PR (I, 1)
PR (I, 2)
PR (I, 3)
: a unit vector version of $\overrightarrow{VP}$

NCC (I) - equals 1 when particle I is particulate; equals 0 when I is continuous

ECONST - energy constant used for calculating crater volume (J/mm^3)

ZSUBO - standoff (mm) from virtual origin to target surface

RHOJ - jet density ρ_j (g/mm^3)

RHOT - target density ρ_t (g/mm^3)

SIGJ - jet strength (MPa)

SIGT - target strength (MPa)

GAMMA - $(\rho_t/\rho_j)^{\frac{1}{2}}$

JMIN - the last crater number that particle I has been known to successfully have passed through

PENSUM - the penetration resulting from PENJET calculations

NQ = 0 - particle I is travelling down hole profile

NQ = 1 - particle I has just struck target; t is decremented until precise impact time is revealed

NQ = 2 - particle I has drifted so far off course as to preclude entry into any part of the hole profile; it therefore strikes the target surface

KZSUM - number of standoffs at which PENJET has just analyzed a drift distribution

PENMAX (K) - the greatest possible penetration at standoff #K

ZSUB (K) - an array of the standoffs at which PENJET has just been run

PENT (K) - penetration predicted by PENJET at standoff #K

DISTRIBUTION LIST

No. of Copies	Organization
12	Commander Defense Technical Info Center ATTN: DTIC-DDA Cameron Station Alexandria, VA 22314
2	HQDA (DAMA-ZA; DAMA-RA, T. Rorstad) Washington, DC 20310
1	Assistant Secretary of the Army (R&D) ATTN: Assistant for Research Washington, DC 20310
1	Deputy Under Secretary of the Army (Operations Research) ATTN: SAUS-OR, D. C. Hardison Room 2E621, The Pentagon Washington, DC 20310
3	Commander US Army Materiel Development and Readiness Command ATTN: DRCDMD-ST DRCCG DRCDE-WM 5001 Eisenhower Avenue Alexandria, VA 22333
5	Commander US Army Armament Research and Development Command ATTN: DRDAR-TSS DRDAR-LCU-D-R/T. Stevens DRDAR-LCU-LT/A. King DRDAR-LCU-DC/J. Pearson Dover, NJ 07801
1	Commander US Army Armament Research and Development Command ATTN: DRDAR-TDC (Dr. D. Gyorog) Dover, NJ 07801
1	Commander US Army Armament Materiel Readiness Command ATTN: DRSAR-LEP-L Rock Island, IL 61299
1	Director US Army ARRADCOM Benet Weapons Laboratory ATTN: DRDAR-LCB-TL Watervliet, NY 12189
1	Commander US Army Aviation Research and Development Command ATTN: DRDAV-E 4300 Goodfellow Blvd St. Louis, MO 63120
1	Director US Army Air Mobility Research and Development Laboratory Ames Research Center Moffett Field, CA 94035
1	Commander US Army Communications Research and Development Command ATTN: DRSEL-ATDD Fort Monmouth, NJ 07703
1	Commander US Army Electronics Research and Development Command Technical Support Activity ATTN: DELSD-L Fort Monmouth, NJ 07703
9	Commander US Army Missile Command ATTN: DRSMI-R DRSMI-J COL C. M. Matthews, Jr. DRSMI-VIT DRCPM-HD/COL Cass DRCPM-HDE-M/R. Nasucci DRCPM-TO DRSMI-YDL TOW-PM/COL Williamson DRSMI-RLA/E. B. Harwell Redstone Arsenal, AL 35898
2	Commandant US Army Infantry School ATTN: ATSH-CD-CSO-OR Fort Benning, GA 31905

DISTRIBUTION LIST

No. of Copies	Organization
3	Commander US Army Tank Automotive Command ATTN: DRDTA-RWL/C. Bradley DRDTA-TSL DRDTA-RC/Dr. J. Jellinek Warren, MI 48090
1	Program Manager XM1 Abrams Tank System ATTN: DRCPM-GCM-S Warren, MI 48090
1	Director US Army TRADOC Systems Analysis Activity ATTN: ATAA-SL White Sands Missile Range NM 88002
2	Commander US Army Materials and Mechanics Research Center ATTN: DRXMR-PDD/J. Prifti Tech Lib Watertown, MA 02172
1	Commander US Army Research Office P. O. Box 12211 Research Triangle Park NC 27709
2	Chief of Naval Research Department of the Navy ATTN: Code 427 Code 470 Washington, DC 20360
1	Commander Naval Sea Systems Command Washington, DC 20360
2	Commander Naval Air Systems Command ATTN: Code AIR-310 Code AIR-350 Washington, DC 20360
2	Commander Naval Surface Weapons Center ATTN: Code DG-50 DX-21, Lib Br Dahlgren, VA 22448 22448
1	Commander Naval Surface Weapons Center ATTN: Code 730, Lib Silver Spring, MD 20910
1	Commander Naval Surface Weapons Center ATTN: N. Coleburn Silver Spring, MD 20910
1	Commander Naval Weapons Center ATTN: Dr. L. Smith China Lake, CA 93555
2	Commander Naval Weapons Center ATTN: Code 4057 Code 3431, Tech Lib China Lake, CA 93555
1	Commander Naval Research Laboratory Washington, DC 20375
1	USAF/AFRDDA Washington, DC 20311
1	AFSC/SDZ/SDOA Andrews AFB Washington, DC 20334
2	US Air Force Academy ATTN: Code FJS-41 (NC) Tech Lib Colorado Springs, CO 80840
1	AFATL/DLJW (Dr. J. Foster) Eglin AFB, FL 32542
1	AFWL/SUL Kirtland AFB, NM 87117

DISTRIBUTION LIST

No. of Copies	Organization
1	AFATL/DLYV (Mr. J. Smith) Eglin AFB, FL 32542
1	AFWL/SUL (LT Tennant) Kirtland AFB, NM 87117
1	AFAL Wright-Patterson AFB, OH 45433
1	AFLC/MMWMC Wright-Patterson AFB, OH 45433
1	Director Lawrence Livermore National Lab. ATTN: Tech Lib P. O. Box 808 Livermore, CA 94550
2	Director Lawrence Livermore National Lab. ATTN: Dr. C. Godfrey Mr. M. Wilkins P. O. Box 808 Livermore, CA 94550
1	AFELM, The Rand Corporation ATTN: Library D 1700 Main Street Santa Monica, CA 90406
1	Sandia Laboratories ATTN: Tech Lib Albuquerque, NM 87115
1	Battelle- Memorial Institute ATTN: Mr. Joseph E. Backofen 505 King Avenue Columbus, OH 43201
1	Dyna East Corporation ATTN: P. C. Chou 227 Hemlock Road Wynnewood, Pa 19096
2	Firestone Defense Research and Products Division of the Firestone Tire and Rubber Company ATTN: R. Berus, L. Swabley 1200 Firestone Parkway Akron, OH 44317
1	Honeywell Inc. Government and Aerospace Products Division ATTN: C. R. Hargreaves 600 Second Street Hopkins, NM 55343
1	Physics International ATTN: Ron E. Brown San Leandro, CA 94577
1	Drexel Institute of Technology 32nd and Chestnut Streets Philadelphia, PA 19104
1	Systems, Science & Software ATTN; Dr. R. Sedgwick P. O. Box 1620 La Jolla, CA 92037

Aberdeen Proving Ground

Dir, USAMSAA
ATTN: DRXSY-D
DRXSY-MP, H. Cohen
DRXSY-G, Mr. Kramer
Cdr, USATECOM
ATTN: DRSTE-TO-E
Dir, USACSL, Bldg. E3516, EA
ATTN: DRDAR-CLB-PA
DRDAR-CLN
DRDAR-CLJ-L

USER EVALUATION OF REPORT

Please take a few minutes to answer the questions below; tear out this sheet, fold as indicated, staple or tape closed, and place in the mail. Your comments will provide us with information for improving future reports.

1. BRL Report Number _____

2. Does this report satisfy a need? (Comment on purpose, related project, or other area of interest for which report will be used.)

_____

_____

_____

3. How, specifically, is the report being used? (Information source, design data or procedure, management procedure, source of ideas, etc.) _____

_____

_____

4. Has the information in this report led to any quantitative savings as far as man-hours/contract dollars saved, operating costs avoided, efficiencies achieved, etc.? If so, please elaborate.

_____

_____

5. General Comments (Indicate what you think should be changed to make this report and future reports of this type more responsive to your needs, more usable, improve readability, etc.) _____

_____

_____

_____

6. If you would like to be contacted by the personnel who prepared this report to raise specific questions or discuss the topic, please fill in the following information.

Name: _____

Telephone Number: _____

Organization Address: _____

_____

_____

FOLD HERE

Director
US Army Ballistic Research Laboratory
ATTN: DRDAR-BLA-S
Aberdeen Proving Ground, MD 21005

NO POSTAGE
NECESSARY
IF MAILED
IN THE
UNITED STATES

OFFICIAL BUSINESS
PENALTY FOR PRIVATE USE, $300

BUSINESS REPLY MAIL
FIRST CLASS PERMIT NO 12062 WASHINGTON, DC
POSTAGE WILL BE PAID BY DEPARTMENT OF THE ARMY

Director
US Army Ballistic Research Laboratory
ATTN: DRDAR-BLA-S
Aberdeen Proving Ground, MD 21005

FOLD HERE